Excited hadrons from data

Michael Döring

Helmholtz-Institut für Strahlen- und Kernphysik, Universität Bonn

Bethe Center for Theoretical Physics

Seminar @ JLab

~~March 06, 2013~~

March 13, 2013

The intermediate energy region...

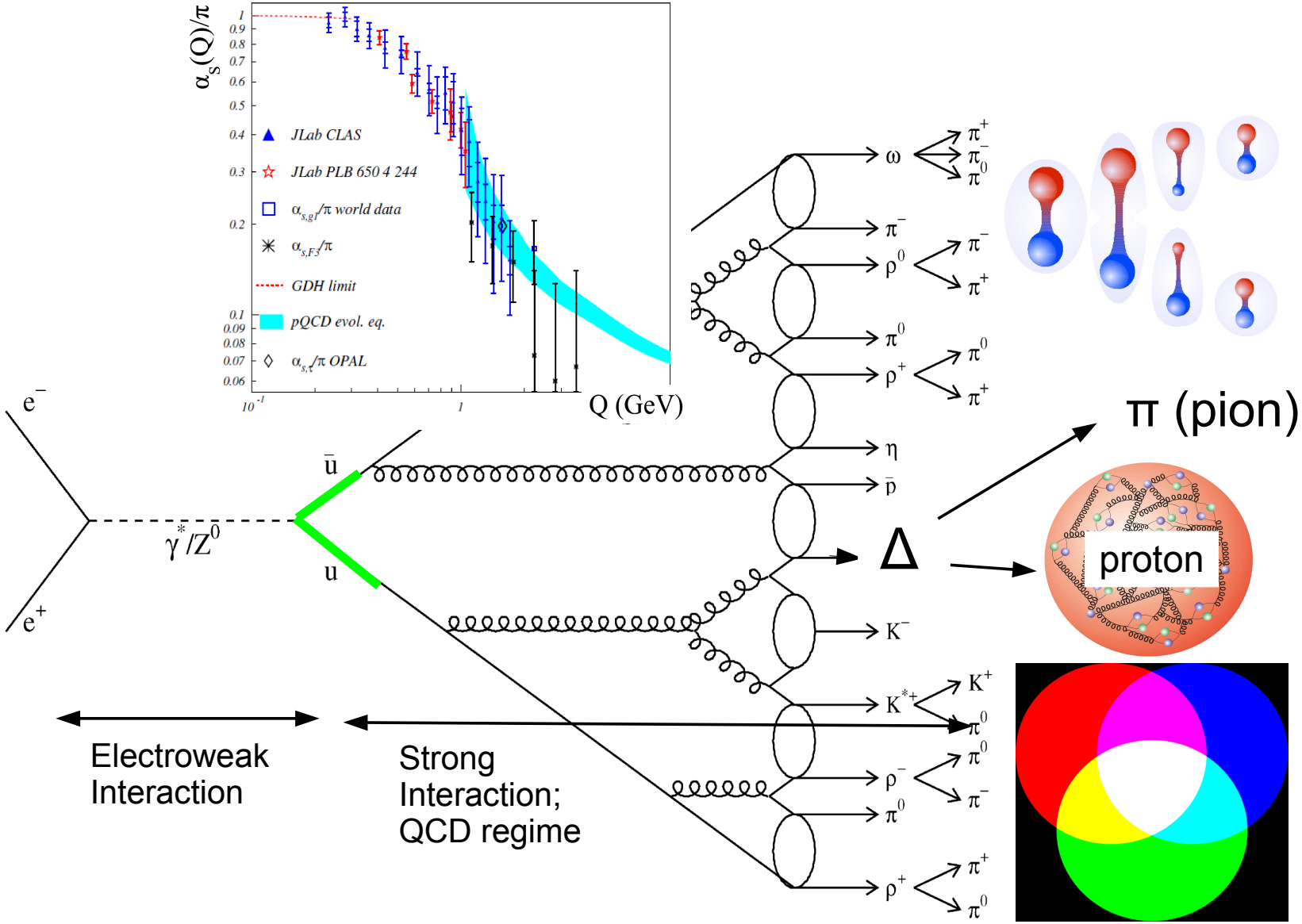

The intermediate energy region...

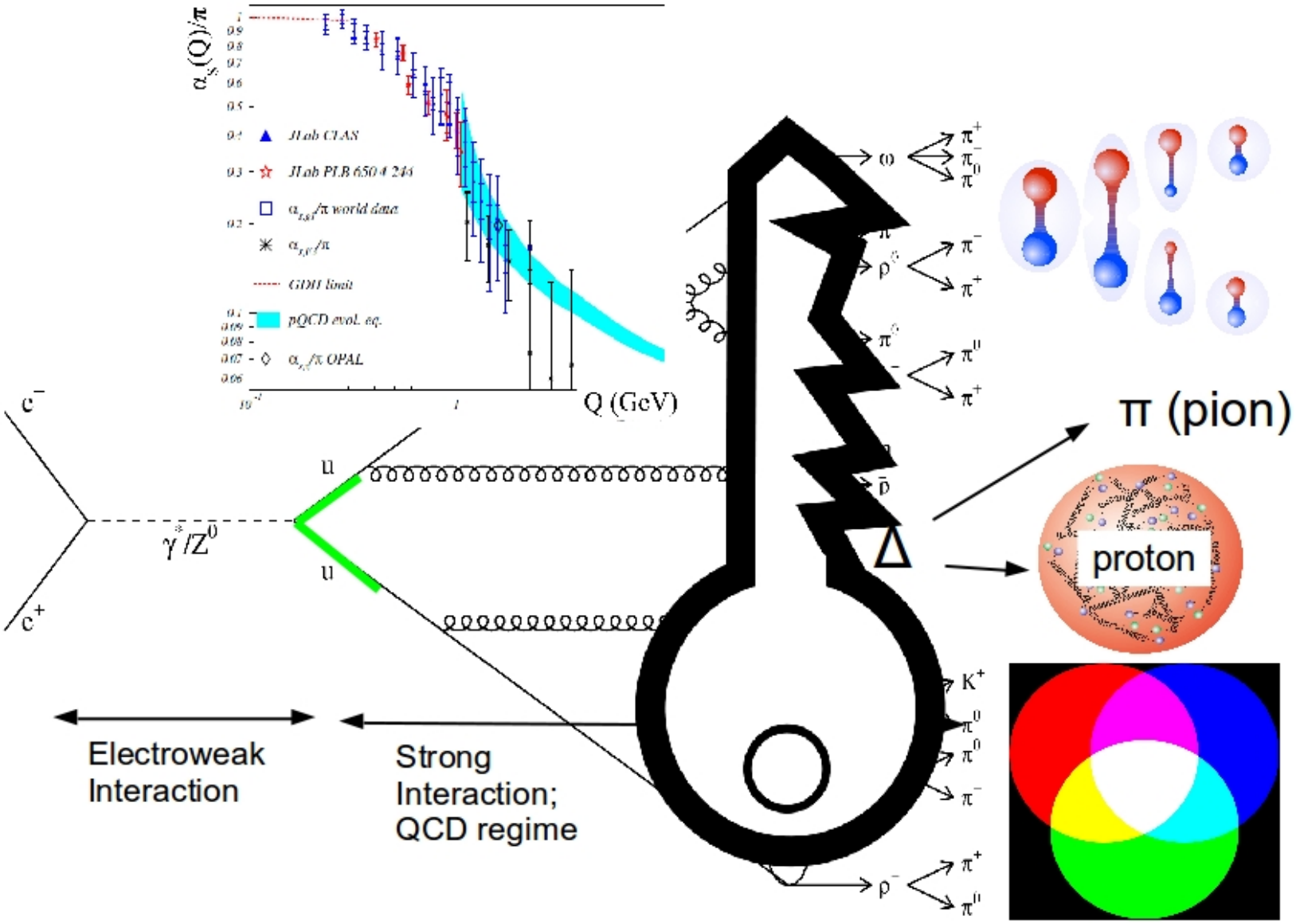

...provides a key to our understanding of QCD.

Outline

- How can ab-initio QCD predictions be matched to the rich phenomenology of excited baryons?
- Are there explicit experimental signatures of gluon dynamics at intermediate energies? Do exotics exist?

- Analysis of excited baryons
- Analysis of excited mesons
- Analysis of lattice data

The baryon spectrum: N^* and Δ resonances

- Many resonances predicted in lattice calculations — Missing resonance problem from quark model reappears [Edwards *et al.*, Phys.Rev. D84 (2011)]:

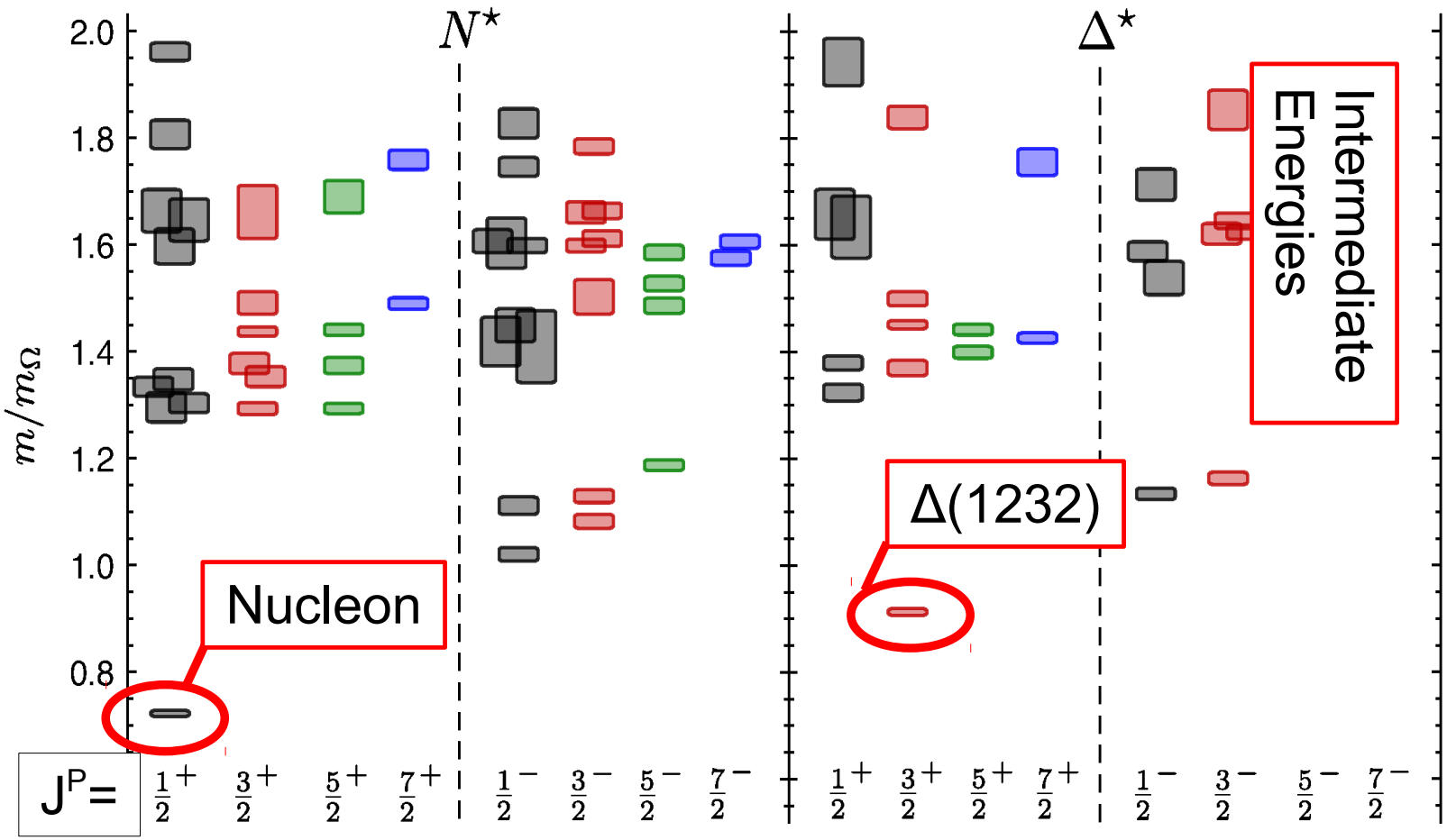

$m_\pi = 396 MeV$ (!)

- Search for these states in dedicated experimental programs

Photoproduction experiments: Jefferson Lab, MAMI, ELSA,...

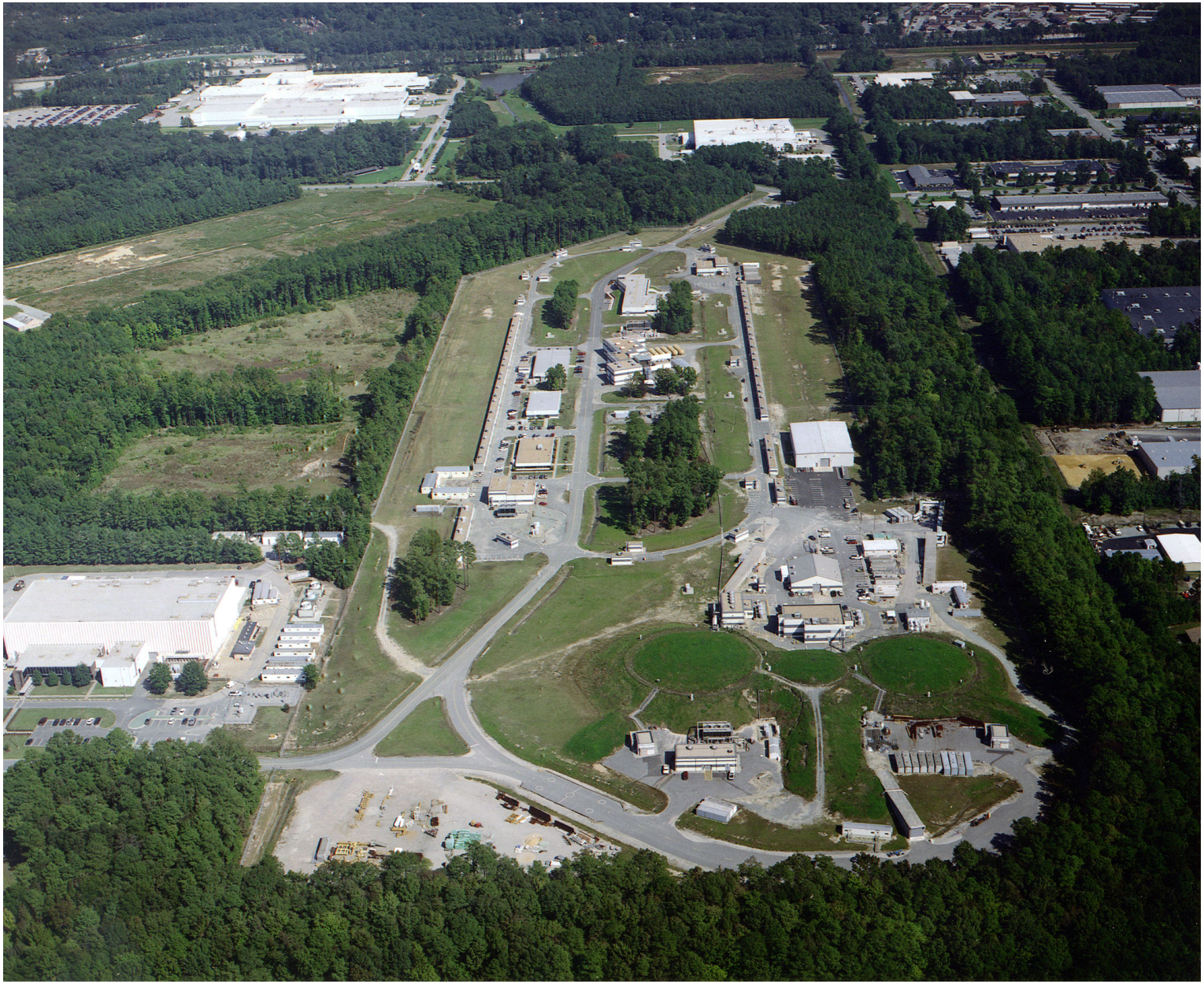

Photoproduction cross sections

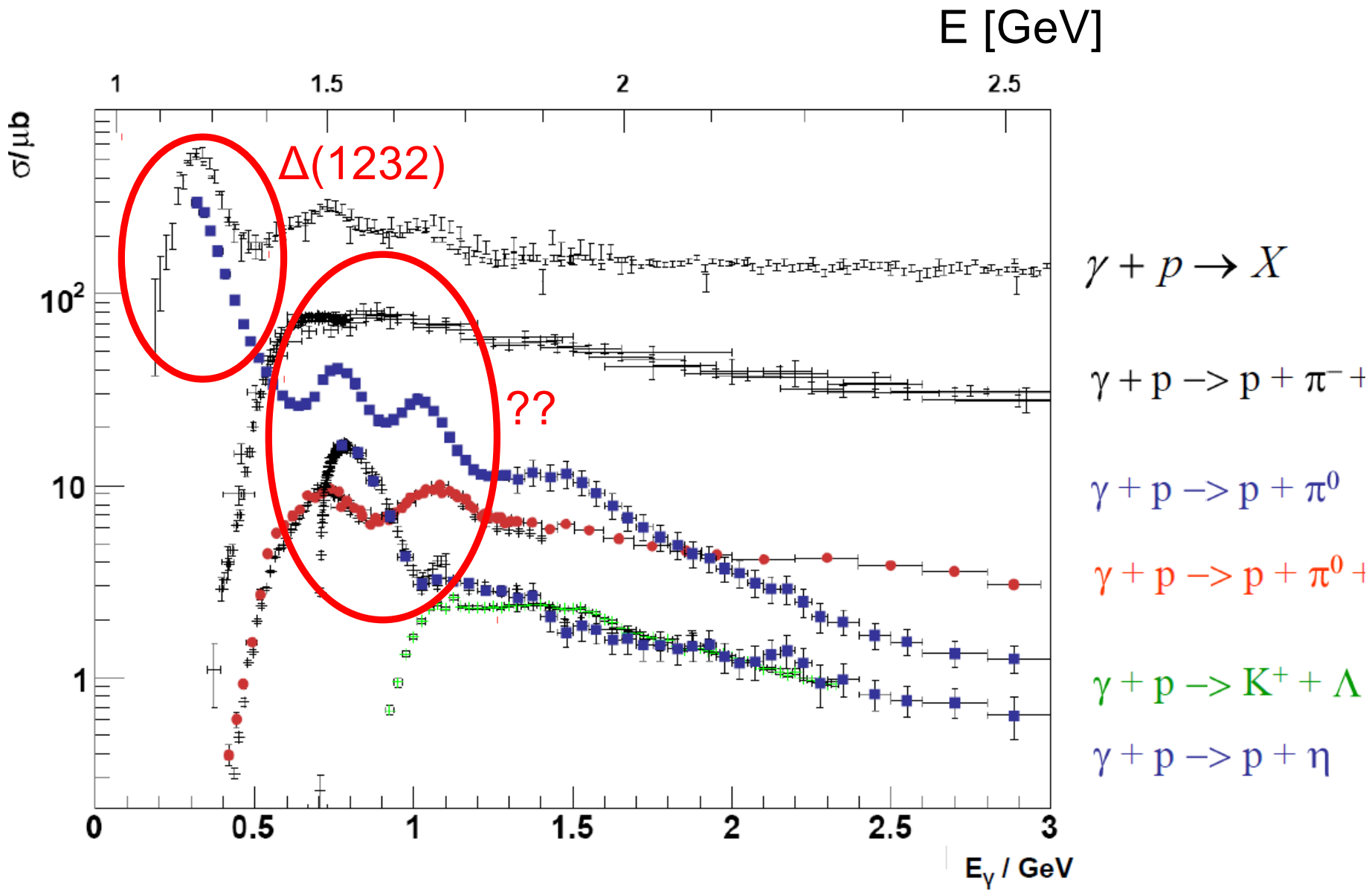

[data: JLab, ELSA, MAMI]

Multipole/PW analysis required

Principles for scattering: 2-body unitarity

$$\mathrm{Im}\, T^{-1} = \sigma, \quad \sigma \sim p_{\mathrm{cms}} \sim \sqrt{z - (m + M)}$$

$\rightarrow$ One branchpoint at $z = m + M$, one cut, two Riemann sheets.

Implementation:

- K-matrix: $T = K - i\, K\, \sigma\, T$
- On-shell: $T = V + V\, G\, T$, Re $G \neq 0$, e.g., from dispersion relation.
- Off-shell: $\boxed{T(q'', q') = V(q'', q') + \int dq\, V(q'', q)\, g(q)\, T(q, q')}$

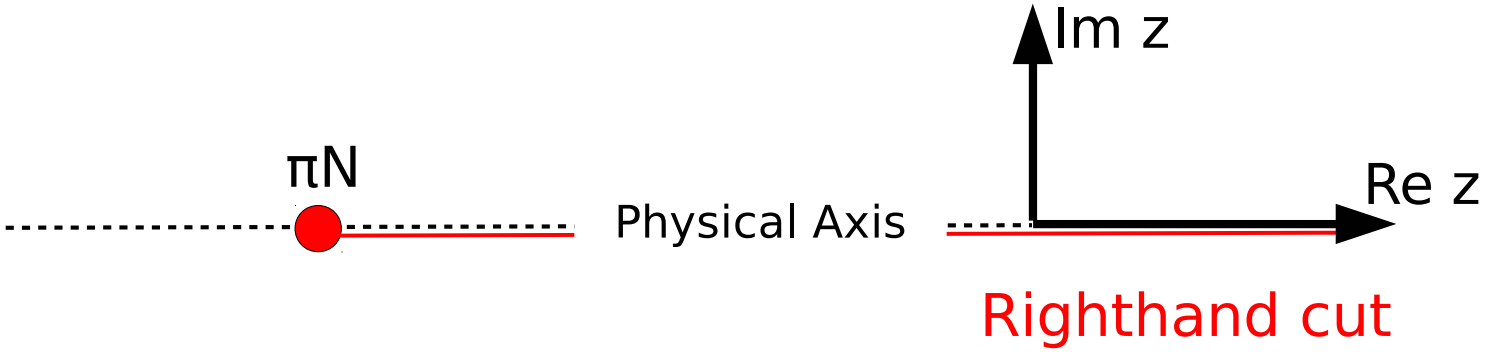
πN
Physical Axis
Im z
Re z
Righthand cut

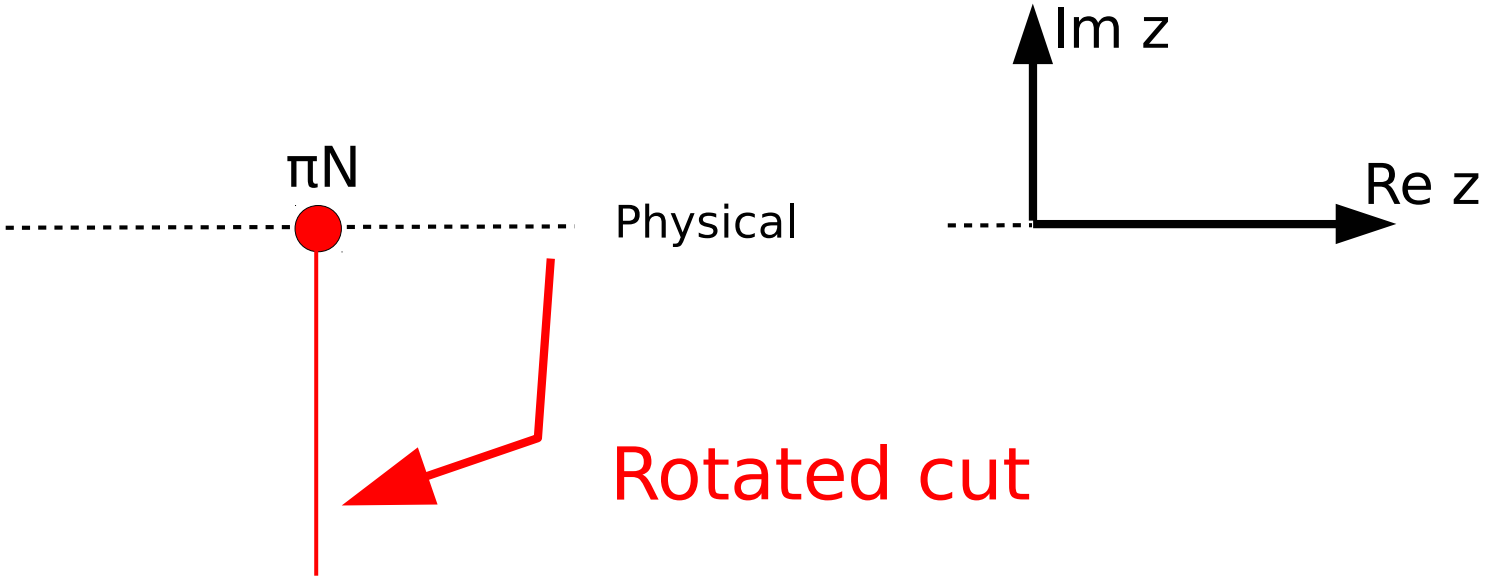
πN
Physical
Im z
Re z
Rotated cut

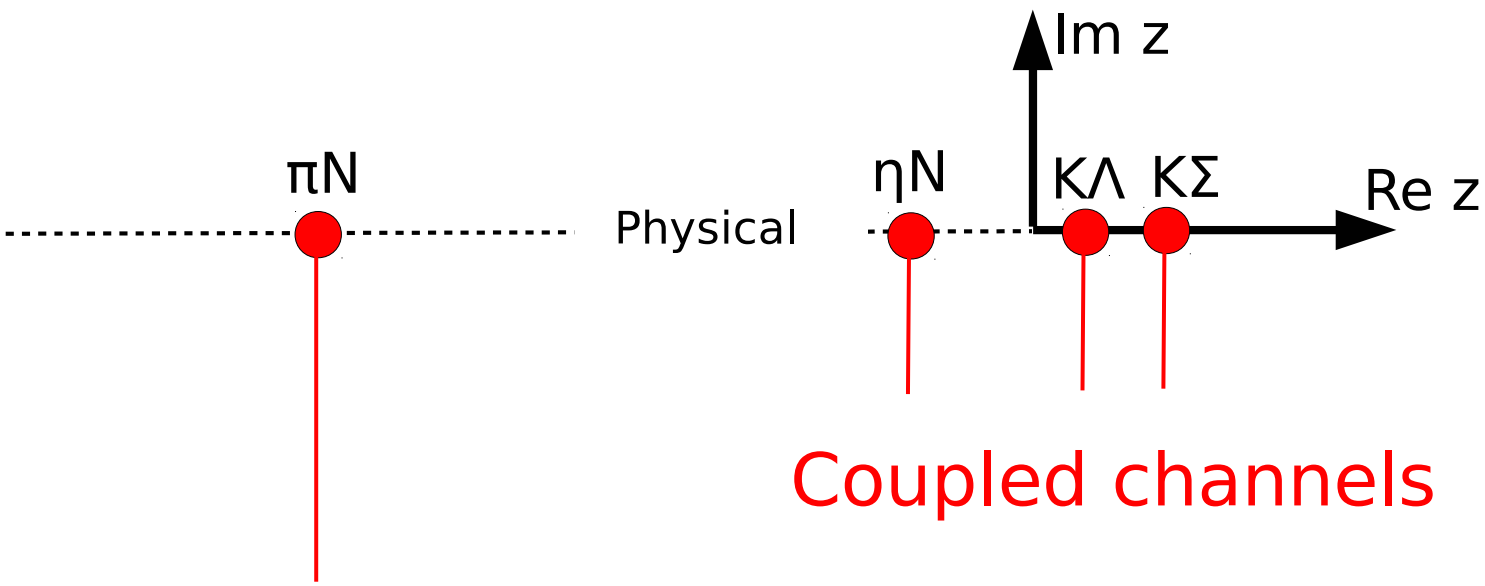

Coupled channels

Three-particle intermediate states

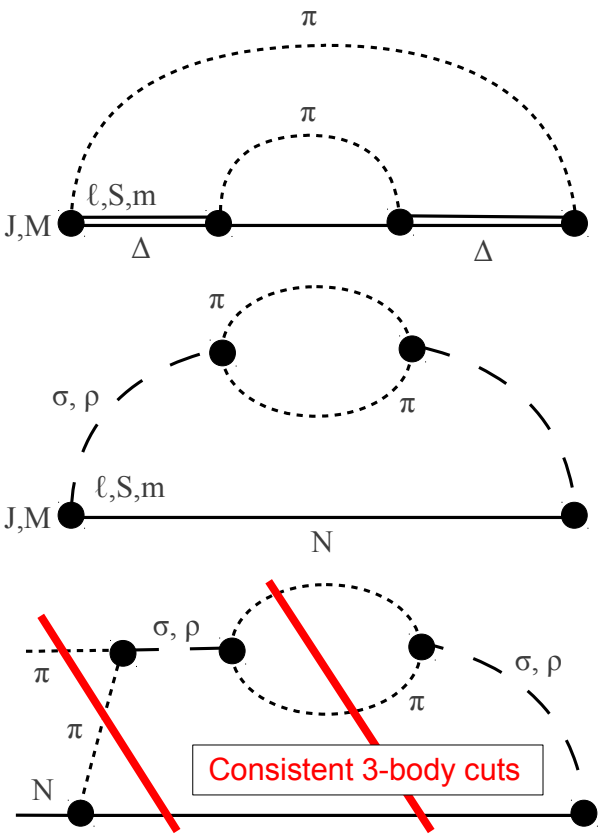

- Known large inelasticities $\pi\pi N$ [$\pi\Delta$, σN, ρN,...]
- $\pi\pi/\pi N$ boosted subsystems constructed to fit the respective phase shifts.
- Is it enough to include (boosted) 2-particle subsystems in the propagator? No.
- Three-body s-channel dynamics requires meson exchange transitions. $\Rightarrow$ Three-body unitarity (also applicable for meson analysis).

  [Aaron, Almado, Young, PR 174 (1968) 2022, Aitchison, Brehm, PLB 84 (1979) 349, PRD 25 (1982) 3069,...]

Consequence: Threshold openings in the complex plane

Existence shown model-independently in [S. Ceci, M.D., C. Hanhart *et. al.*, PRC 84 (2011)]

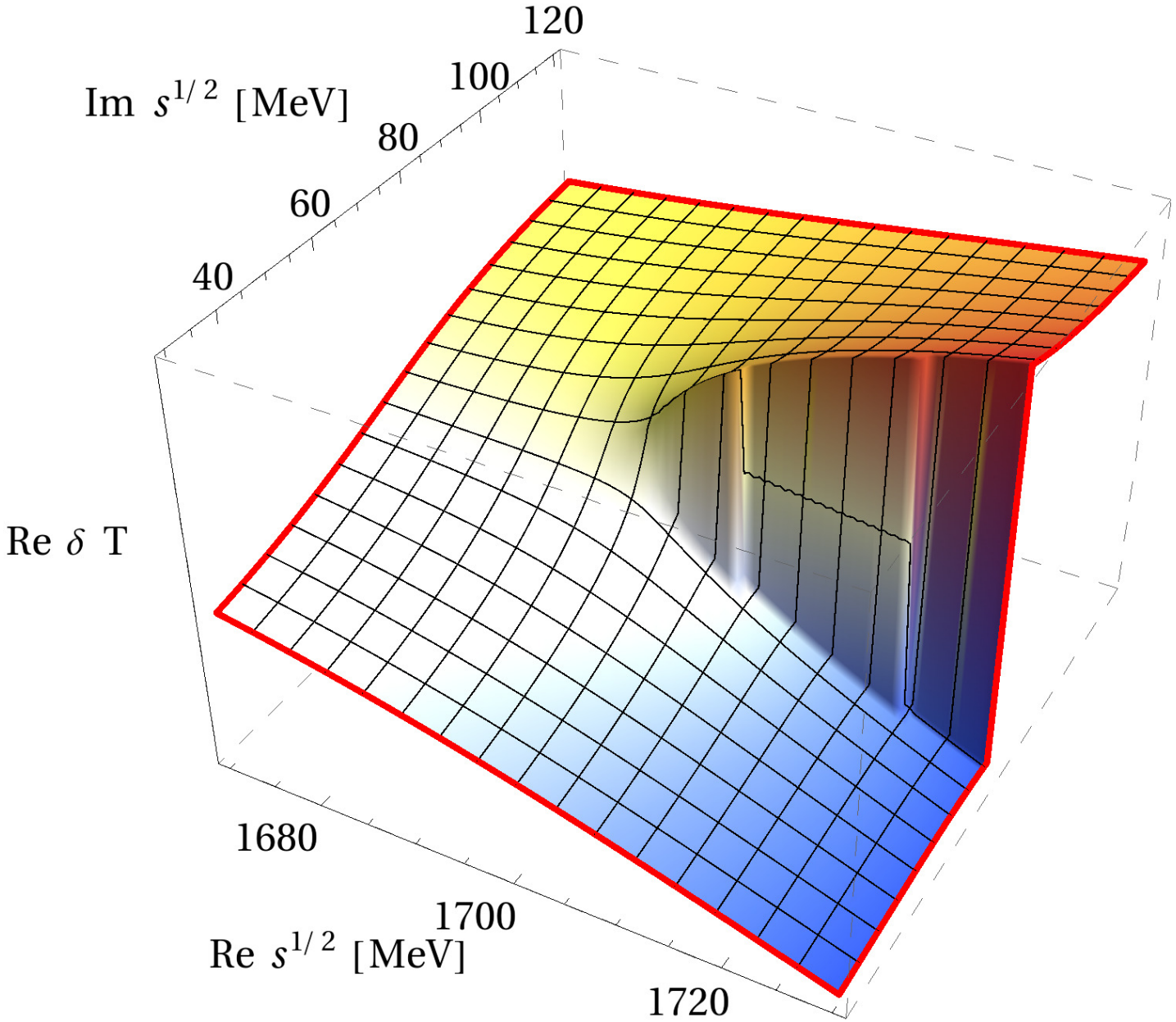

Further consequences

[S. Ceci, M.D., C. Hanhart *et. al.*, PRC 84 (2011)]

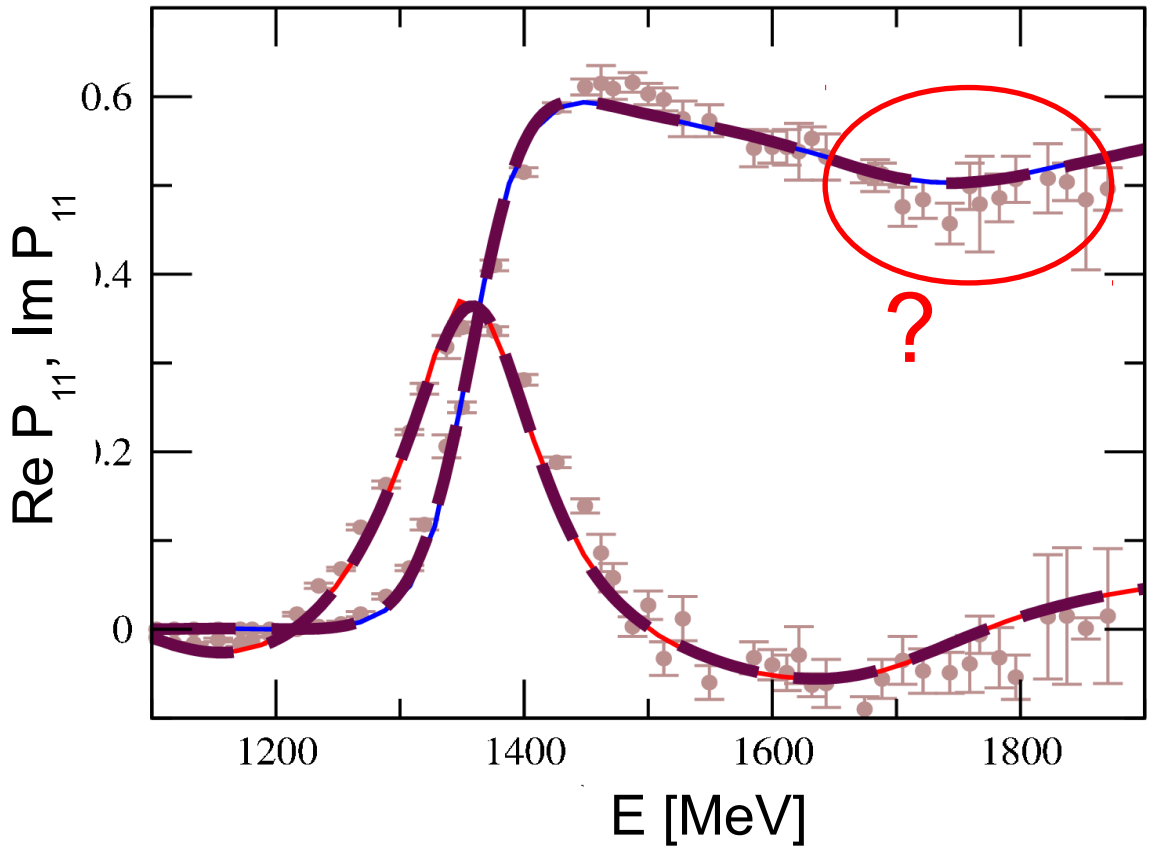

Amplitude **A** with complex ρN branchpoint at E= 1700 - i 70 MeV

Fit to **A** using model **B** <u>without</u> this branchpoint

→ **B** needs fake resonance at E= 1700 - i 130 MeV

→ Erroneous resonance signal induced by wrong analytic structure

Definitely. . .

. . . the wrong analytic structure.

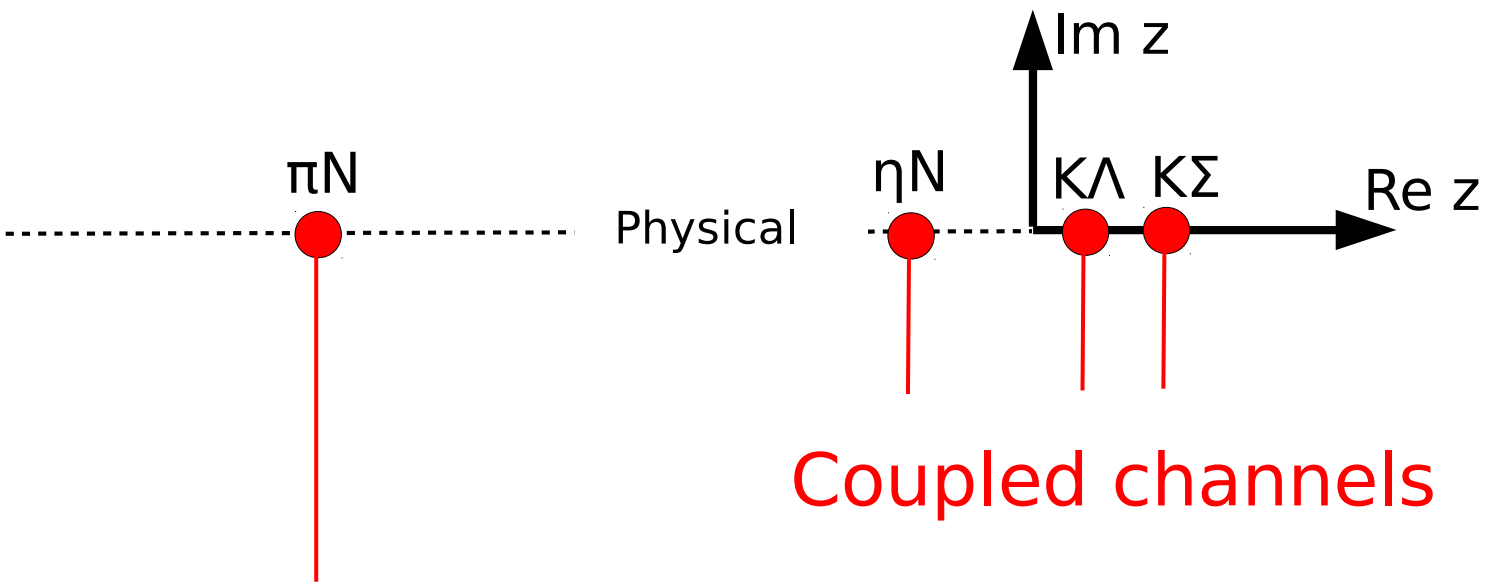

Coupled channels

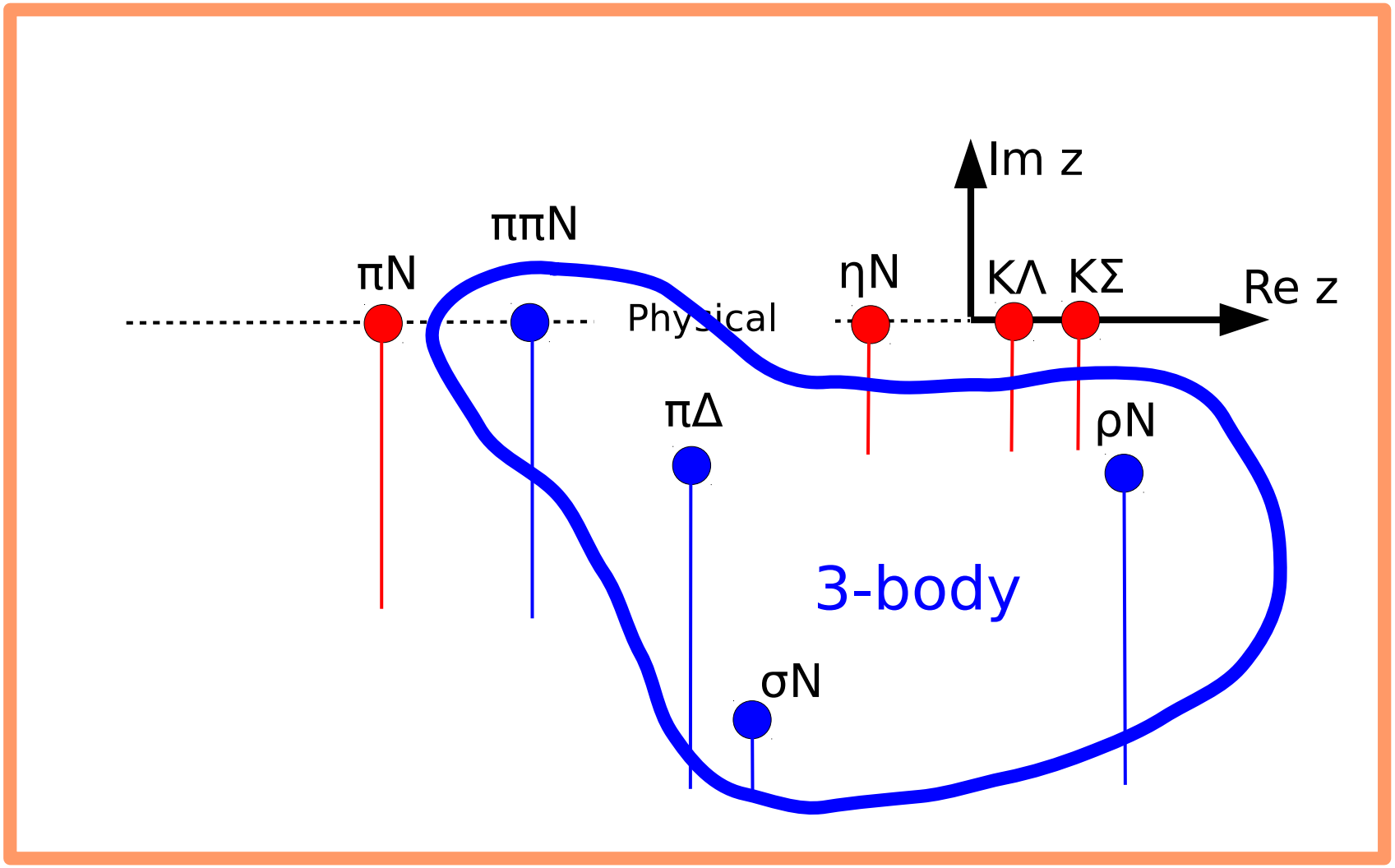
Im z
ππN
πN
ηN
KΛ
KΣ
Re z
Physical
πΔ
ρN
3-body
σN

Left-hand, short nucleon and circular cut

- Circular cut: Induced by partial wave projection, NOT present in the amplitude in plane-wave basis.

$$V_u = \int_{-1}^{1} dx \, \frac{P_\ell(x)}{u - m_N^2 + i\epsilon}, \quad V_t = \int_{-1}^{1} dx \, \frac{P_\ell}{t - m_t^2 + i\epsilon}$$

Branch points given where integration border hits pole:

$$m_N^2 - u|_{x=\pm 1} = 0, \quad u = (p_\pi^f - p_N^i)^2$$

$\rightarrow$ u-channel exchanges to obtain and approximate left-hand & other cuts

- (Excited) t- and u-channel exchanges relate all partial waves and, at the same time, provide the background of s-channel resonances.

Approximations of crossing symmetry

at the level of the potential (not the amplitude)

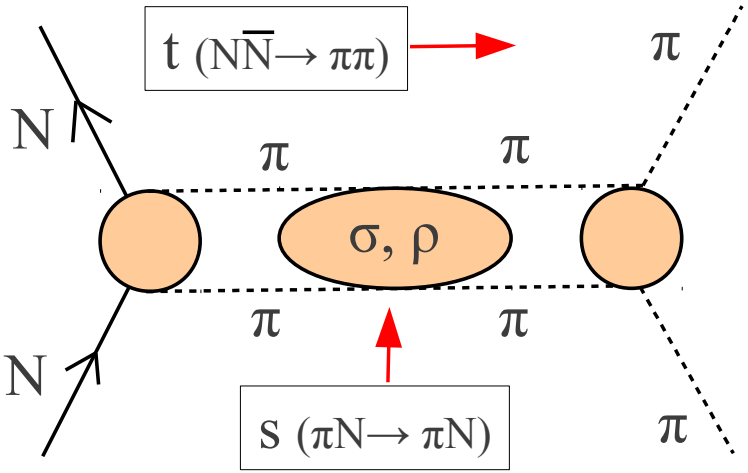

- For $\sigma(600)$ and $\rho(770)$ quantum numbers: πN t-channel interaction from $\bar{N}N \to \pi\pi$ (analytically continued) data.
- Use of crossing symmetry and dispersion techniques [Schütz *et al.* PRC 49 (1994) 2671].

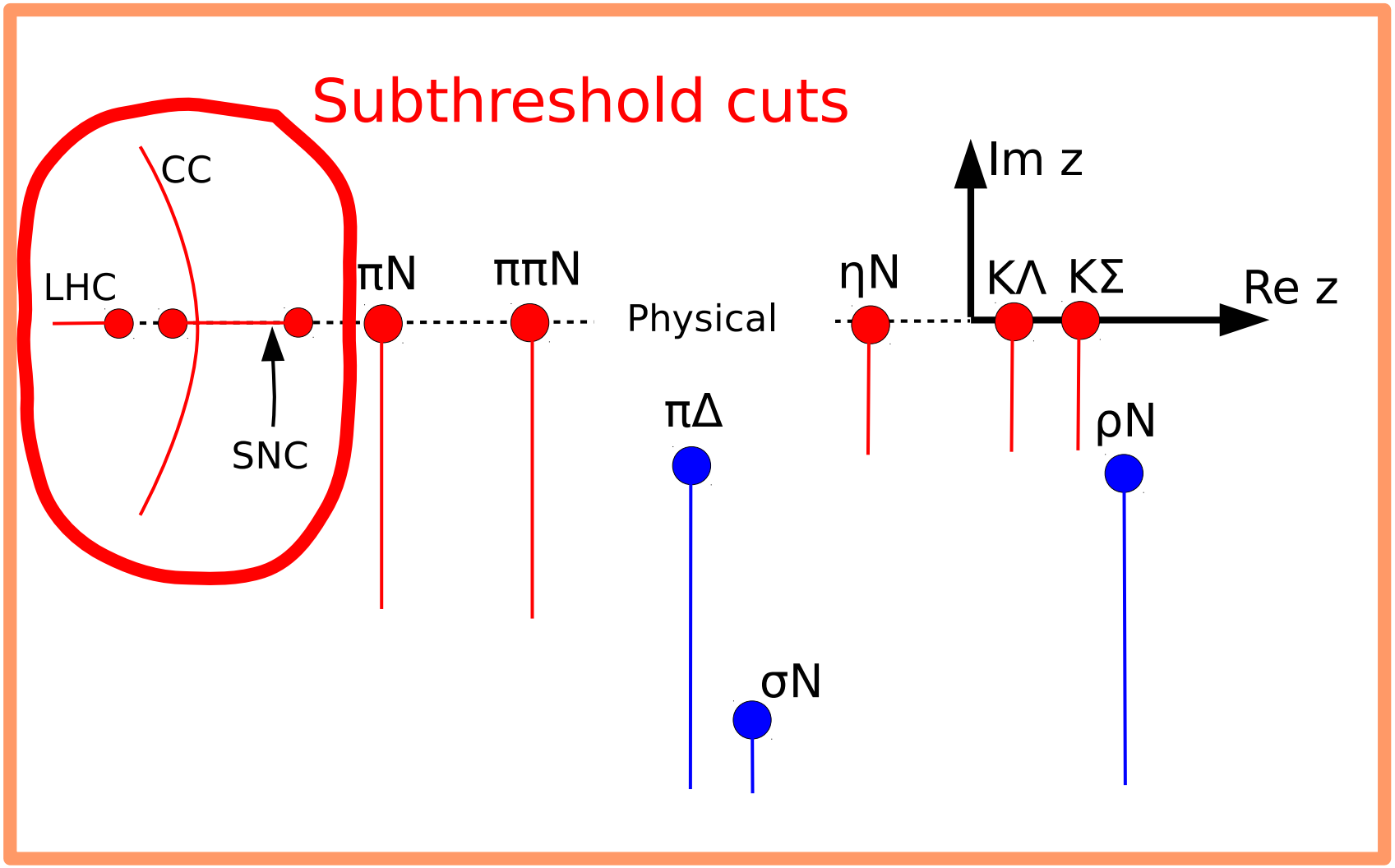
Subthreshold cuts
CC
LHC
SNC
πN
ππN
Physical
ηN
KΛ
KΣ
Im z
Re z
πΔ
σN
ρN

The scattering equation

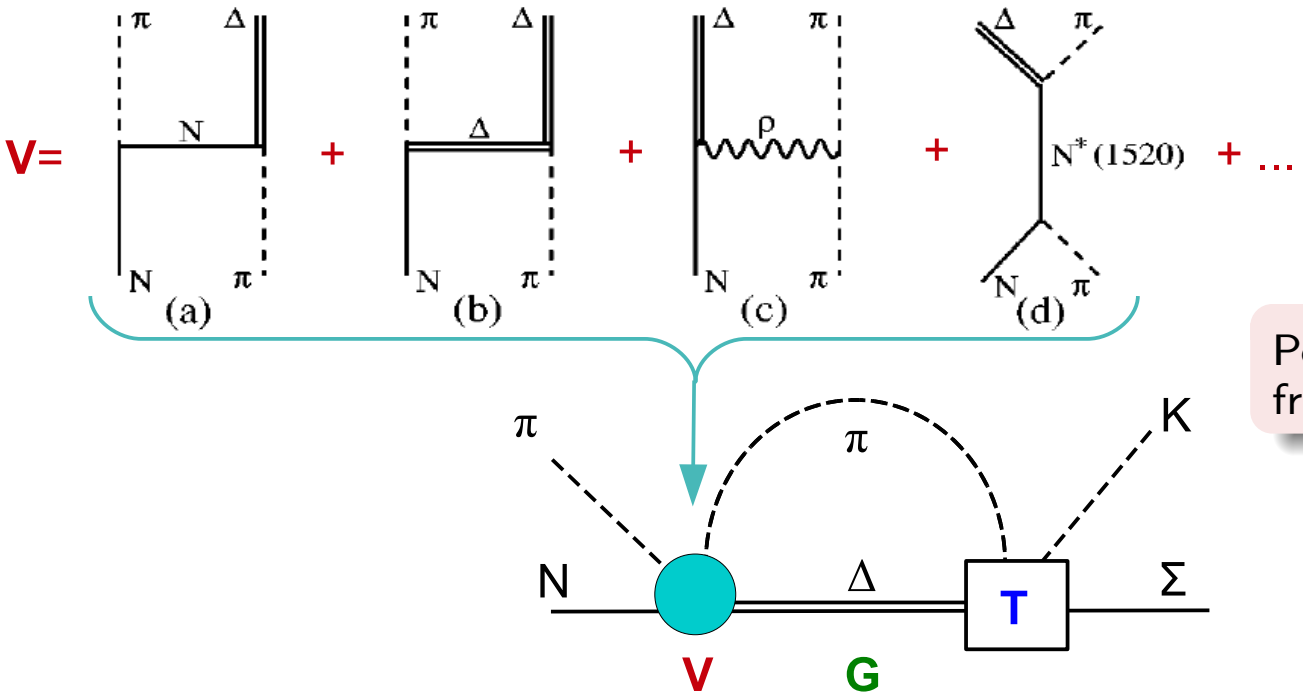

Potentials V constructed from Wess-Zumino $\mathcal{L}$

$$T^I_{\mu\nu}(\vec{k}',\lambda',\vec{k},\lambda) = V^I_{\mu\nu}(\vec{k}',\lambda',\vec{k},\lambda) + \sum_{\gamma,\lambda''}\int d^3q\, V^I_{\mu\gamma}(\vec{k}',\lambda',\vec{q},\lambda'')\frac{1}{Z-E_\gamma(q)+i\epsilon}\,T^I_{\gamma\nu}(\vec{q},\lambda'',\vec{k},\lambda)$$

Data base

Analysis of the world data base on ηN, $K\Lambda$, $K\Sigma$

	PWA	σ_{tot}	$\frac{d\sigma}{d\Omega}$	P	β
$\pi N \to \pi N$	GWU/SAID 2006 up to J=9/2				
$\pi^- p \to \eta n$		62 data points	38 energy points E=1489 to 2235 MeV	12 energy points 1740 to 2235 MeV	
$\pi^- p \to K^0 \Lambda$		66 data points	46 energy points 1626 to 1405 MeV	27 energy points 1633 to 2208 MeV	7 energy points 1852 to 2262 MeV
$\pi^- p \to K^0 \Sigma^0$		16 data points	29 energy points 1694 to 2405 MeV	19 energy points 1694 to 2316 MeV	
$\pi^- p \to K^+ \Sigma^-$		14 data points	15 energy points 1739 to 2405 MeV		
$\pi^+ p \to K^+ \Sigma^+$		18 data points	32 energy points 1729 to 2318 MeV	32 energy points 1729 to 2318 MeV	2 energy pionts 2021 and 2107 MeV

$\sim$ 6000 data points

plus $\sim$ 2000 data points for photoproduction:
differential cross section and spin asymmetry for

$$\gamma p \to \pi^+ n,\ \gamma p \to \pi^0 p,\ \gamma n \to \pi^- p,\ \gamma n \to \pi^0 n$$

$\pi N \to \pi N$: Partial wave amplitudes I=1/2 PWA data: SAID [Phys.Rev. C 74 (2006)]

[Rönchen, M.D. *et al.*, arXiV: 1211.6998, accepted for publication in EPJA]

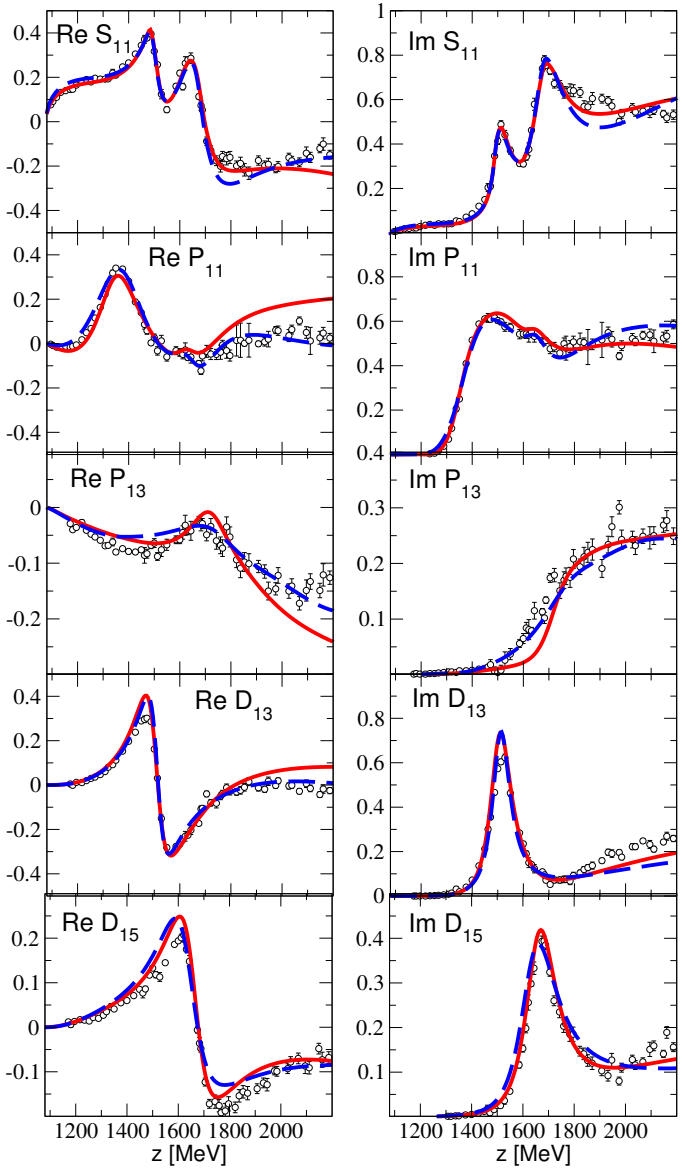

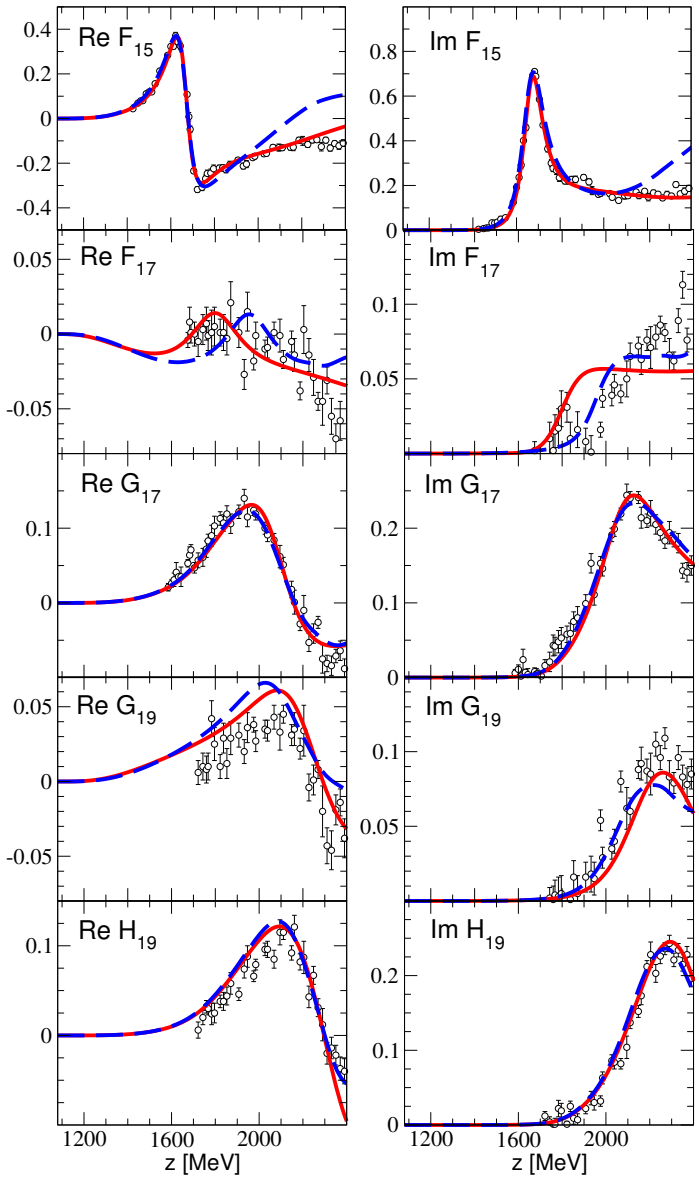

$\pi N \to \pi N$: Partial wave amplitudes I=3/2

[Rönchen, M.D. *et al.*, arXiV: 1211.6998, accepted for publication in EPJA]

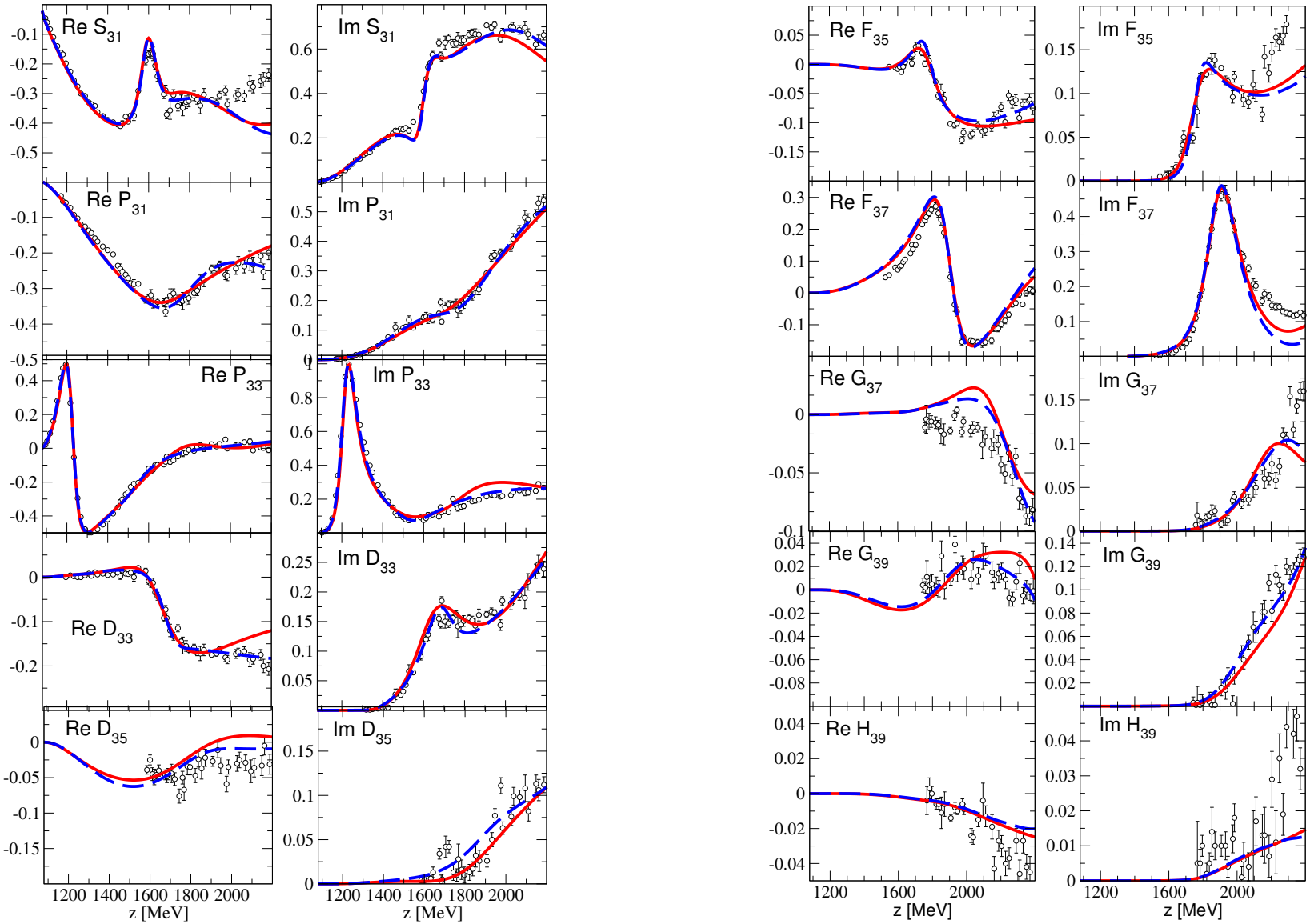

Selected results for $\pi^- p \to K^0 \Lambda$

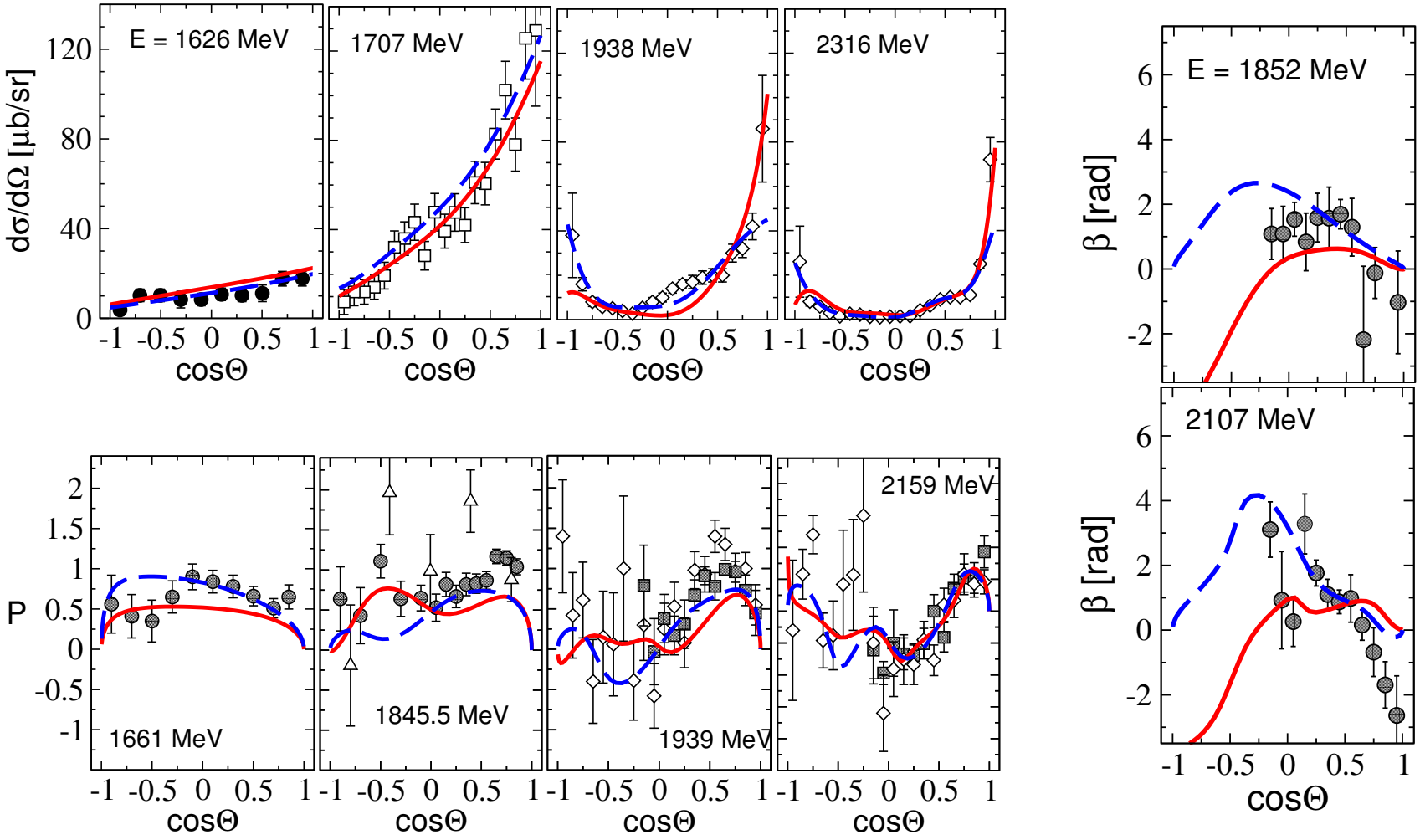

This is a complete experiment

in the sense that it fixes the amplitude up to one energy-dependent, overall phase.

$\pi^- p \to K^0 \Lambda$: Total cross section

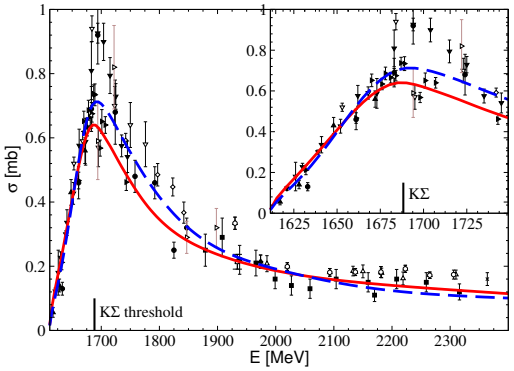

Result: Partial wave content.

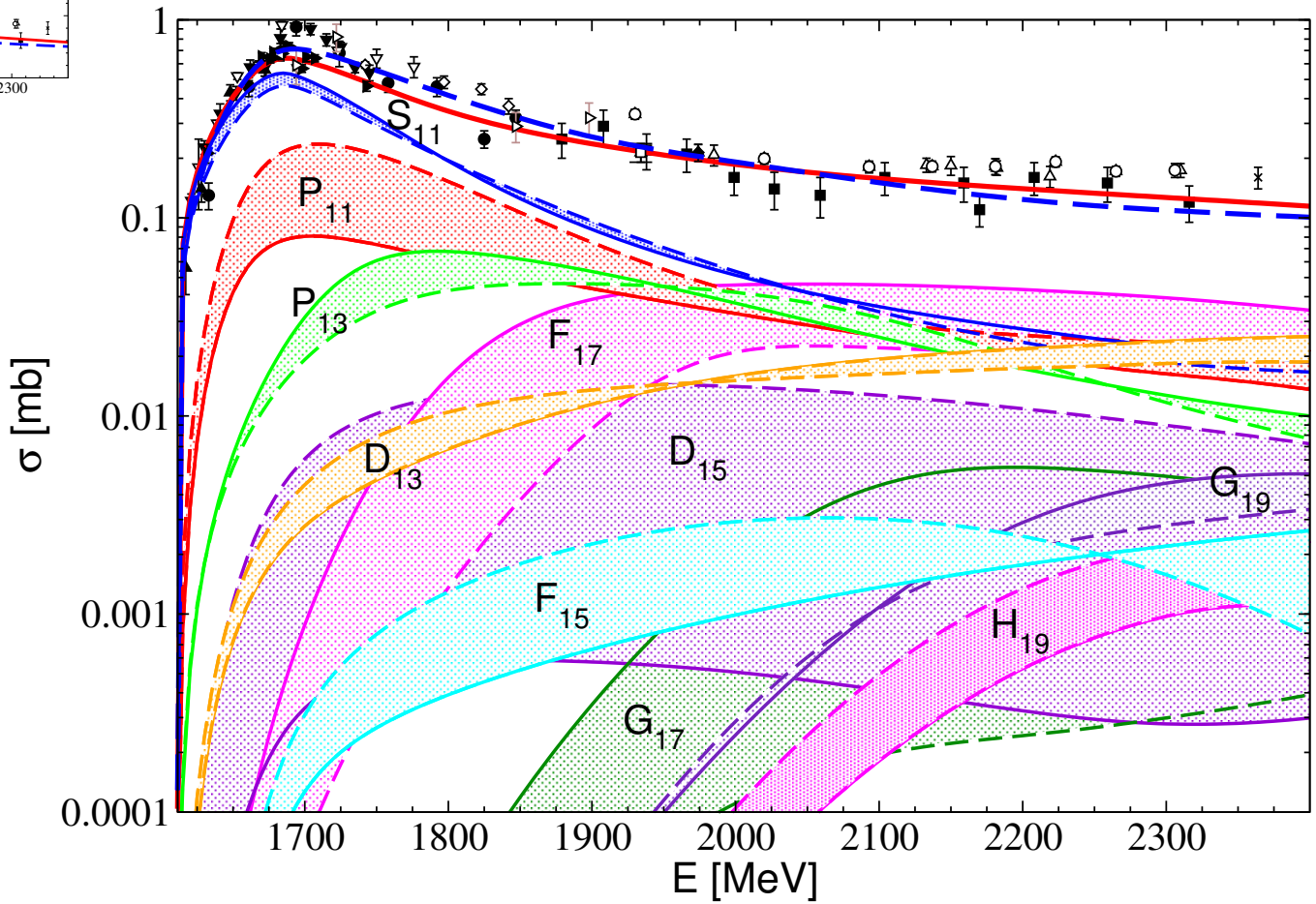

The P_{11} partial wave

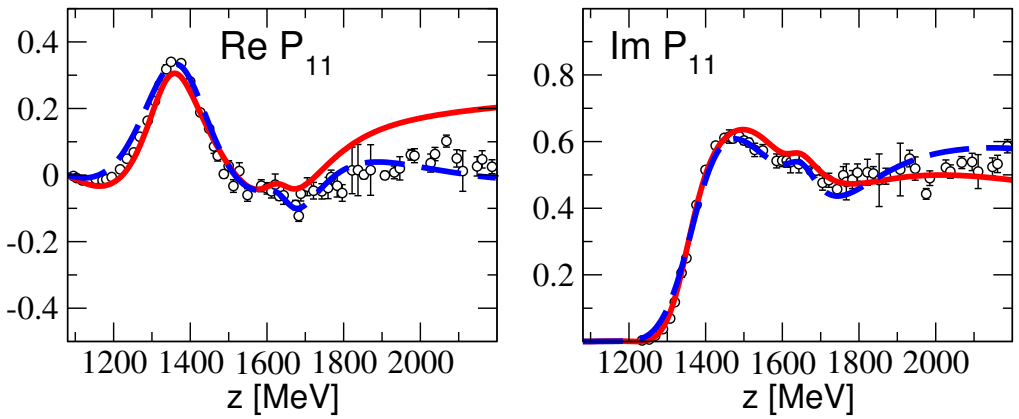

Nucleon
Dynamical Roper $P_{11}(1440)$
Genuine $P_{11}(1710)$
(Dynamical $P_{11}(1750)$)

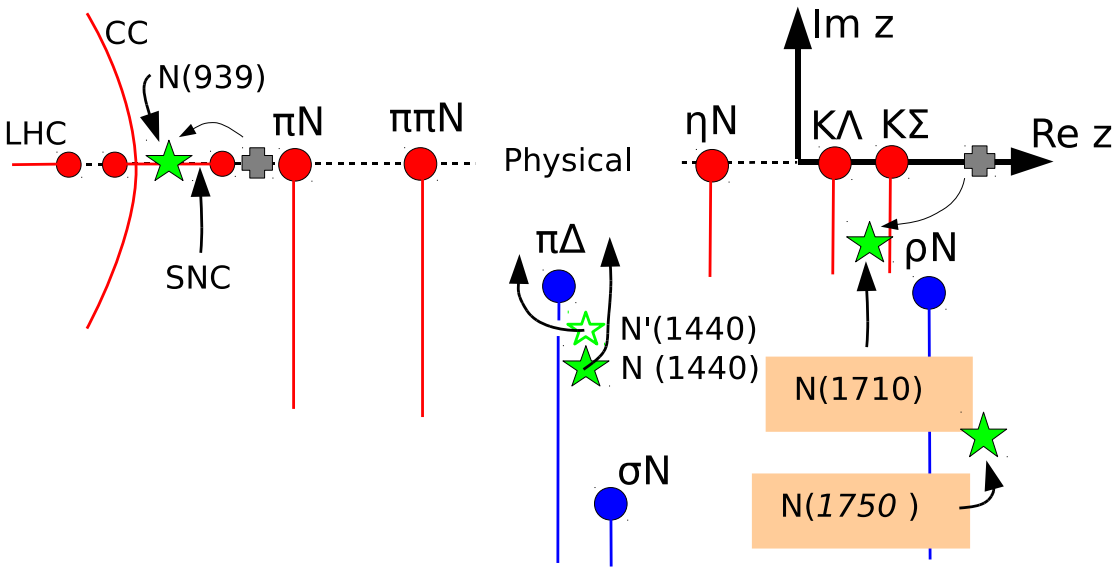

The P_{11} partial wave

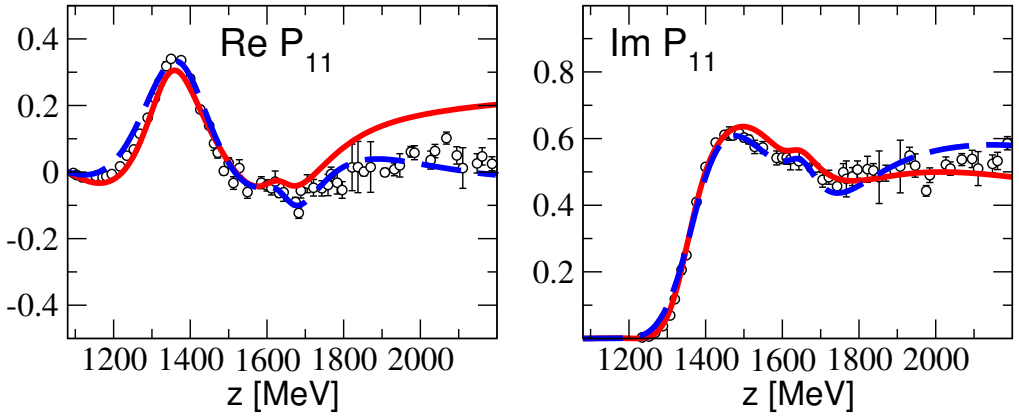

Nucleon
Dynamical Roper $P_{11}(1440)$
Genuine $P_{11}(1710)$
(Dynamical $P_{11}(1750)$)

Genuine $P_{11}(1710)$:

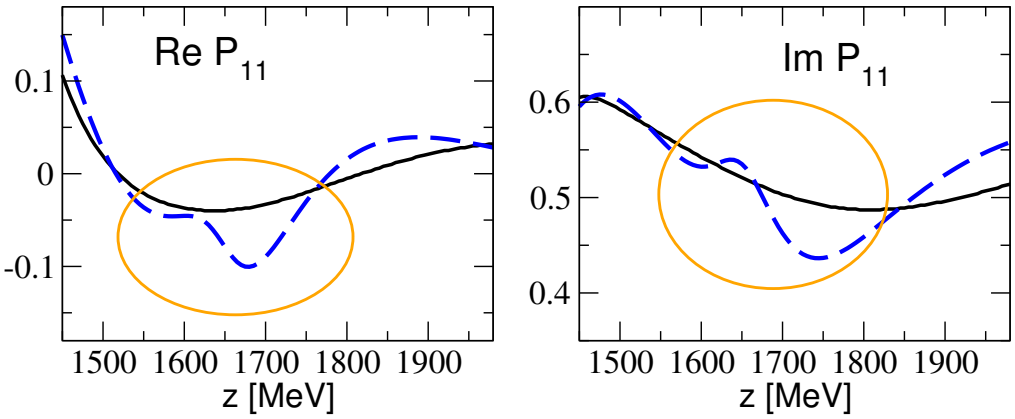

- Input for our fit (blue dashed): energy-dependent SAID solution (black solid)
- Inclusion of $P_{11}(1710)$ necessary from $K\Lambda$ data

The P_{11} partial wave

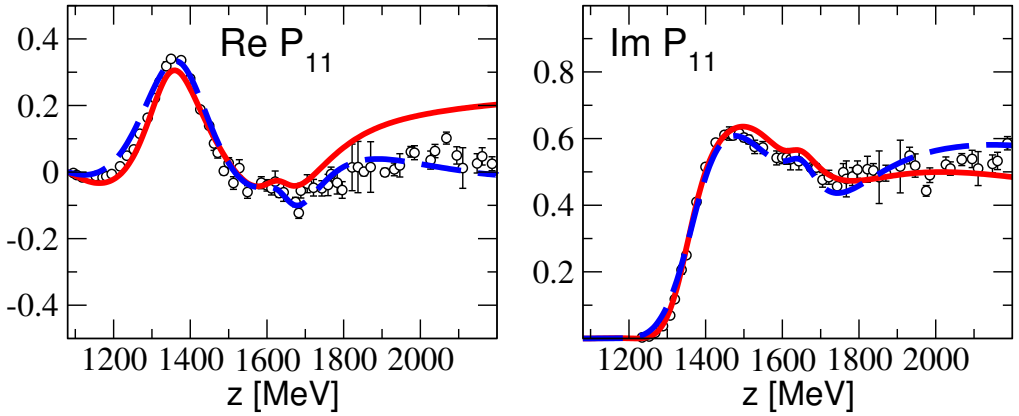

Nucleon
Dynamical Roper $P_{11}(1440)$
Genuine $P_{11}(1710)$
(Dynamical $P_{11}(1750)$)

Genuine $P_{11}(1710)$:

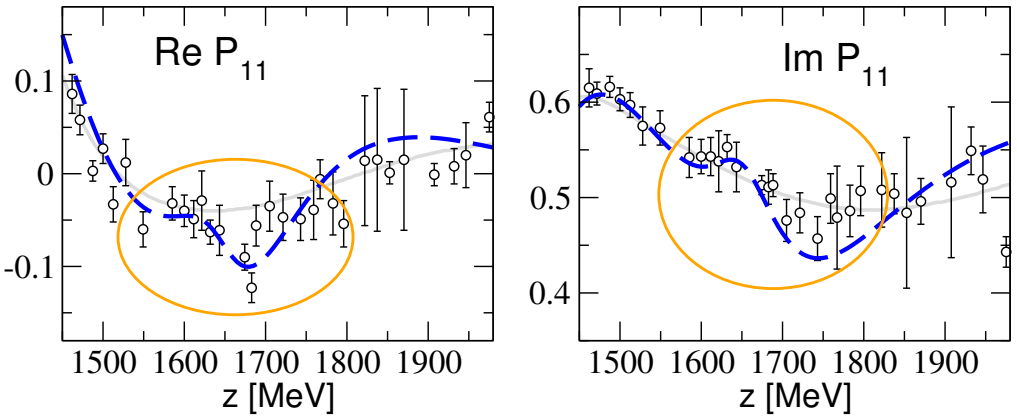

- Input for our fit (blue dashed): energy-dependent SAID solution (black solid)
- Inclusion of $P_{11}(1710)$ necessary from $K\Lambda$ data
- But: Our solution matches single-energy solution ("data" points)

- Coupled-channel dynamics at work

Gauge invariance for photoproduction

Haberzettl, PRC56 (1997), Haberzettl, Nakayama, Krewald, PRC74 (2006)

Gauge invariance: Generalized Ward-Takahashi identity (WTI)

$$k_\mu M^\mu = -|F_s\tau\rangle S_{p+k} Q_i S_p^{-1} + S_{p'}^{-1} Q_f S_{p'-k} |F_u\tau\rangle + \Delta^{-1}_{p-p'+k} Q_{pi} \Delta_{p-p'} |F_t\tau\rangle$$

Photoproduction amplitude:

$$M^\mu = \underbrace{M_s^\mu + M_u^\mu + M_t^\mu}_{\gamma \text{ to external legs}} + \underbrace{M_{int}^\mu}_{\gamma \text{ inside hadronic vertex}}$$

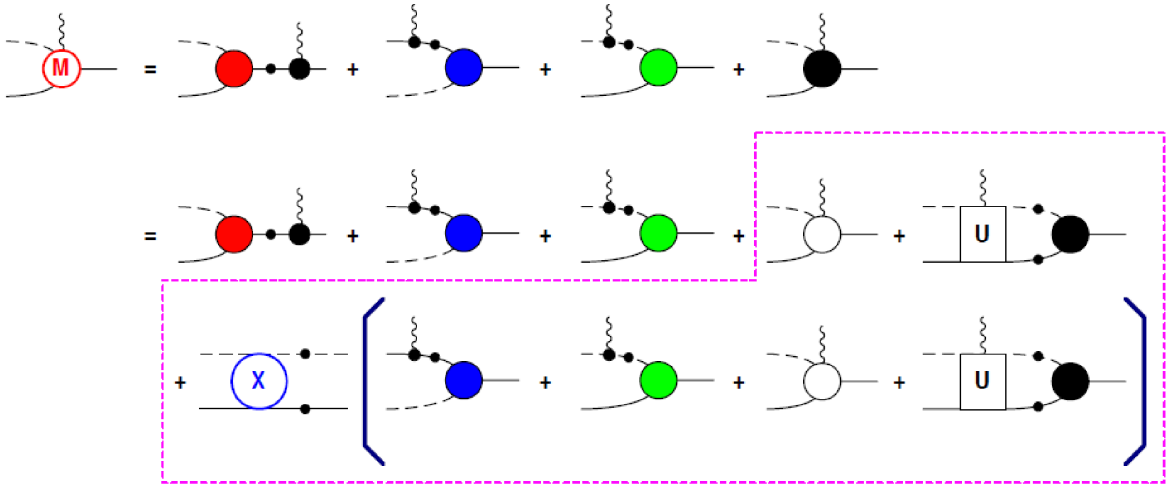

Strategy: Replace 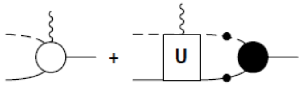

by phenomenological contact term such that the generalized WTI is satisfied

The importance of Gauge Invariance

[Huang, M.D., Haberzettl, Haidenbauer, Hanhart, Krewald, Meißner, Nakayama, PRC 85 (2011)]

[data: GWINS/DAC data base; JLab, ELSA, MAMI]

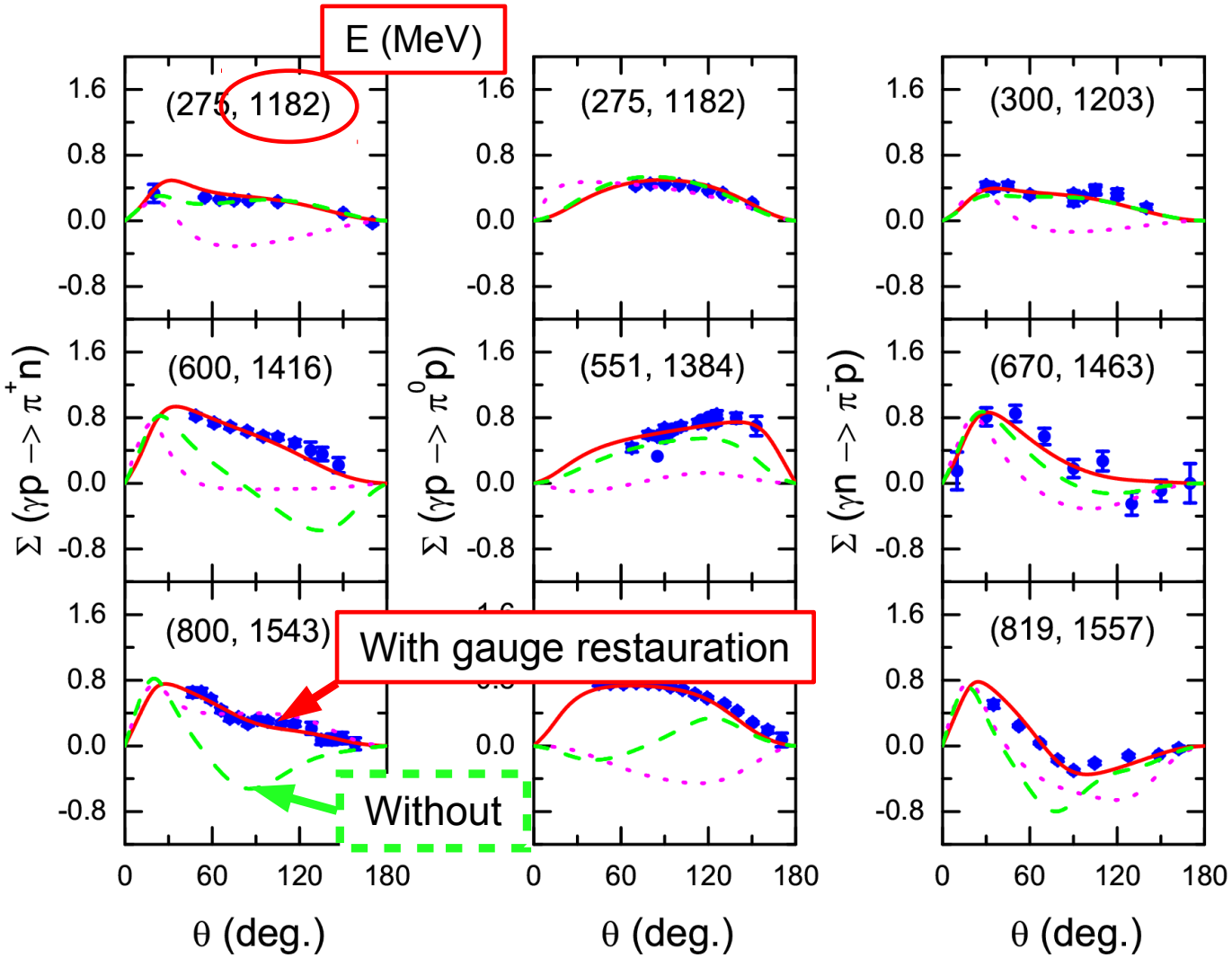

Pion photoproduction: $d\sigma/d\Omega$ and Σ_γ for $\gamma p \to \pi^+ n$

F. Huang, M. Döring, K. Nakayama *et al.*, Phys. Rev. C85 (2012) 054003

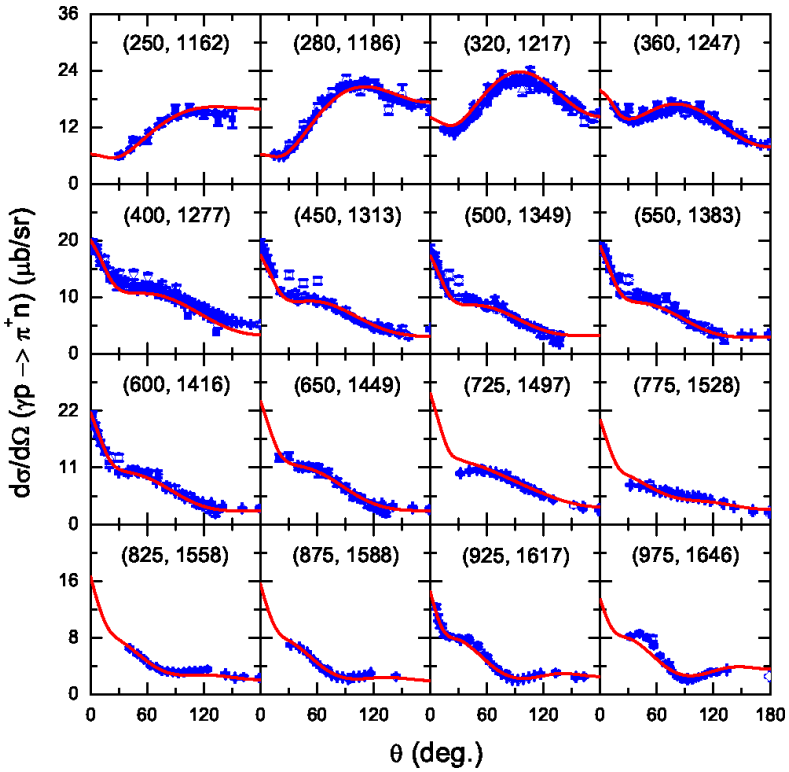

Differential cross section for $\gamma p \to \pi^+ n$

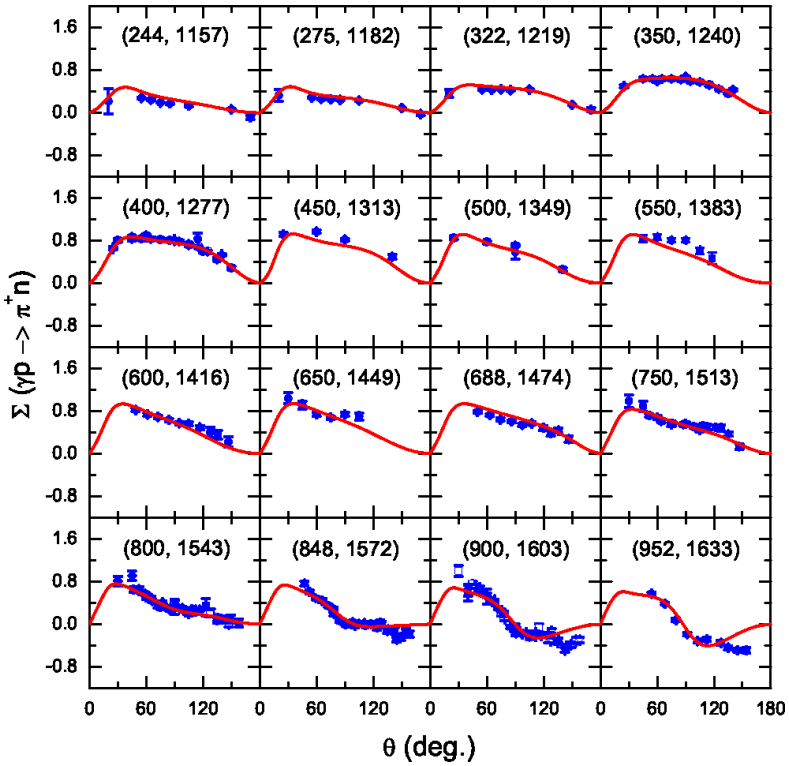

Photon spin asymmetry for $\gamma p \to \pi^+ n$

Data: CNS Data analysis center [CBELSA/TAPS, JLAB, MAMI,...]

Pion photoproduction: $d\sigma/d\Omega$ and Σ_γ for $\gamma n \to \pi^- p$

F. Huang, M. Döring, K. Nakayama *et al.*, Phys. Rev. C85 (2012) 054003

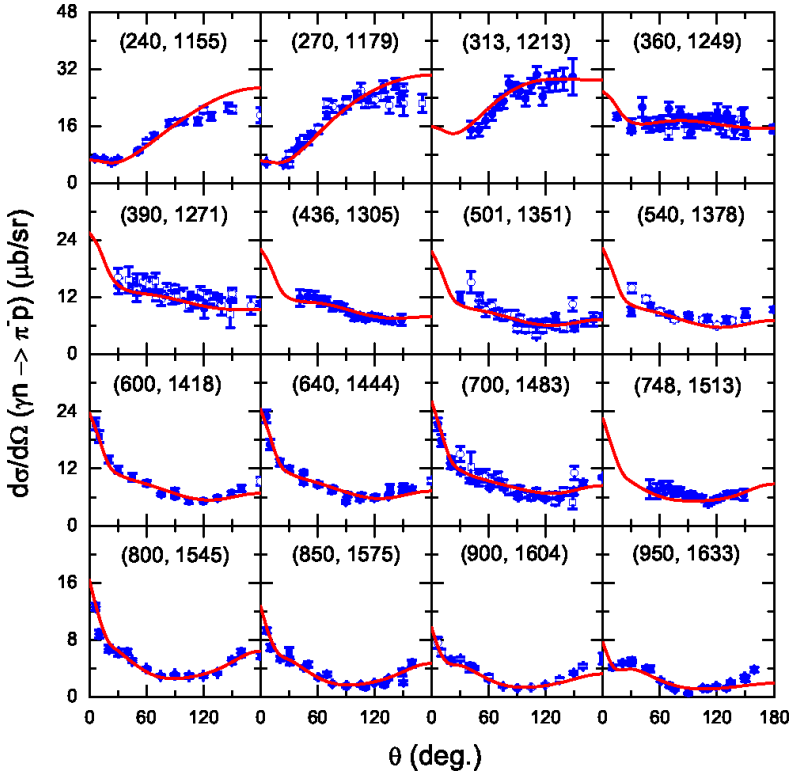

Differential cross section for $\gamma n \to \pi^- p$

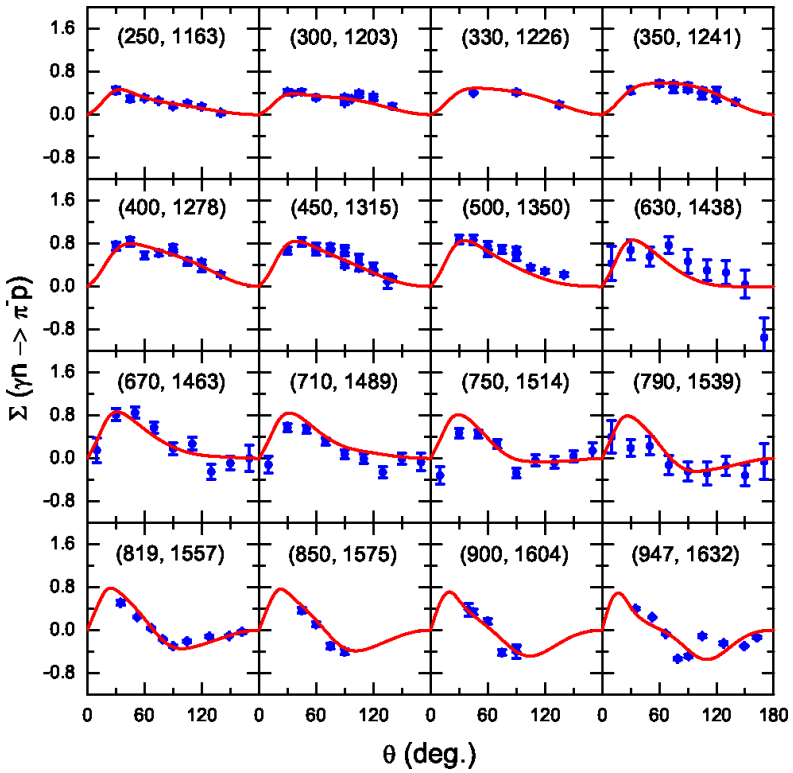

Photon spin asymmetry for $\gamma n \to \pi^- p$

Data: CNS Data analysis center [CBELSA/TAPS, JLAB, MAMI,...]

Pion photoproduction: $d\sigma/d\Omega$ and Σ_γ for $\gamma p \to \pi^0 p$

F. Huang, M. Döring, K. Nakayama *et al.*, Phys. Rev. C85 (2012) 054003

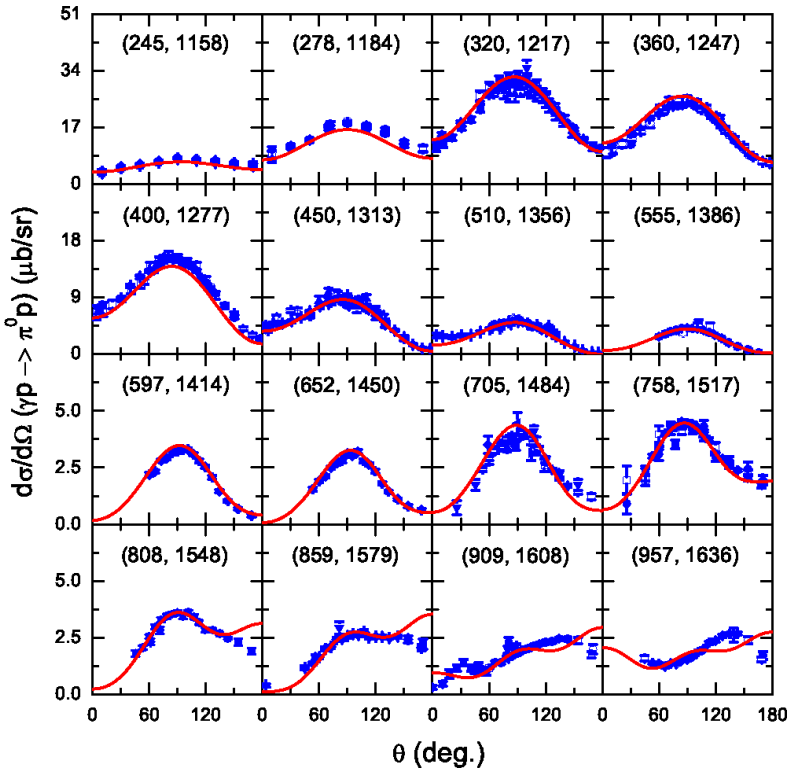

Differential cross section for $\gamma p \to \pi^0 p$

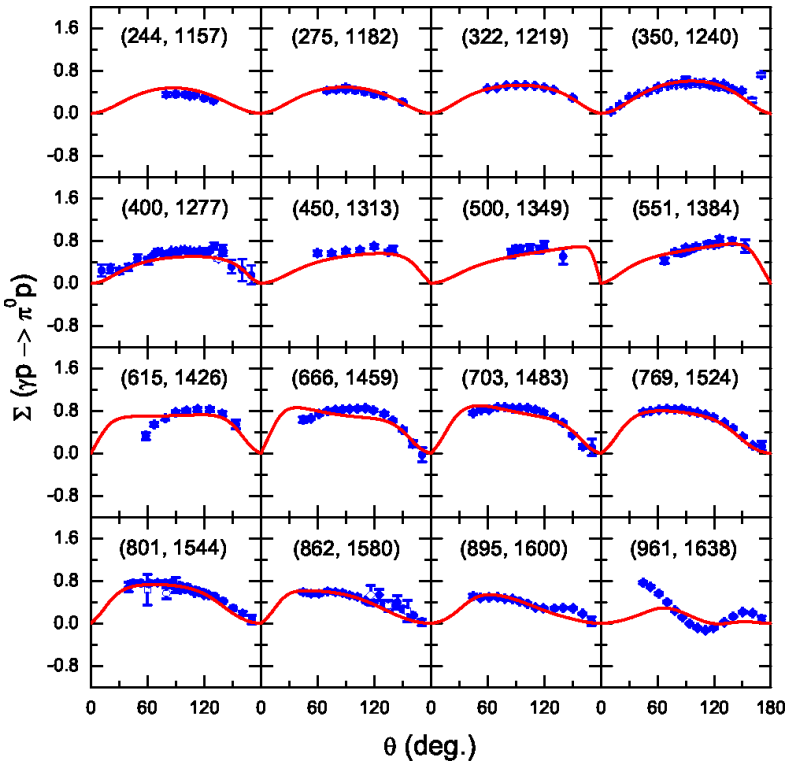

Photon spin asymmetry for $\gamma p \to \pi^0 p$

Data: CNS Data analysis center [CBELSA/TAPS, JLAB, MAMI,...]

Multipole amplitudes I=3/2

not included in the fit

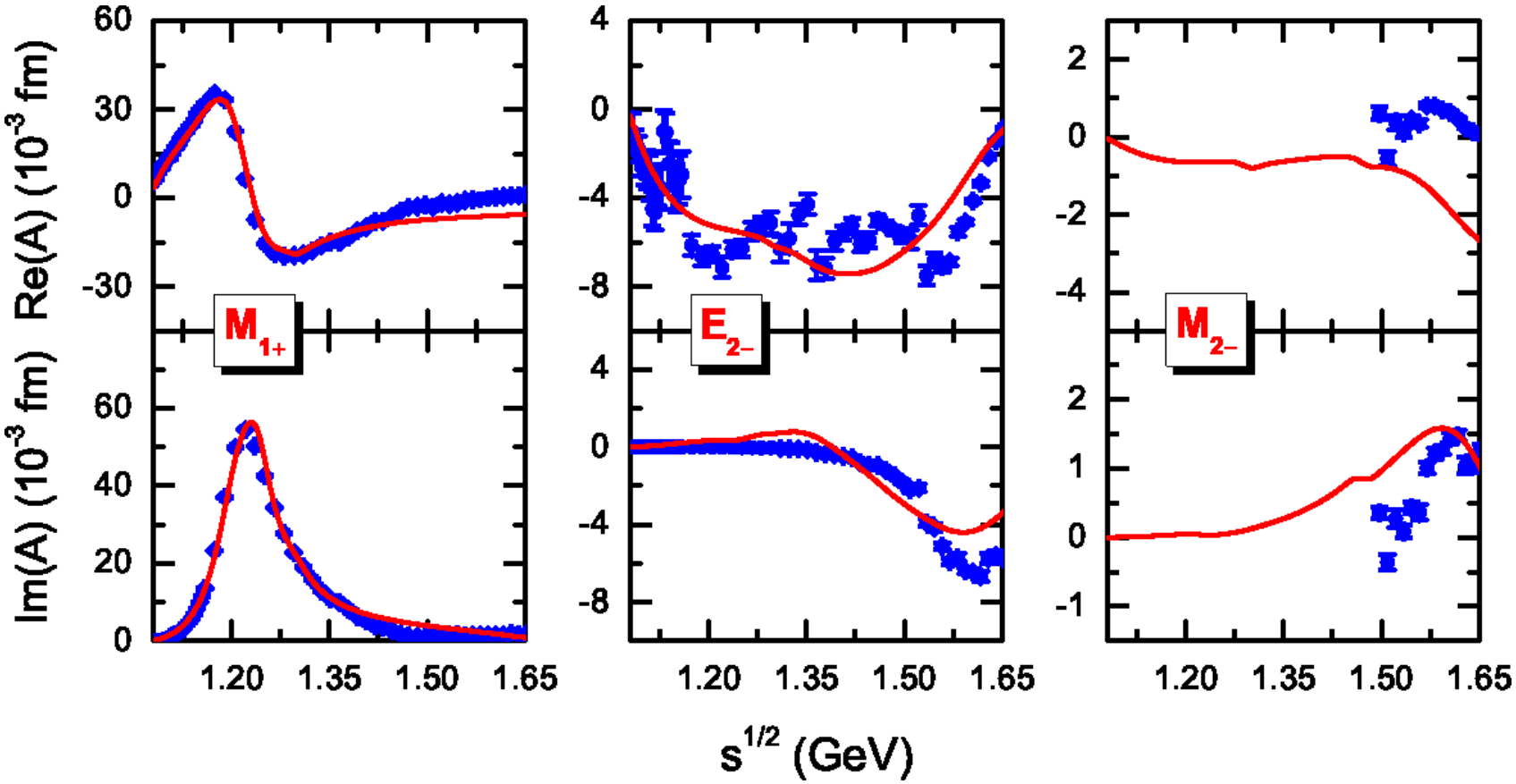

Wealth of new data arriving from JLab, MAMI, ELSA,. . .

Resonance content: Nucleon-like resonances

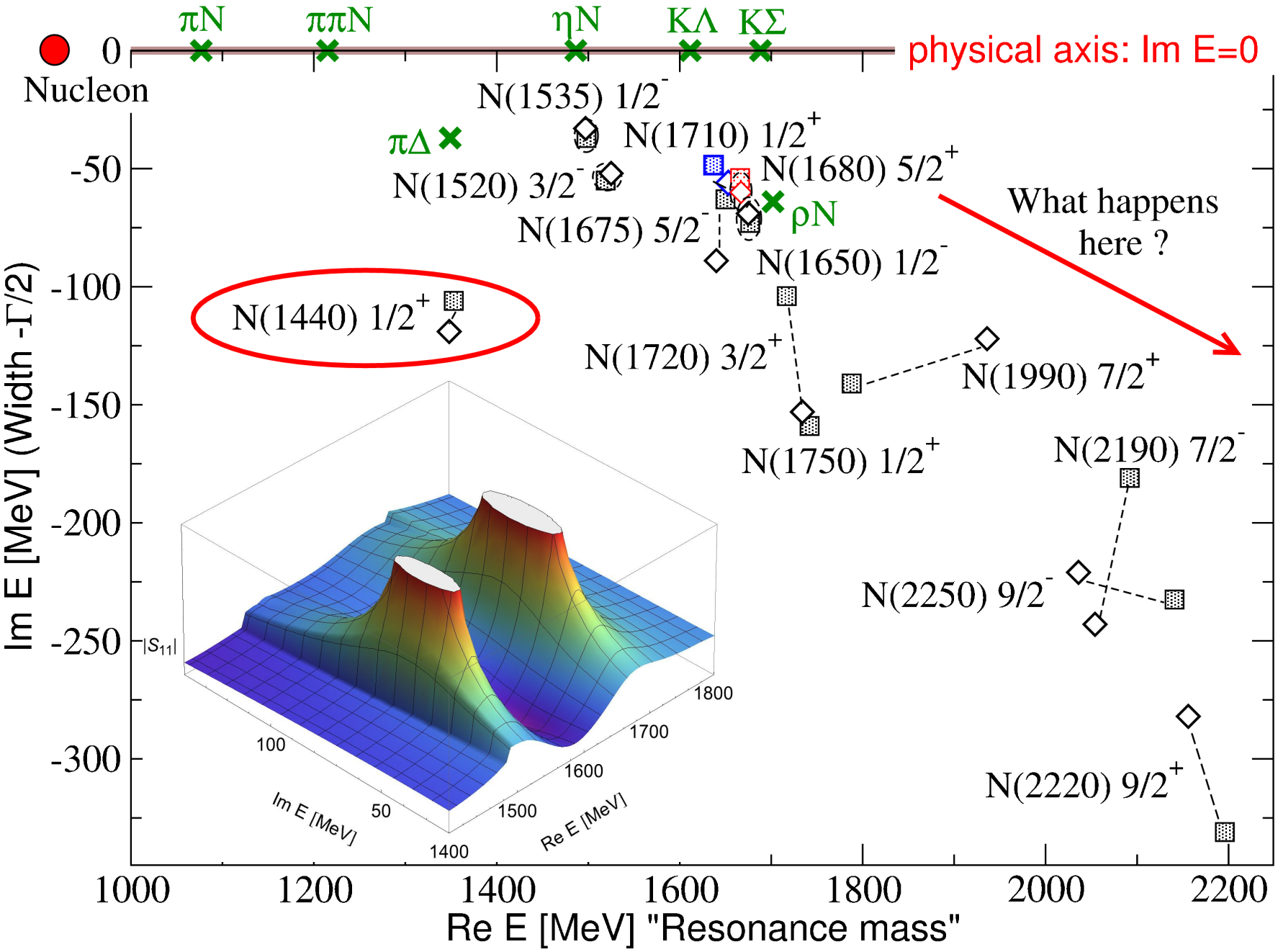

Perspectives

Meson spectroscopy @ GlueX

Hadronic approaches for the lattice

From 2 to 3 particles in the final state: an example

[M. D., E. Oset, Ulf-G. Meißner, EPJA 46 (2010)]

- 3-bodies in the final state: complex kinematics
- Many observables
- Illustrated for

$$\boxed{\vec{\gamma}p \to \pi^0 \eta p}$$

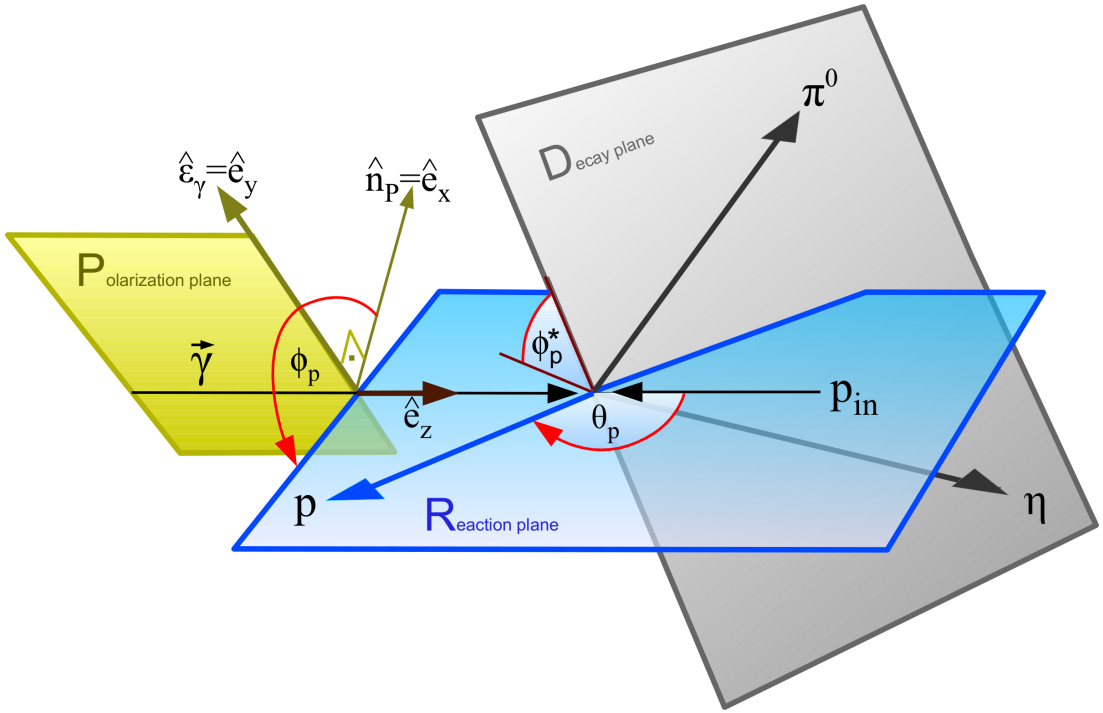

First measurement of I^S, I^C (fixed ϕ^*)

$$\frac{d\sigma}{d\phi} = \sigma_0[1 + I^S \sin(2\phi) + I^C \cos(2\phi)]$$

by CBELSA/TAPS E. Gutz *et al.*, Phys.Lett.B **687**,11,2010

Predictions for I^C DATA: CBELSA/TAPS, E. Gutz *et al.*, Phys.Lett.B **687**,11,2010

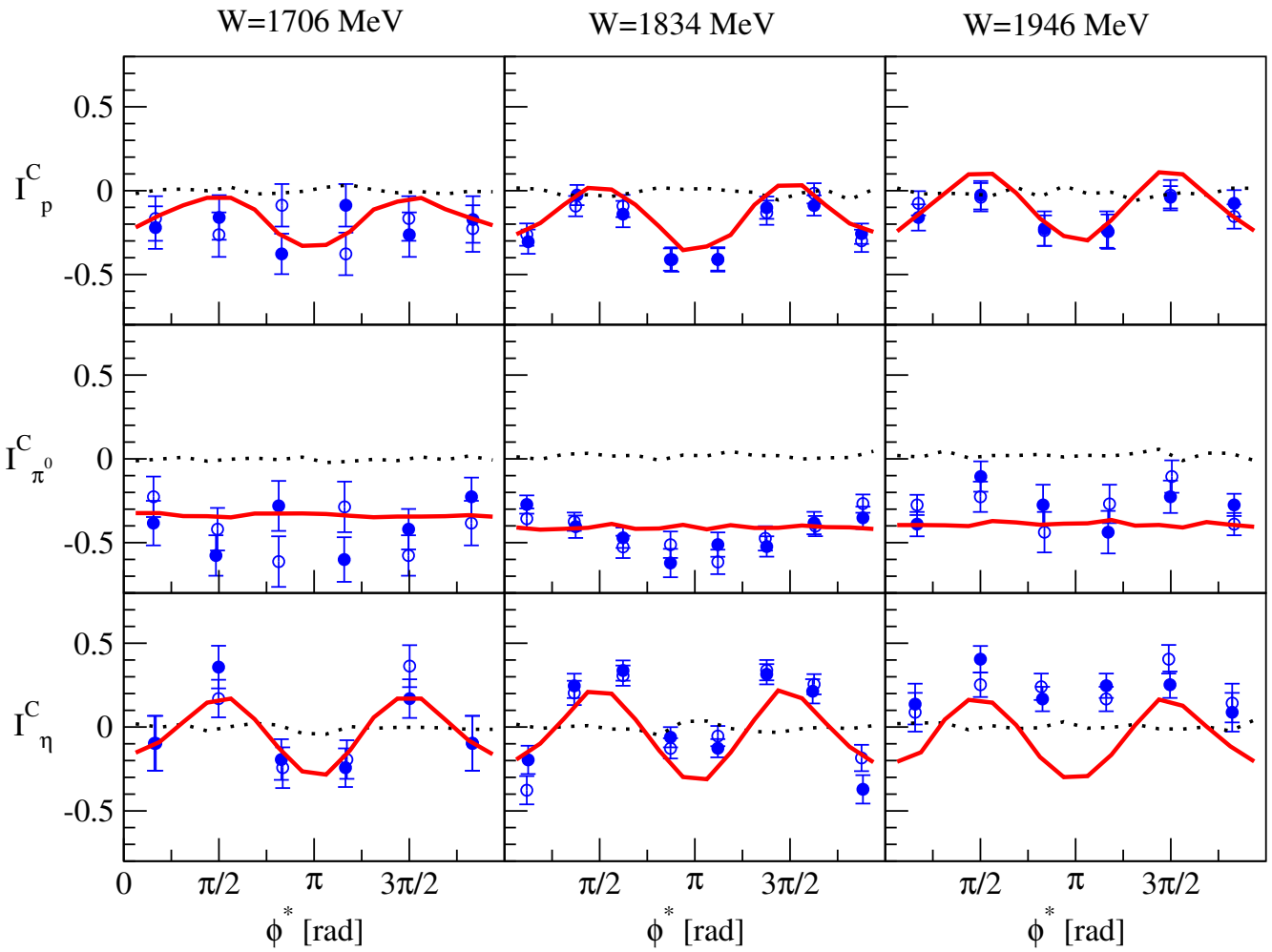

Red solid lines: Predicted results.

Black dotted lines: Without the strong $\Delta(1700) \to \eta\Delta(1232)$ coupling predicted from UχPT.

Hybrids and exotics in recent lattice calculations

Dudek PRD 83 (2011) 111502, Dudek PRD 84 (2011) 074023

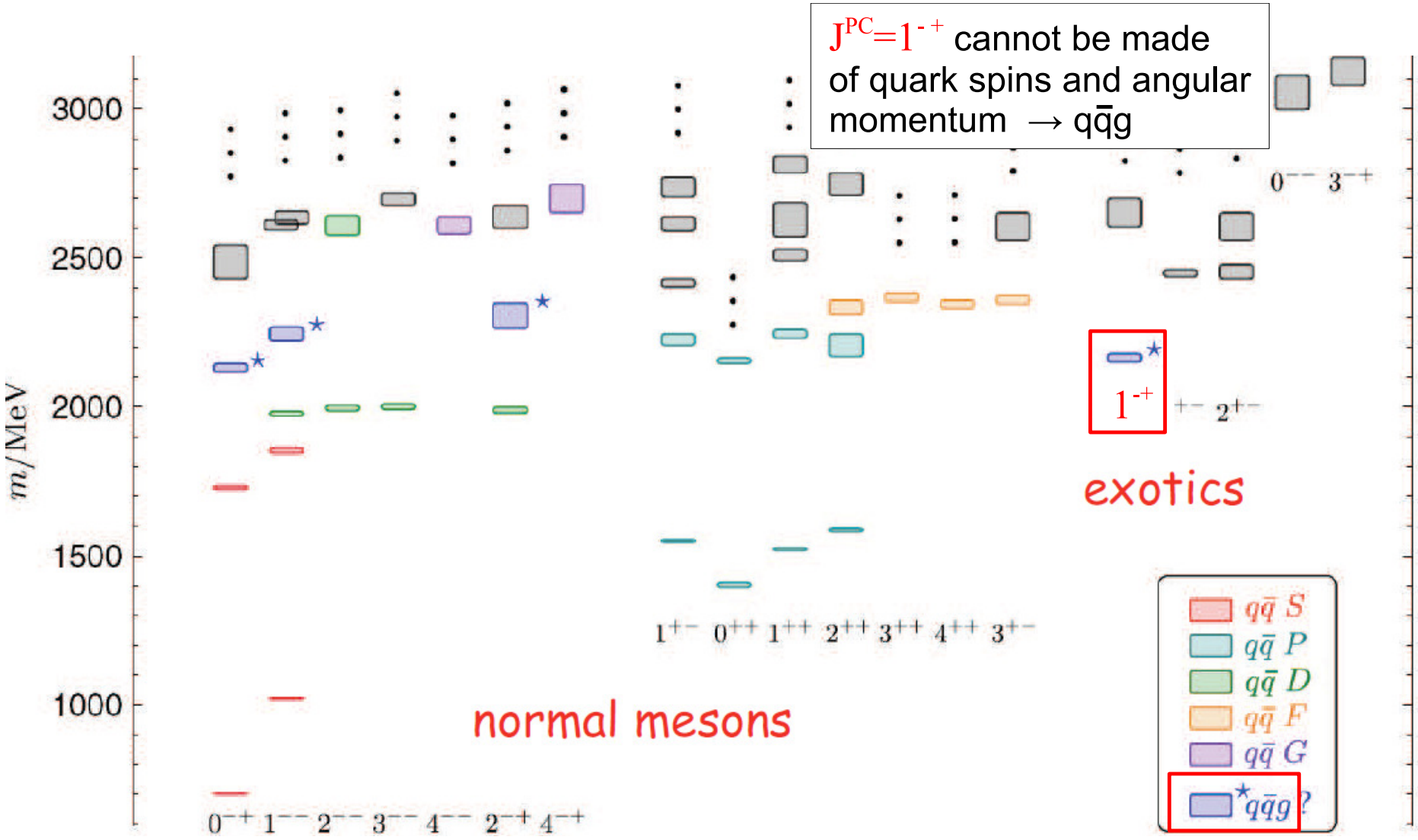

Partial wave analysis – the isobar model

A. R. Dzierba *et al.*, Phys.Rev. D73 (2006) 072001, **CLAS**: Phys. Rev. Lett. **102**, 102002 (2009)

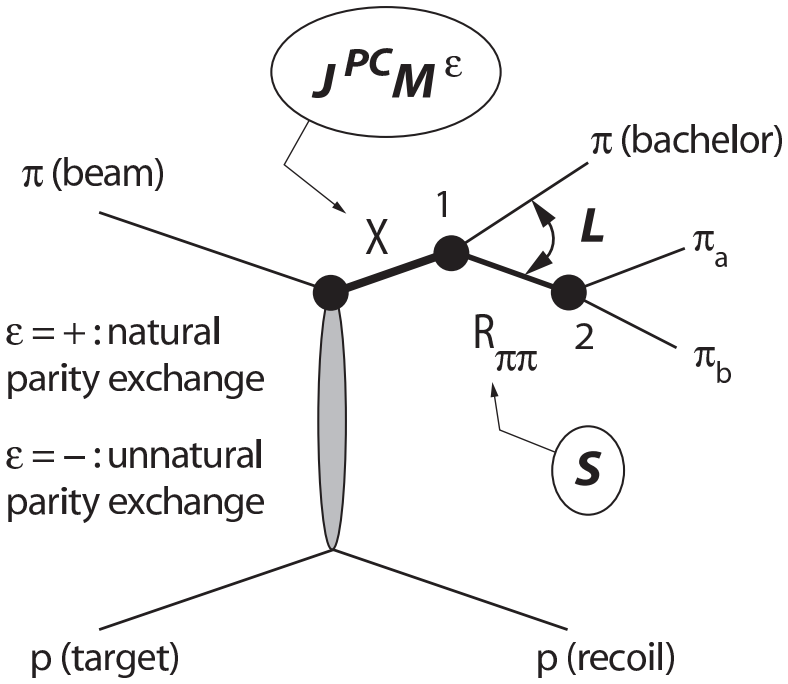

- Binning in $m_{3\pi}$ and t.
- $\rightarrow$ No assumption on resonances.
- Event-based log-likelihood fit.
- Future: effective Regge-parameterization.

Next-generation experiments @ JLab

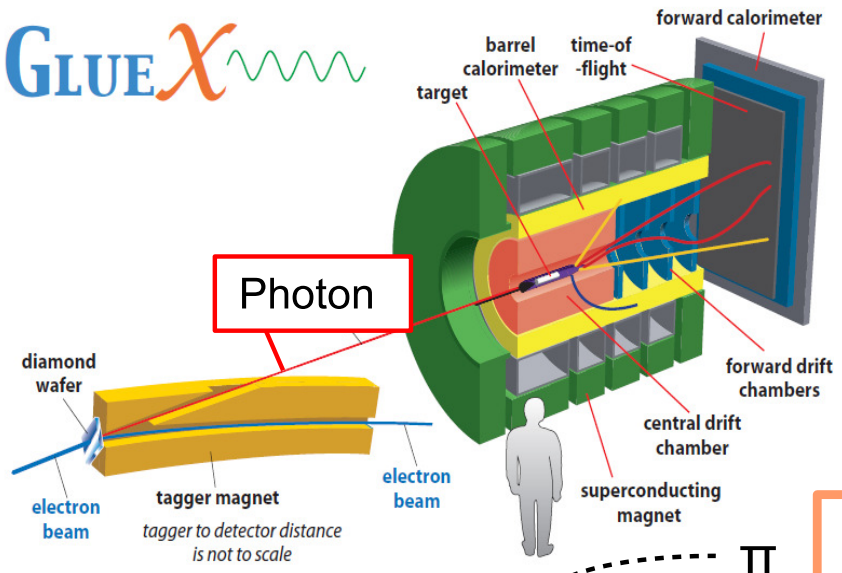

Transfer of methods from baryon to meson analysis

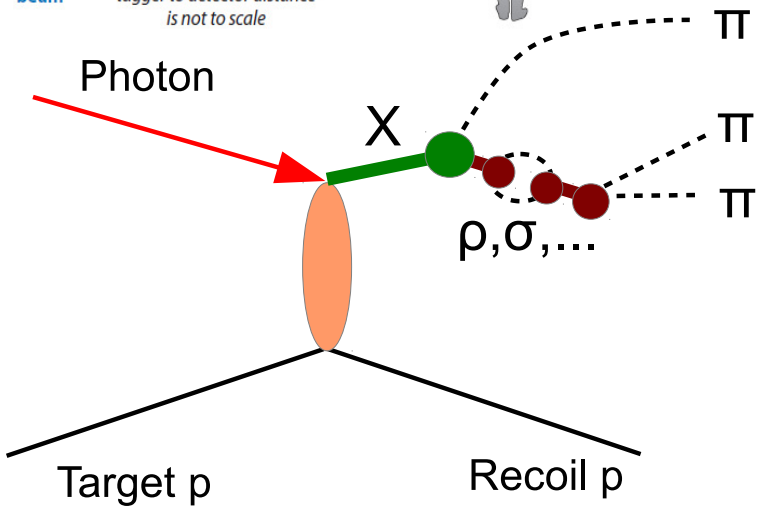

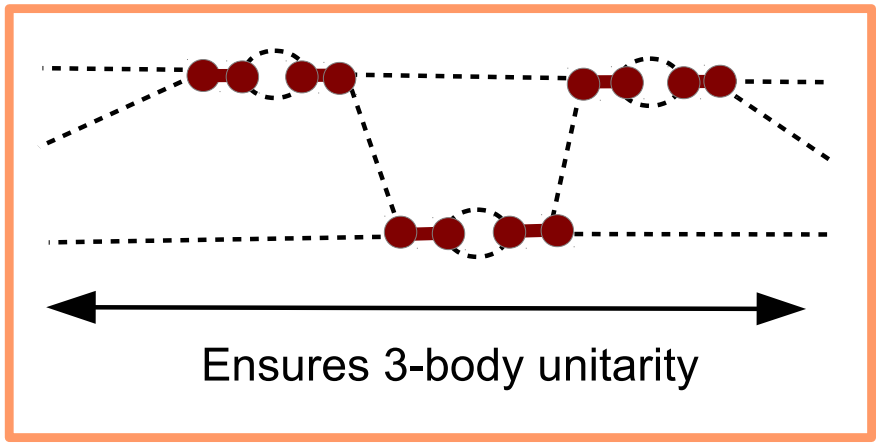

+ pions from N* and Δ's

Beyond the isobar model

1) no FSI, no 3-body unitarity, commonly used.

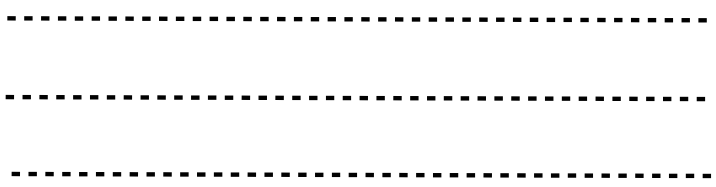

3) "Isobars" from unitarized χPT

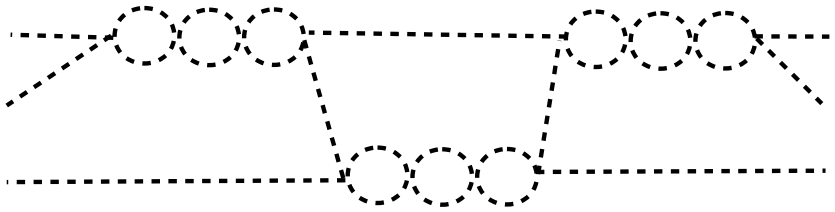

Match to [X→π isobar] not straightforward

2) 3-body unitary isobars, off or on-shell reduction.

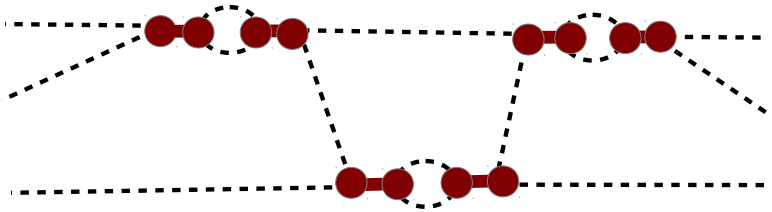

Match to [X→π isobar] natural

4) Faddeev calculation.

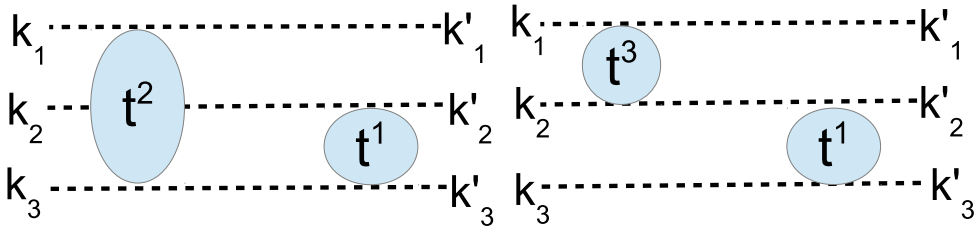

(shown only subprocesses)

- Usually integral equations → on-shell simplifications possible?
- Effective isobar parameterizations (Pelaez, Caprini,. . .): take account of Adler zero, increased convergence by complex mapping techniques,. . .

Perspectives

Meson spectroscopy @ GlueX

Hadronic approaches for the lattice

The world as lattice sees it

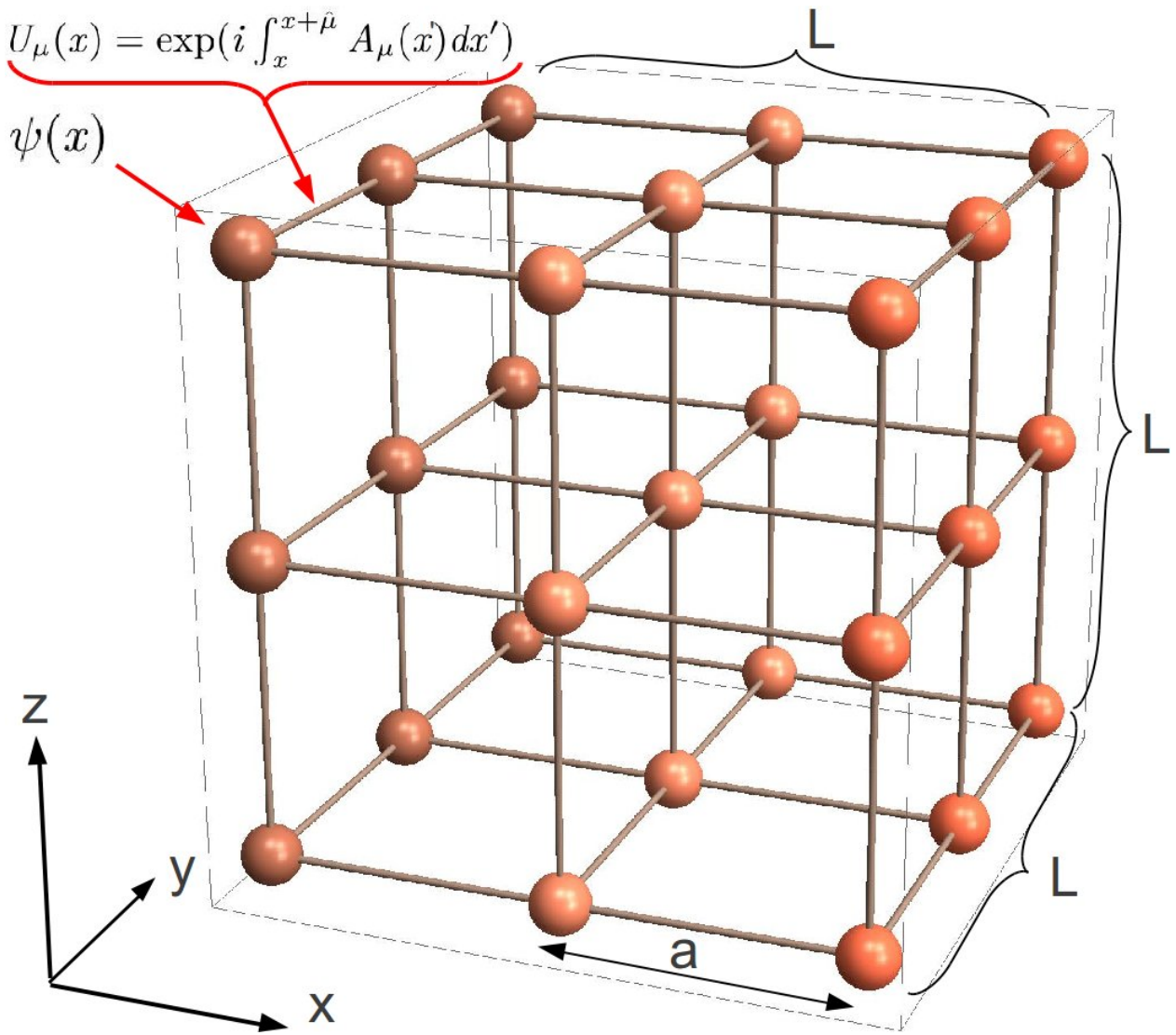

- Finite volume L^3
- Finite lattice spacing a
- m_q(Lattice) $\neq m_q$

Resonances decaying on the lattice

Eigenvalues in the finite volume

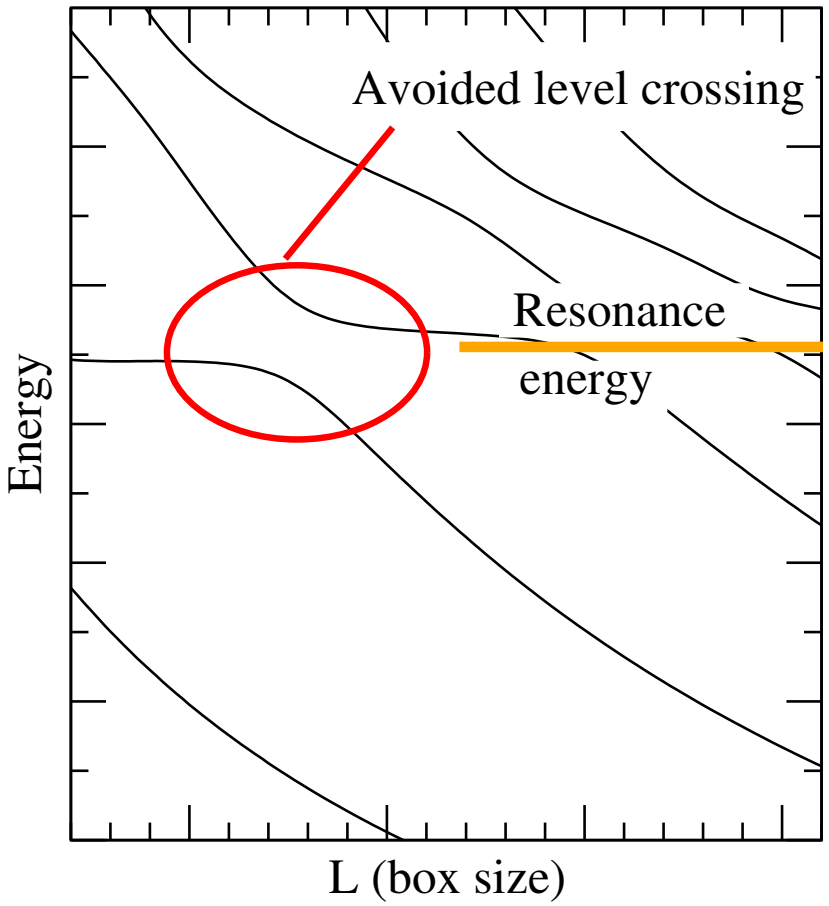

Resonances in the finite volume

[M.D., M. Mai, U.-G. Meißner, arXiV: 1302.4065, hep-lat]

- Unitarized chiral interaction with NLO contact terms

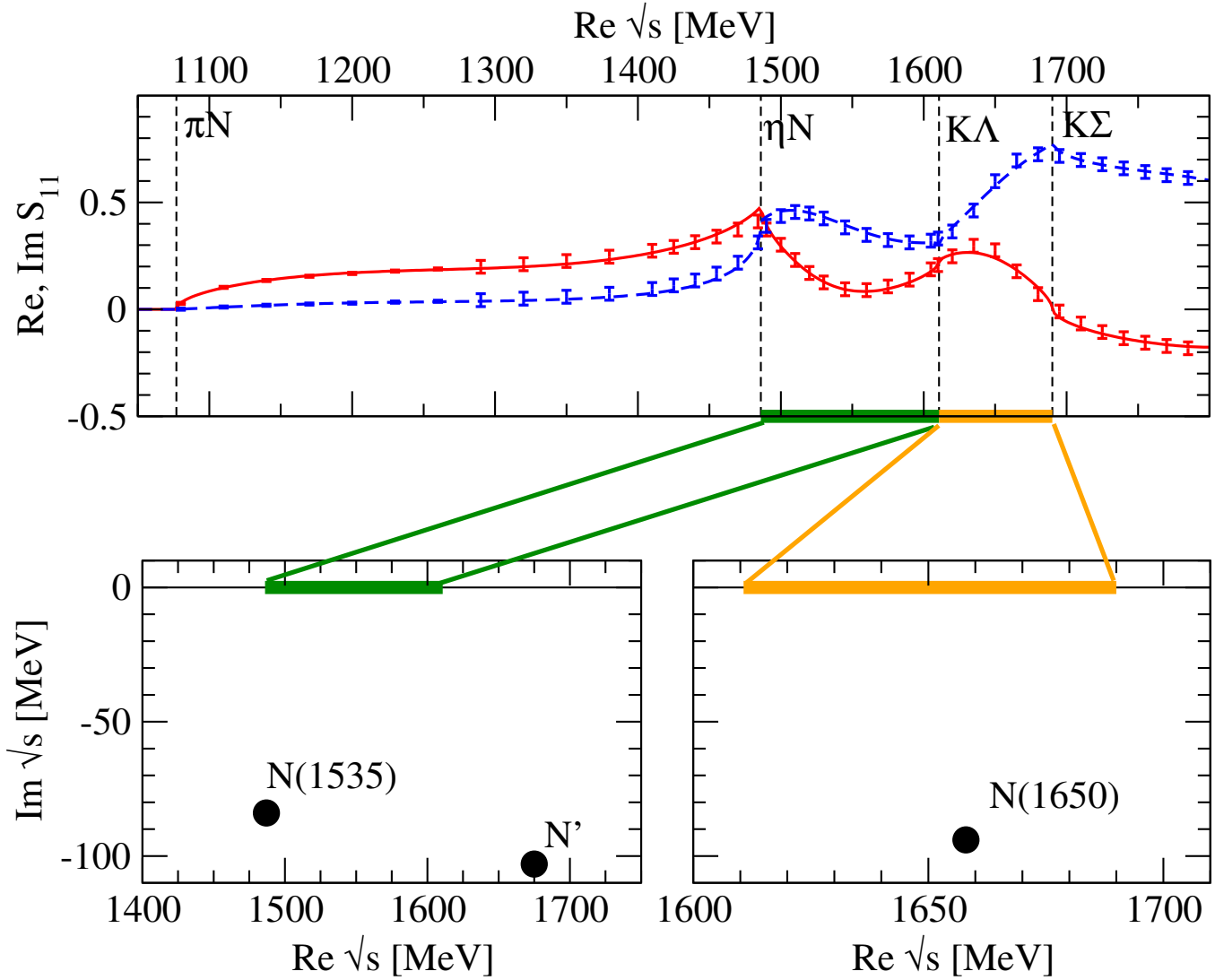

Data: SAID (2006)

Chiral extrapolation to a QCDSF lattice setup

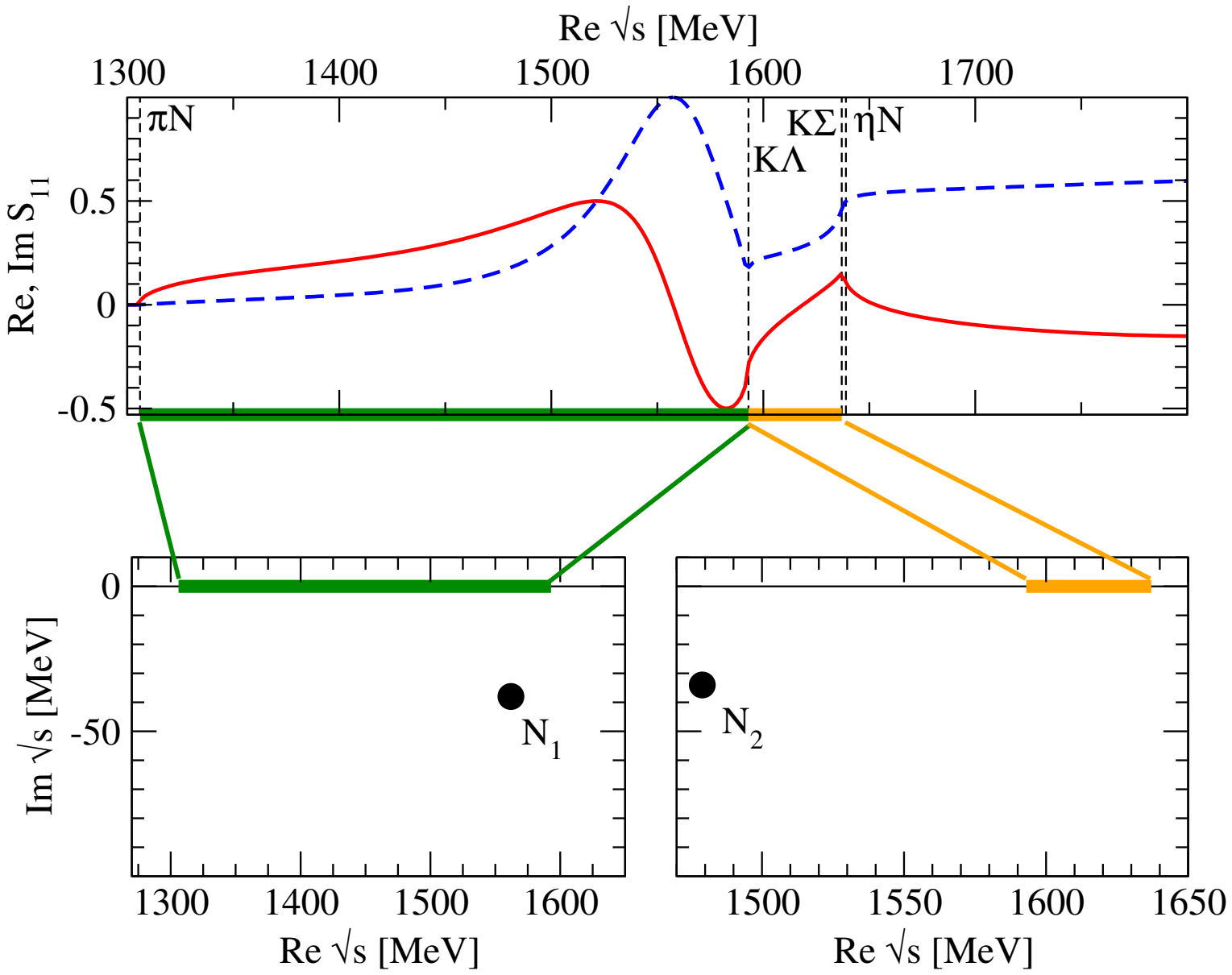

Prediction of the lattice spectrum

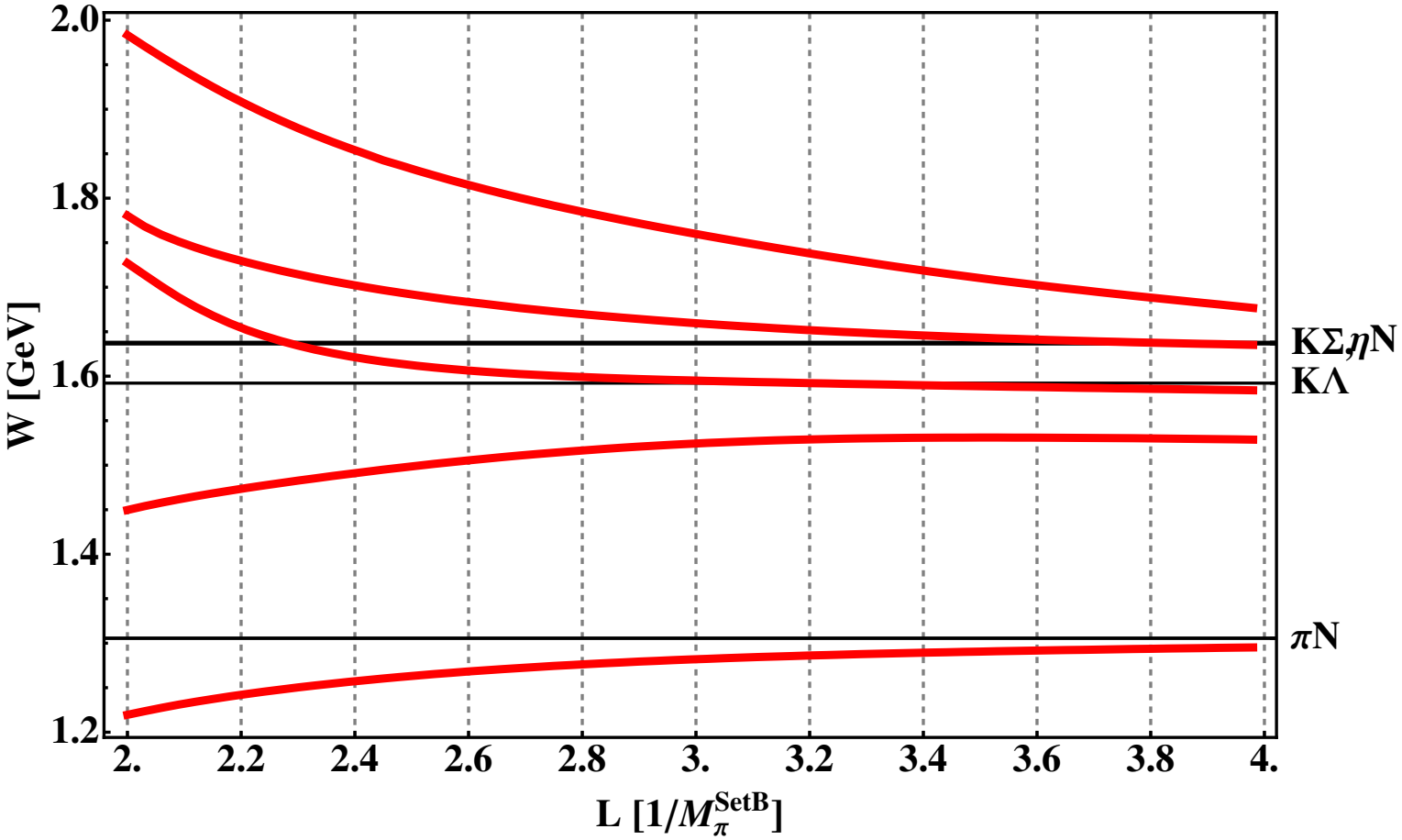

- The inverse process:

Analyze <u>existing</u> lattice spectra to <u>extract</u> hadronic resonances!

Extracting resonances from lattice data

[M.D., Meißner, Oset/Rusetsky, EPJA **47** (2011)]

Three unknown potentials

- $V(\pi\pi \to \pi\pi)$
- $V(\pi\pi \to \bar{K}K)$
- $V(\bar{K}K \to \bar{K}K)$

- Expand a two-channel potential V in energy (i, j: $\pi\pi$, $\bar{K}K$):

$$V_{ij}(E) = a_{ij} + b_{ij}(E^2 - 4M_K^2)$$

to extract phase shifts/resonances

lattice data & fit

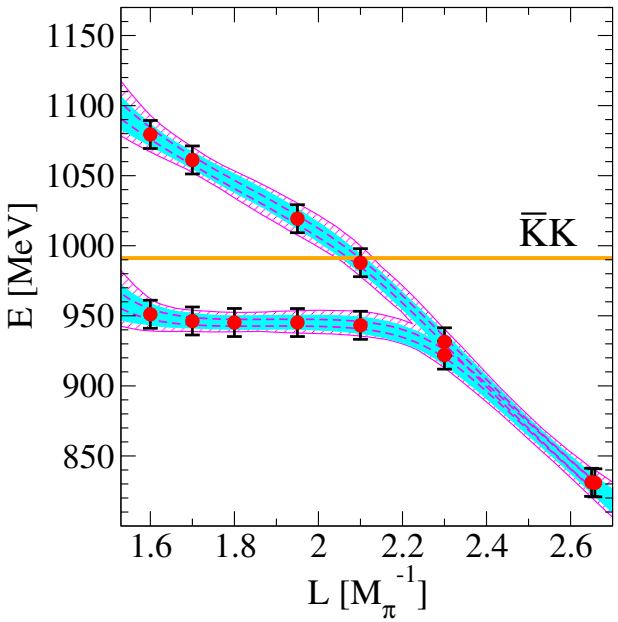

extracted phase shift

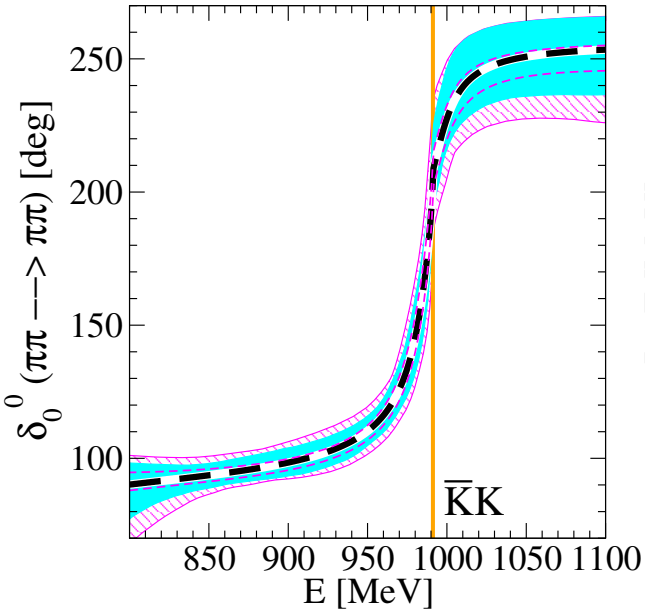

$f_0(980)$ pole position

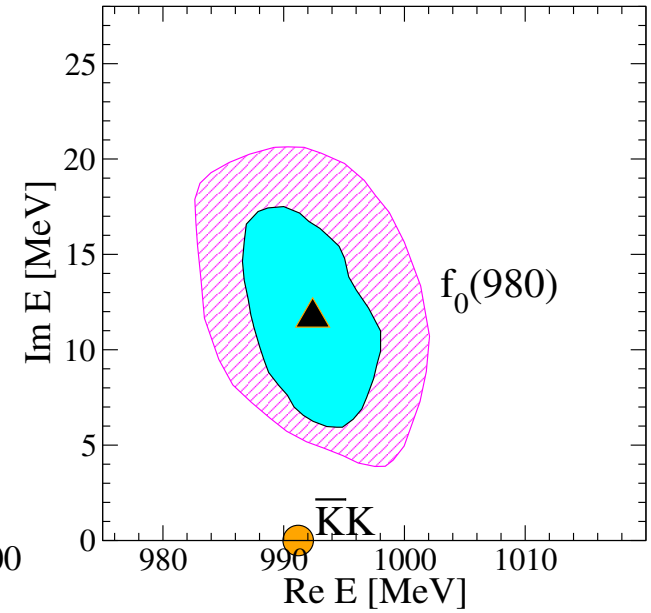

κ/K^* in moving frames: complexity of data at physical masses

Lattice spectrum simulated from NLO UχPT [M.D. *et al.*, EPJ **A** 48 (2012)]

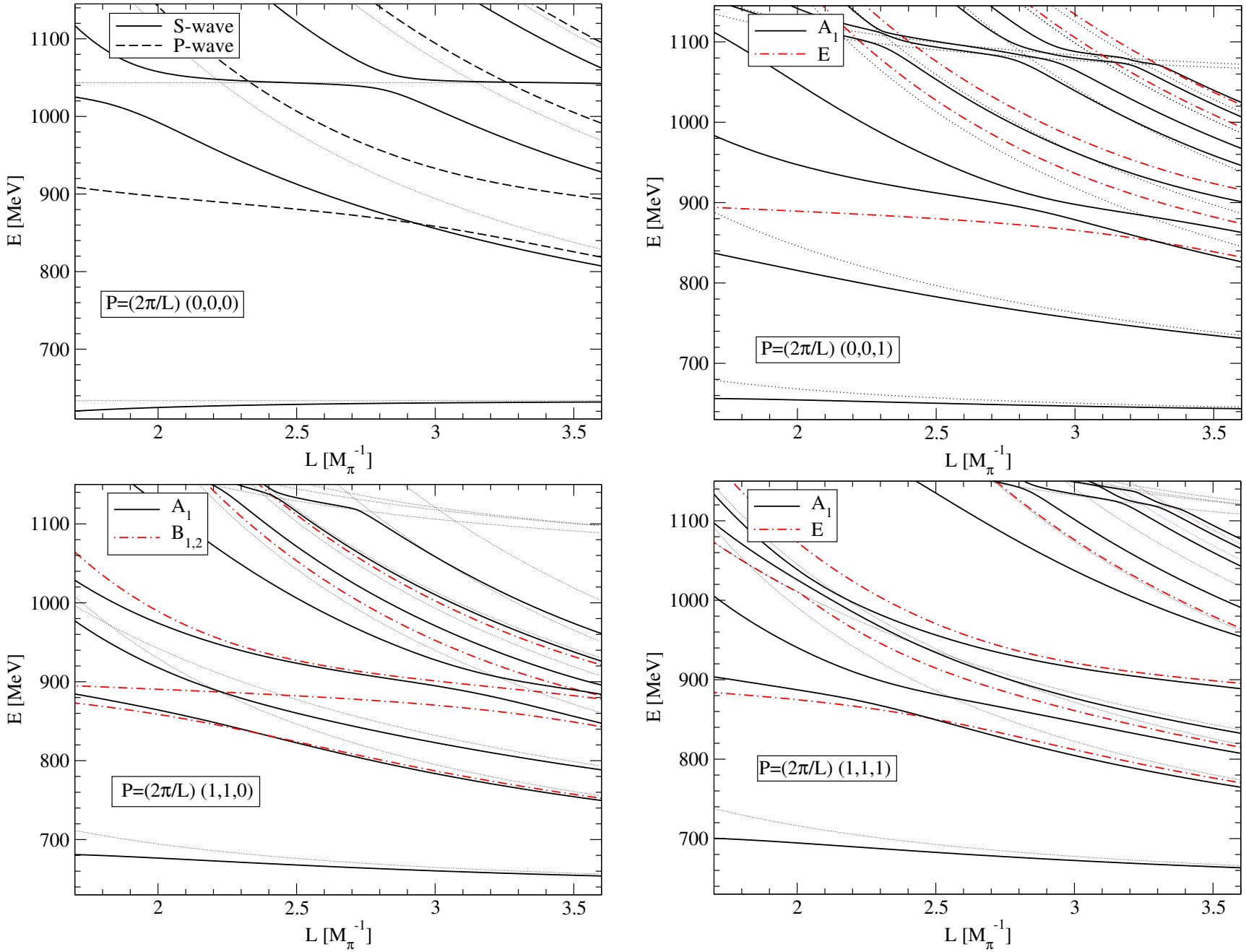

κ/K^* in moving frames: complexity of data at physical masses

Lattice spectrum simulated from NLO UχPT [M.D. *et al.*, EPJ **A** 48 (2012)]

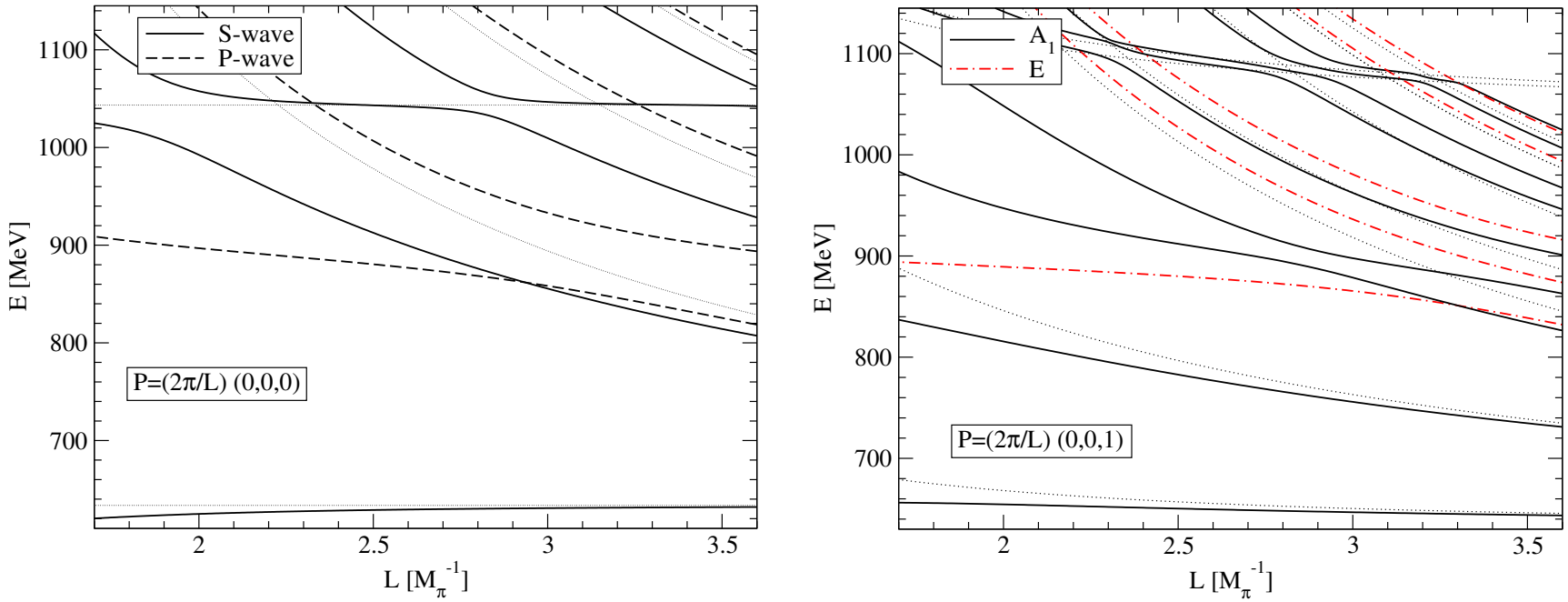

- Mixing of partial waves, coupled channels.
- Eventually three particles on-shell (large finite-volume corrections to the Roper?), isobar schemes including rearrangement for 3-body unitarity,. . .

Principles and tools from data analysis become useful.

Perspectives

- The study of resonances at intermediate energies provides a key to our understanding of Quantum Chromodynamic.
- JLab, MAMI, ELSA, ... provide high-precision photoprodution data.
- The analysis allows to extract the resonance spectrum to test QCD predictions.
- Tools and principles used in baryon analysis can boost the analysis of meson data (GlueX) and lattice eigenvalues.

s-, t- and u-channel exchanges

- s-channel states coupling to πN, ηN, $K\Lambda$, $K\Sigma$, $\pi\Delta$, ρN.
- t- and u-channel exchanges:

	πN	ρN	ηN	$\pi\Delta$	σN	$K\Lambda$	$K\Sigma$
πN	$N, \Delta, (\pi\pi)_\sigma, (\pi\pi)_\rho$	N, Δ, Ct., π, ω, a_1	N, a_0	N, Δ, ρ	N, π	Σ, Σ^*, K^*	$\Lambda, \Sigma, \Sigma^*, K^*$
ρN		N, Δ, Ct., ρ	-	N, π	-	-	-
ηN			N, f_0	-	-	K^*, Λ	Σ, Σ^*, K^*
$\pi\Delta$				N, Δ, ρ	π	-	-
σN					N, σ	-	-
$K\Lambda$						$\Xi, \Xi^*, f_0, \omega, \phi$	Ξ, Ξ^*, ρ
$K\Sigma$							$\Xi, \Xi^*, f_0, \omega, \phi, \rho$

$\pi^- p \to \eta N$: Cross section and Polarization

Selected results

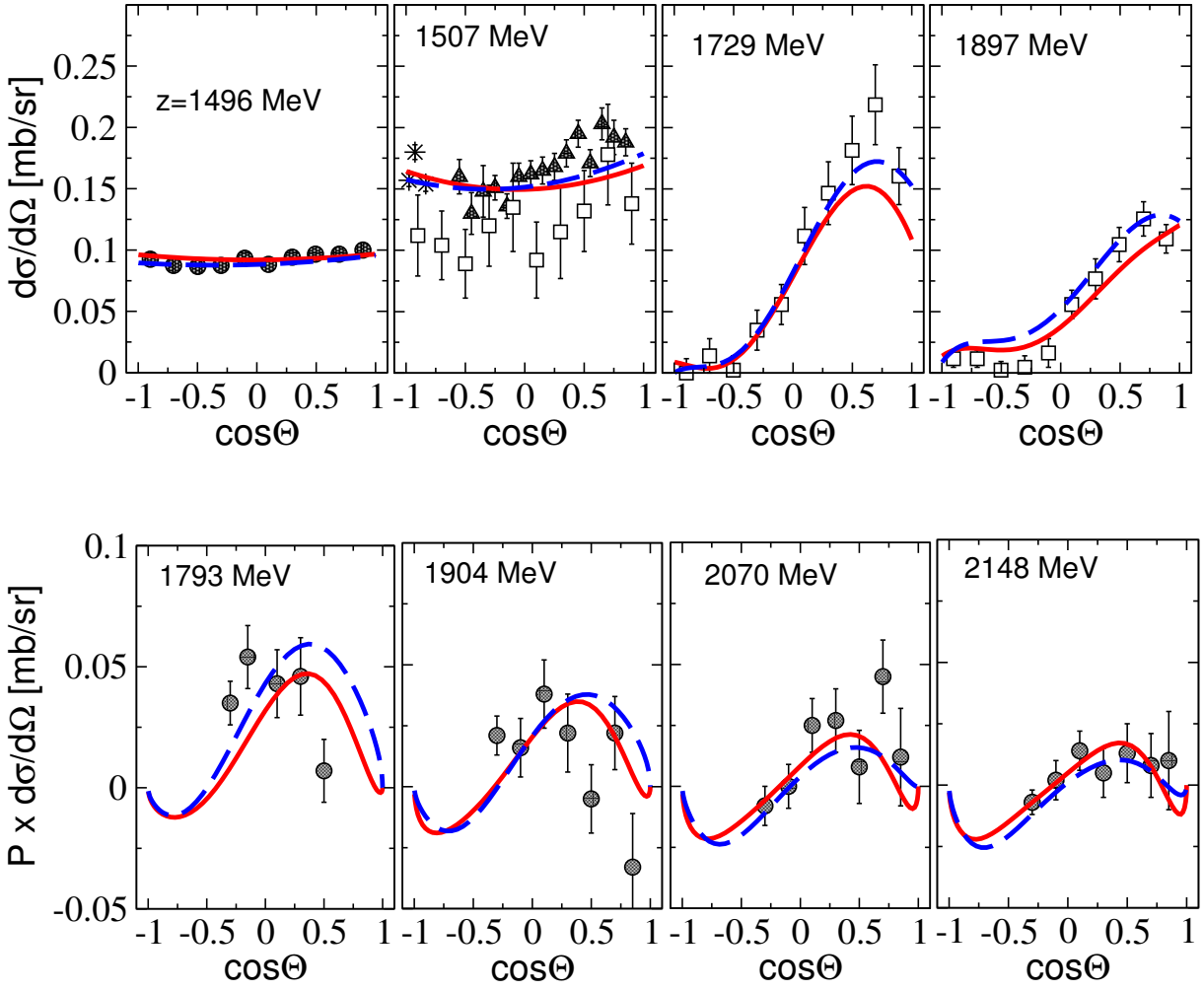

Difficult data situation

- Inconsistencies among different data sets
- Data at higher energies questionable
- Polarization data questionable

$\pi^- p \to \eta N$: Total cross section

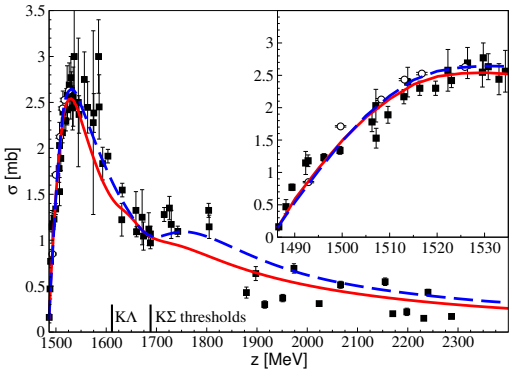

Partial wave content:

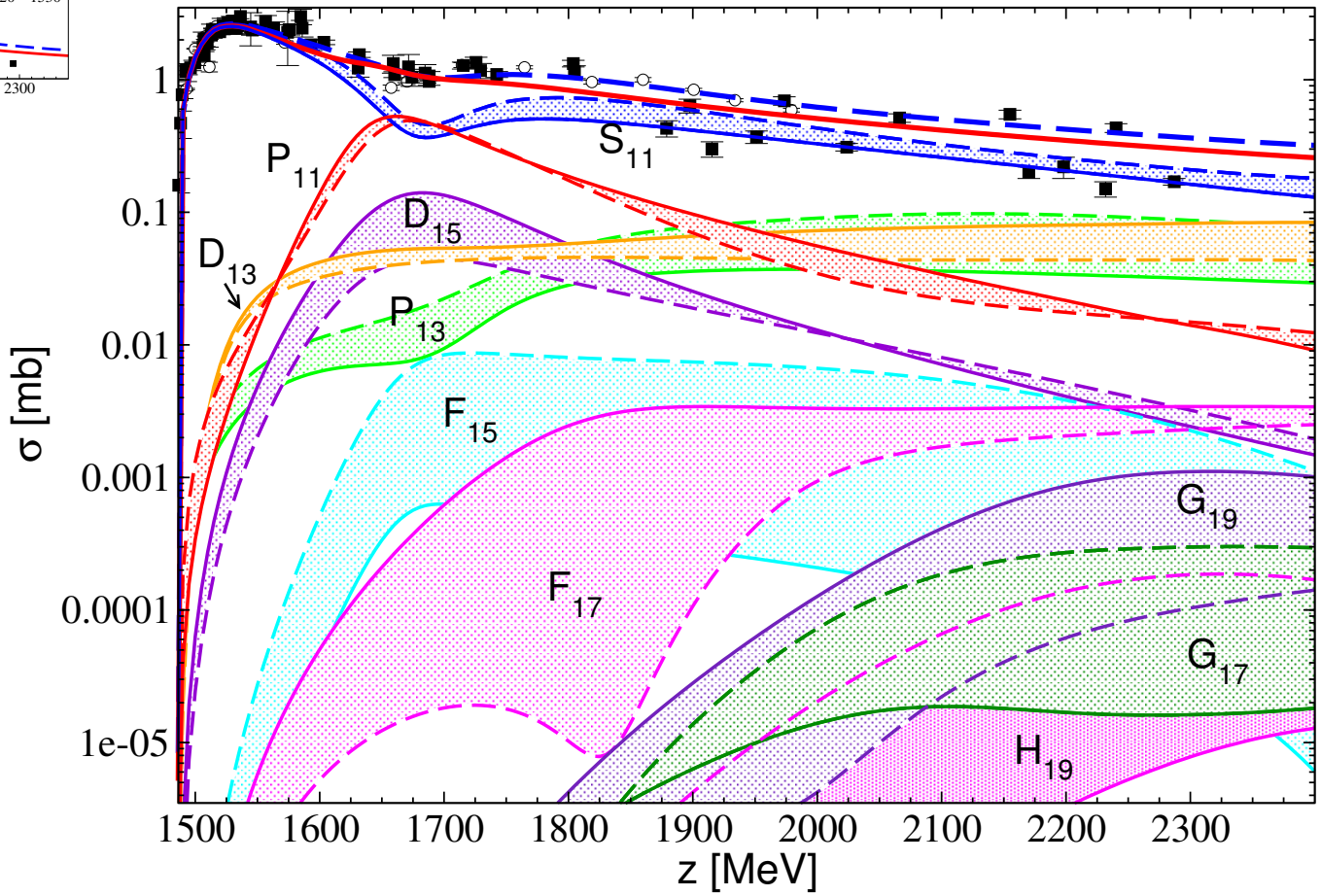

$\pi^- p \to K^0 \Sigma^0$: $d\sigma/d\Omega$ & Polarization

Selected results

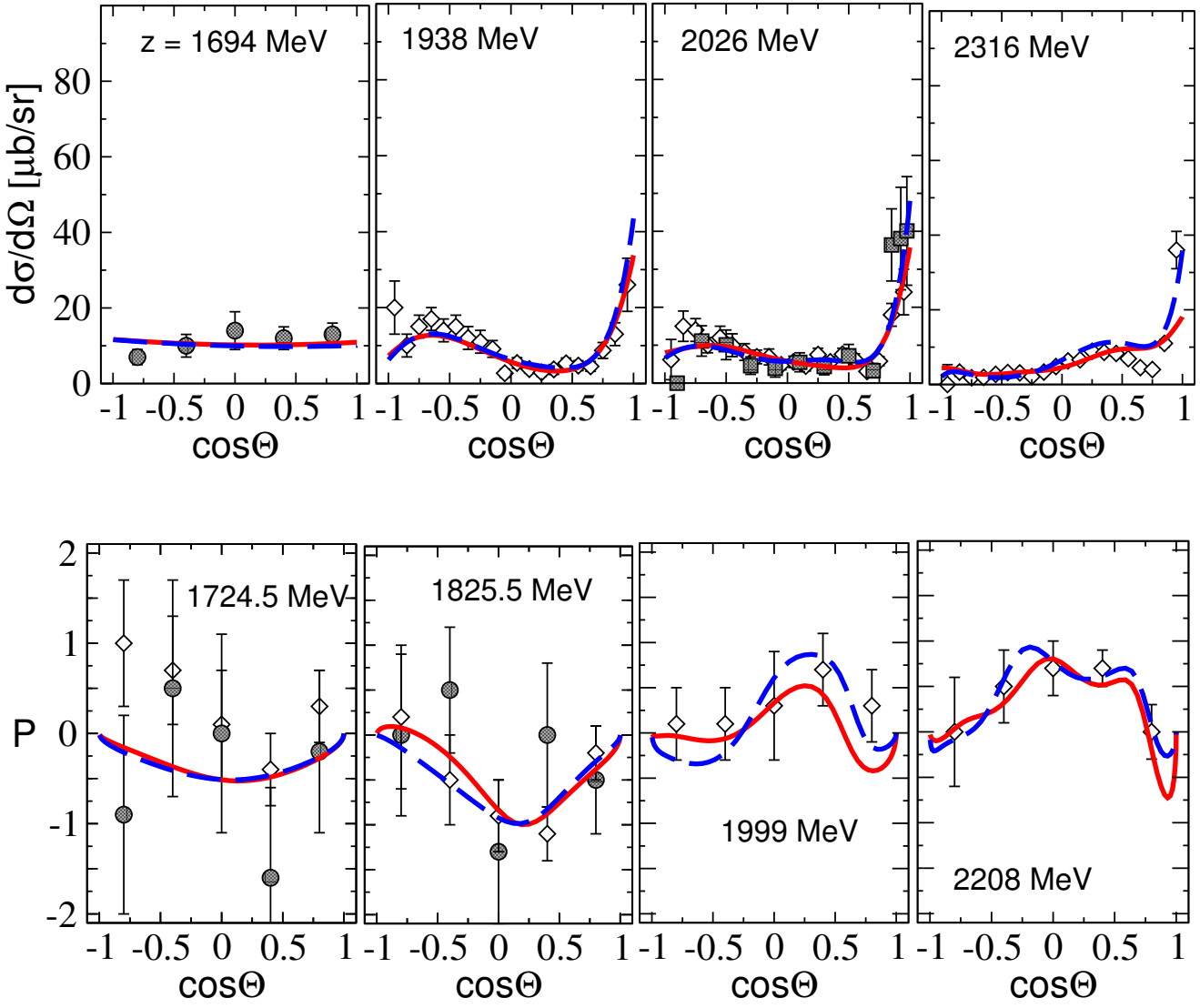

$\pi^- p \to K^0 \Sigma^0$: Total cross section

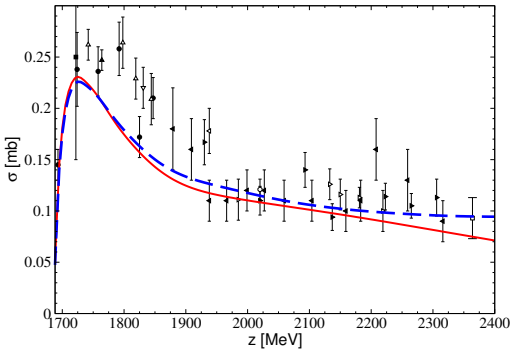

Partial wave content $I = 1/2$:

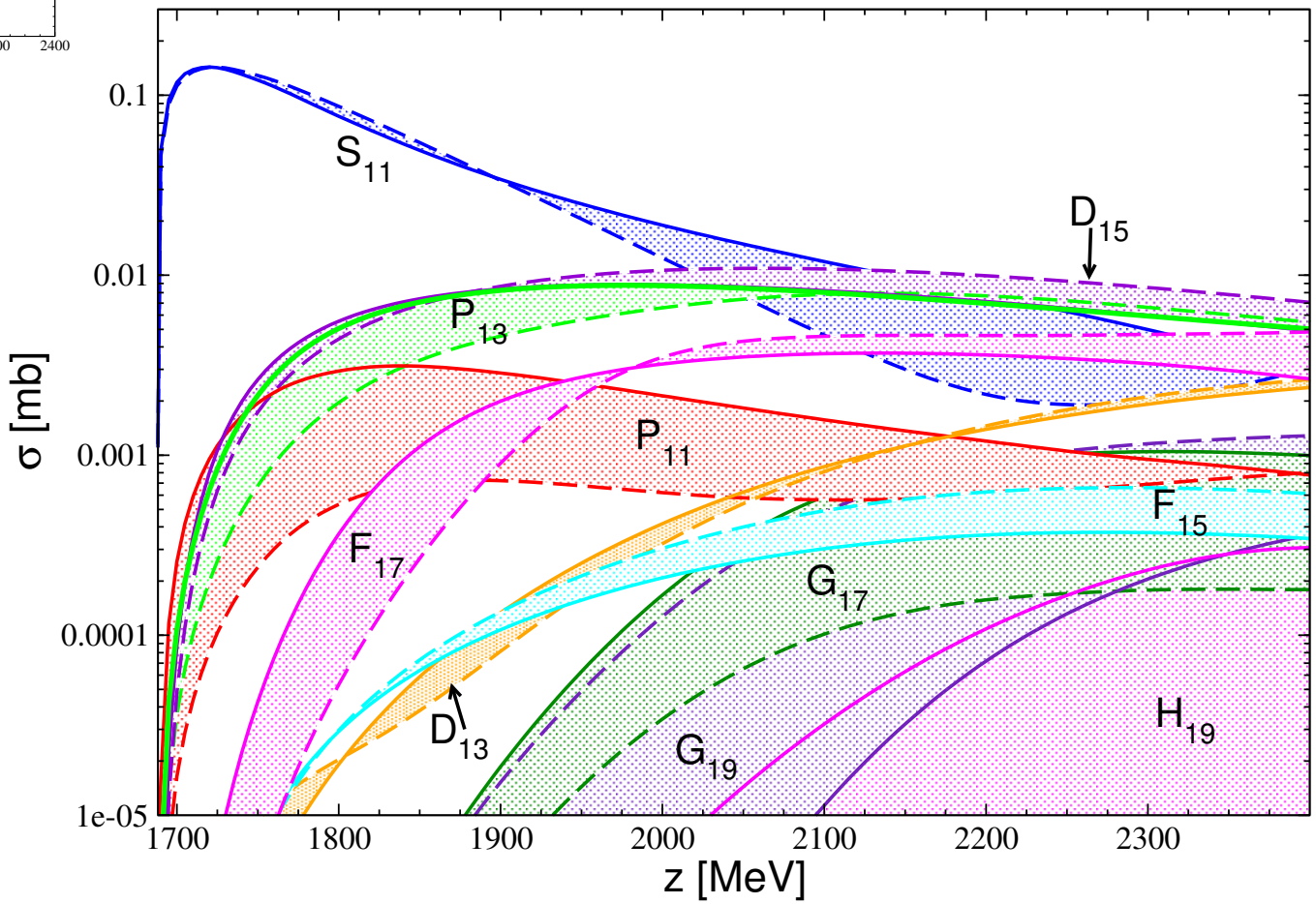

$\pi^- p \to K^0 \Sigma^0$: Total cross section

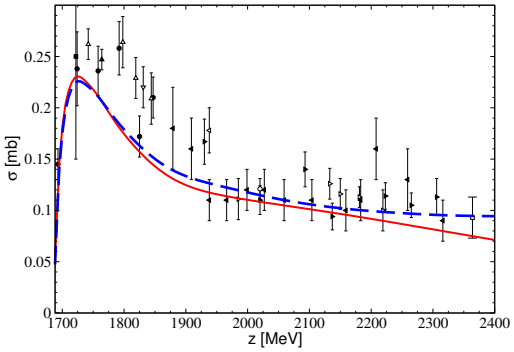

Partial wave content $I = 3/2$:

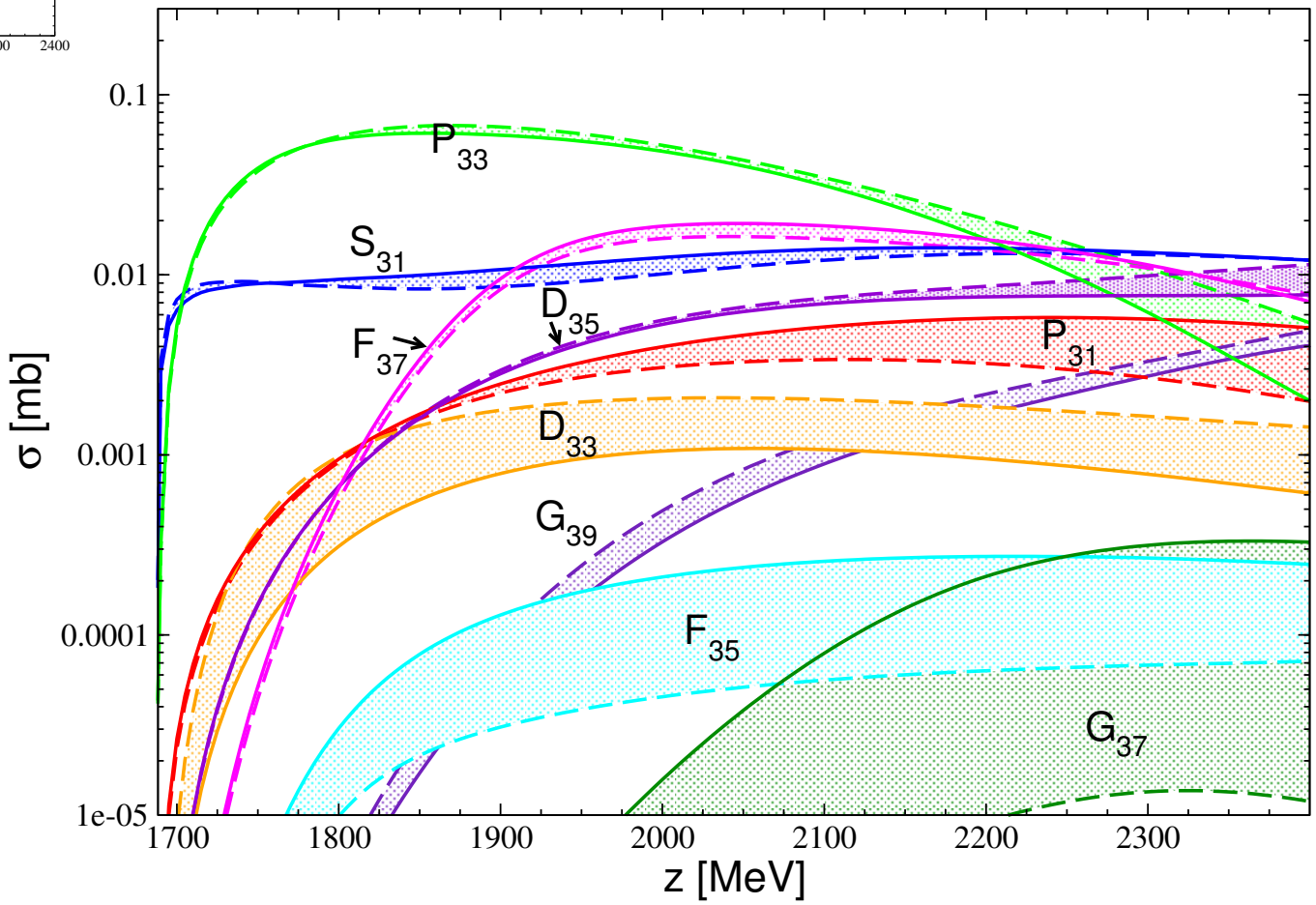

$\pi^- p \to K^+ \Sigma^-$: $d\sigma/d\Omega$

Selected results

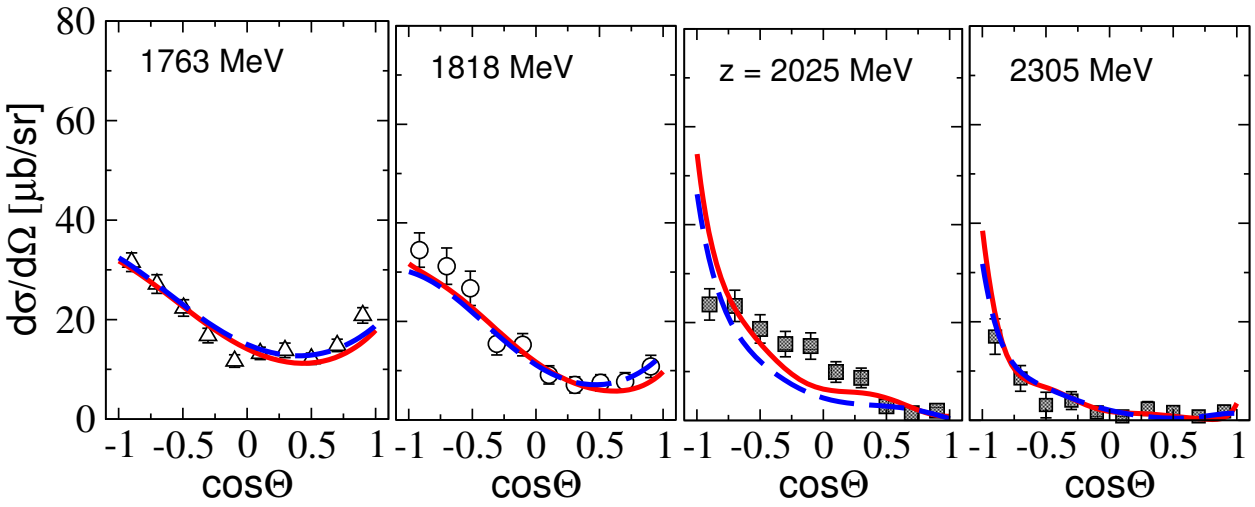

No polarization data

$\pi^+ p \to K^+\Sigma^+$: $d\sigma/d\Omega$, polarization & spinrotation angle

Seclected results

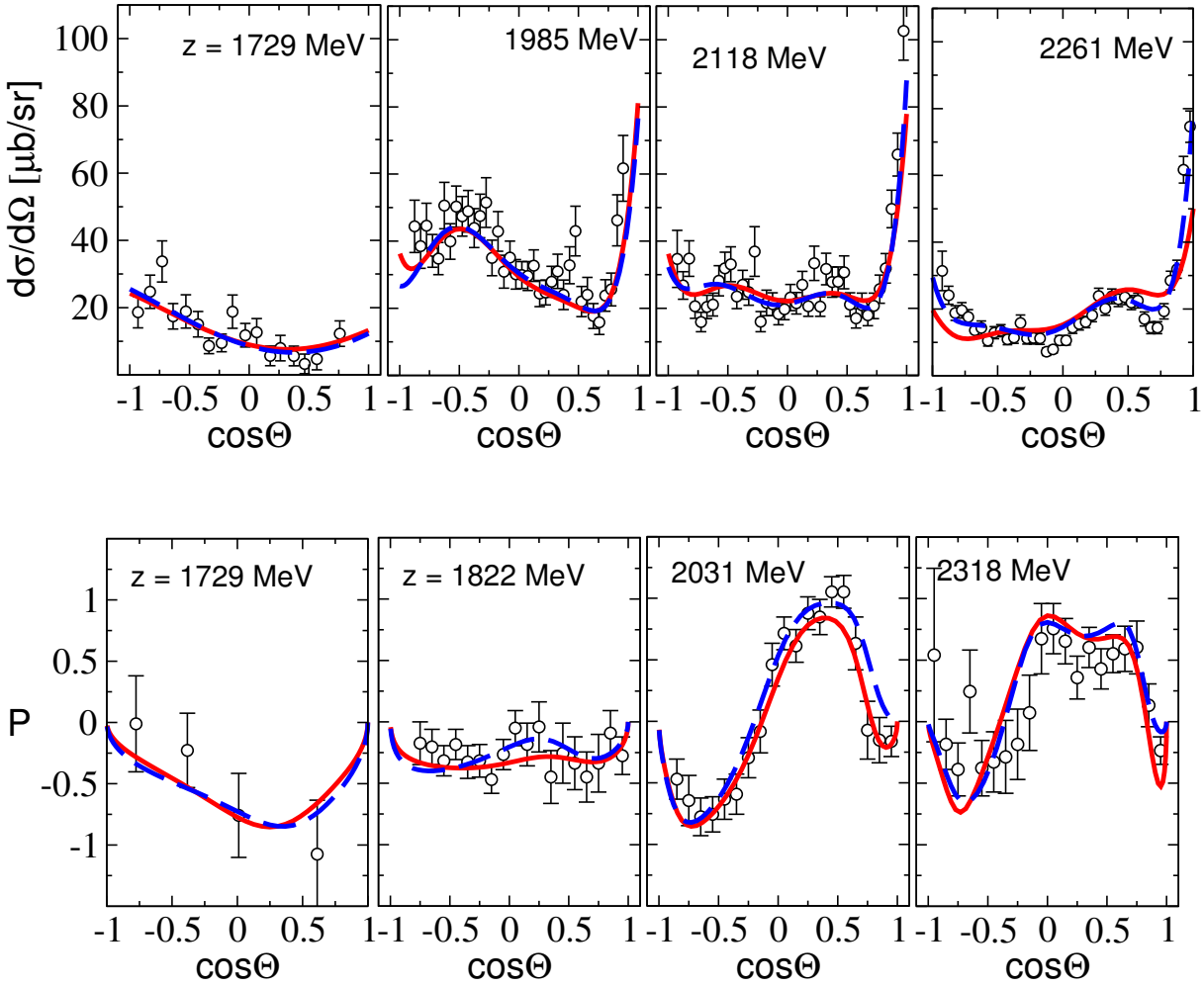

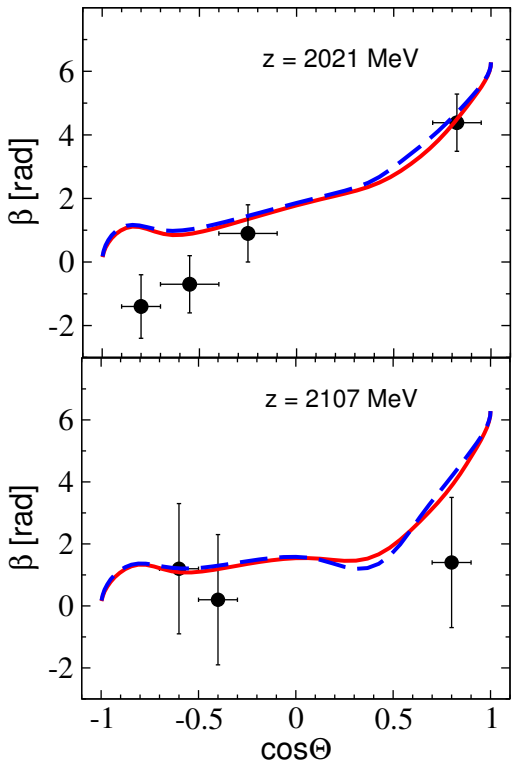

Exciting CLAS data to come from FROST, HD-ICE, . . .

from: Eugene Pasyuk @ *Meson 2012*

	σ	Σ	T	P	E	F	G	H	T_x	T_z	L_x	L_z	O_x	O_z	C_x	C_z
Proton target																
$p\pi^0$	✔	✓	✓	✓	✓	✓	✓	✓								
$n\pi^+$	✔	✓	✓	✓	✓	✓	✓	✓								
$p\eta$	✔	✓	✓	✓	✓	✓	✓	✓								
$p\eta'$	✔	✓	✓	✓	✓	✓	✓	✓								
$p\omega$	✔	✓	✓		✓	✓	✓	✓								
$K^+\Lambda$	✔	✓	✓	✔	✓	✓	✓	✓	✓	✓	✓	✓	✓	✓	✔	✔
$K^+\Sigma^0$	✔	✓	✓	✔	✓	✓	✓	✓	✓	✓	✓	✓	✓	✓	✔	✔
$K^{0*}\Sigma^+$	✔	✓	✓	✓	✓	✓	✓	✓								
"Neutron" target																
$p\pi^-$	✔	✓	✓		✓	✓	✓	✓								
$p\rho^-$	✓	✓	✓		✓	✓	✓	✓								
$K^+\Sigma^-$	✔	✓	✓		✓	✓	✓	✓								
$K^0\Lambda$	✓	✓	✓	✓	✓	✓	✓	✓	✓	✓	✓	✓	✓	✓	✓	✓
$K^0\Sigma^0$	✓	✓	✓	✓	✓	✓	✓	✓	✓	✓	✓	✓	✓	✓	✓	✓
$K^{0*}\Sigma^0$	✓	✓														

✔ - published ✔ - acquired

- Unitarity of the scattering matrix S: $SS^\dagger = \mathbb{1}$ $\qquad [S = \mathbb{1} - i\,\frac{p}{4\pi E}\,T]$.

$$\mathrm{Im}\; T^{-1}(E) = \sigma \equiv \frac{p}{8\pi\, E}$$

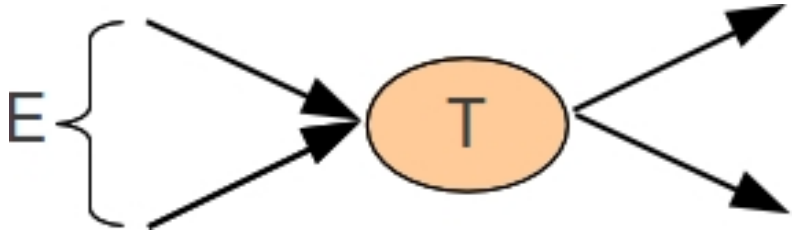

- $\rightarrow$ Generic (Lippman-Schwinger) equation for unitarizing the T-matrix:

$$T = V + V\,G\,T \qquad \mathrm{Im}\; G = -\sigma$$

V: (Pseudo)potential, σ: phase space.

- G: Green's function:

$$\begin{aligned} G &= \int \frac{d^3\vec{q}}{(2\pi)^3}\,\frac{f(|\vec{q}|)}{E^2 - (\omega_1+\omega_2)^2 + i\epsilon}, \\ \omega_{1,2}^2 &= m_{1,2}^2 + \vec{q}^{\,2} \end{aligned}$$

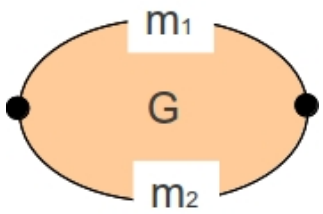

Discretization

Discretized momenta in the finite volume with periodic boundary conditions

$$\Psi(x) \stackrel{!}{=} \Psi(x + \hat{\mathbf{e}}_i\, L) = \exp\left(i\, L\, q_i\right) \Psi(x) \quad \Longrightarrow \quad q_i = \frac{2\pi}{L}\, n_i, \quad n_i \in \mathbb{Z}, \quad i = 1, 2, 3$$

$$\boxed{\int \frac{d^3\vec{q}}{(2\pi)^3}\, g(|\vec{q}\,|^2) \to \frac{1}{L^3} \sum_{\vec{n}} g(|\vec{q}|^2), \quad \vec{q} = \frac{2\pi}{L}\, \vec{n}, \quad \vec{n} \in \mathbb{Z}^3}$$

$$G \to \tilde{G} = \frac{1}{L^3} \sum_{\vec{q}} \frac{f(|\vec{q}|)}{E^2 - (\omega_1 + \omega_2)^2}$$

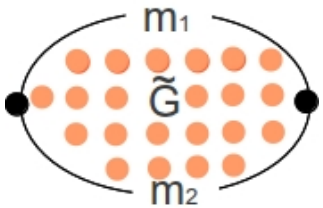

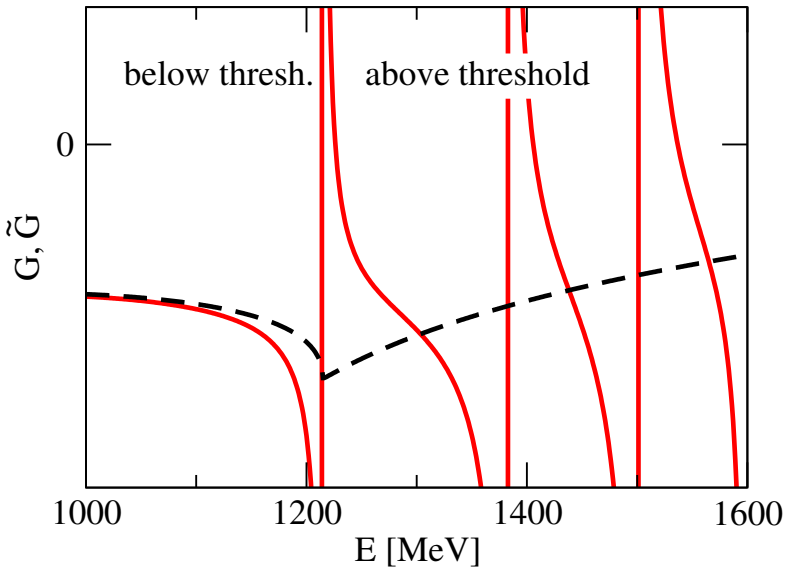

- $E > m_1 + m_2$: $\tilde{G}$ has poles at *free energies in the box*, $E = \omega_1 + \omega_2$
- $E < m_1 + m_2$: $\tilde{G} \to G$ exponentially with L (regular summation theorem).
- Formalism can be mapped to Lüscher's $\mathcal{Z}_{\ell m}$.

Finite $\to$ infinite volume: the Lüscher equation

Warning: Very crude re-derivation.

- Measured eigenvalues of the Hamiltonian (tower of *lattice levels* $E(L)$) $\to$ Poles of scattering equation $\tilde{T}$ in the finite volume $\to$ determines V:

$$\tilde{T} = (1 - V\tilde{G})^{-1} V \;\to\; V^{-1} - \tilde{G} \stackrel{!}{=} 0 \;\to\; V^{-1} = \tilde{G}$$

- The interaction V determines the T-matrix in the infinite volume limit:

$$T = \left(V^{-1} - G\right)^{-1} = \left(\tilde{G} - G\right)^{-1}$$

- Re-derivation of Lüscher's equation (T determines the phase shift δ):

$$\boxed{p \cot \delta(p) = -8\pi\sqrt{s}\left(\tilde{G}(E) - \mathrm{Re}\, G(E)\right)}$$

- V and dependence on renormalization have disappeared (!)

Twisting the boundary conditions (B.C.)

[M.D., Meißner, Oset, Rusetsky, **47** (2011)]

- Periodic B.C.:
  $\Psi(\vec{x} + \hat{\mathbf{e}}_i L) = \Psi(\vec{x})$
- Periodic in 2 dim.:

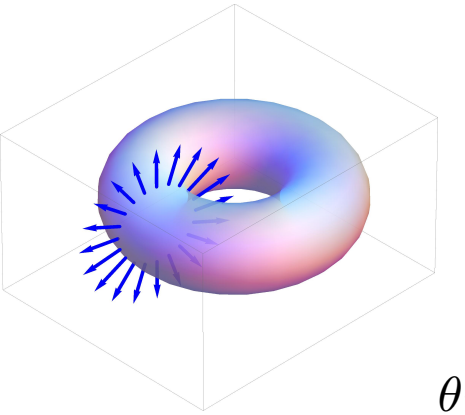

$\theta_1 = 0$

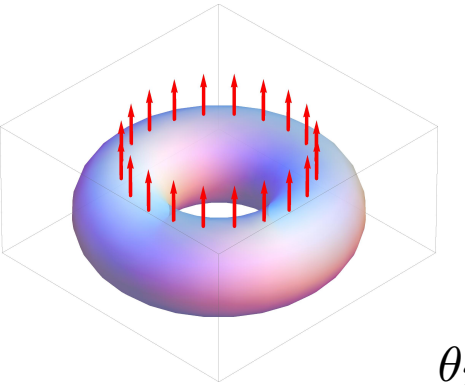

$\theta_2 = 0$

- Twisted B.C.:
  $\Psi(\vec{x} + \hat{\mathbf{e}}_i L) = e^{i\theta_i}\Psi(\vec{x})$
- Periodic/antiperiodic:

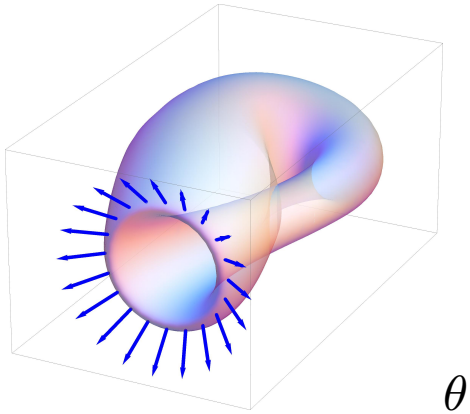

$\theta_1 = 0$

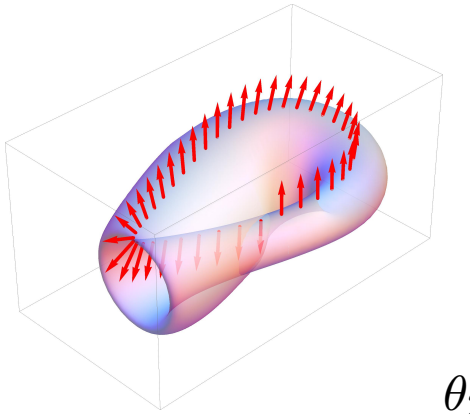

$\theta_2 = \pi$

Example: the $f_0(980)$

- S-wave, coupled-channels $\pi\pi$, $\bar{K}K$.
- Twisted B.C. for the s-quark:
  $u(\vec{x} + \hat{\mathbf{e}}_i L) = u(\vec{x})$
  $d(\vec{x} + \hat{\mathbf{e}}_i L) = d(\vec{x})$
  $s(\vec{x} + \hat{\mathbf{e}}_i L) = e^{i\theta_i} s(\vec{x})$
- Three unknown potentials
  - $V(\pi\pi \to \pi\pi)$
  - $V(\pi\pi \to \bar{K}K)$
  - $V(\bar{K}K \to \bar{K}K)$

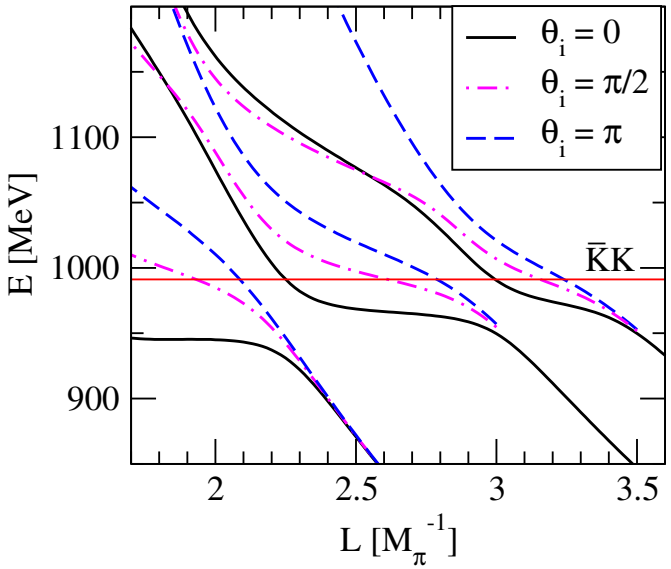

Mixing of partial waves
Example: S- and P-waves

- Infinite volume limit: Rotational symmetry

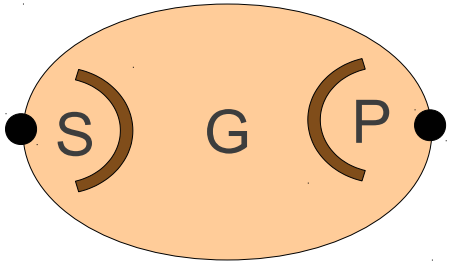

$$\int \frac{d^3\vec{q}}{(2\pi)^3}\, g(|\vec{q}|)\; Y_{\ell m}(\theta,\phi)\, Y^*_{\ell' m'}(\theta,\phi) \sim \delta_{\ell\ell'}\delta_{mm'}\,.$$

S→S	0	0	0
0	$P_{-1} \to P_{-1}$	0	0
0	0	$P_0 \to P_0$	0
0	0	0	$P_1 \to P_1$

Mixing of partial waves
Example: S- and P-waves

- Infinite volume limit: Rotational symmetry

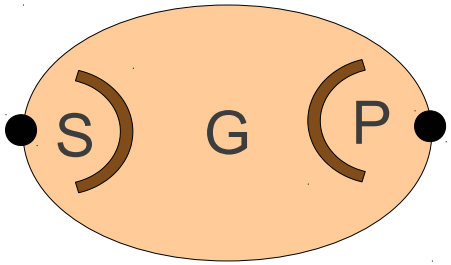

$$\int \frac{d^3\vec{q}}{(2\pi)^3}\, g(|\vec{q}|)\; Y_{\ell m}(\theta,\phi)\, Y^*_{\ell' m'}(\theta,\phi) \sim \delta_{\ell\ell'}\delta_{mm'}\,.$$

- Wigner-Eckart theorem:

S→S	0	0	0
0	P_{-1} →	0	0
0	0		0
0	0	0	→ P_1

Equal

Mixing of partial waves
Example: S- and P-waves

- Finite volume: Rotational symmetry $\rightarrow$ Cubic symmetry

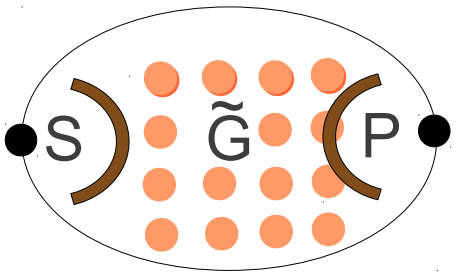

$$\frac{1}{L^3}\sum_{\vec{n}} g(|\vec{q}|)\, Y_{\ell m}(\theta,\phi)\, Y^*_{\ell' m'}(\theta,\phi) \sim A_{\ell\ell' mm'}.$$

- $S-G$-wave mixing, but $S-P$ waves still orthogonal:

S→S	0	0	0
0	$P_{-1} \rightarrow P_{-1}$	0	0
0	0	$P_0 \rightarrow P_0$	0
0	0	0	$P_1 \rightarrow P_1$

Breaking of cubic symmetry through boost

Example: Lattice points $\vec{q}^*$ boosted with $P = (0,0,0) \to \frac{2\pi}{L}\,(0,0,2)$:

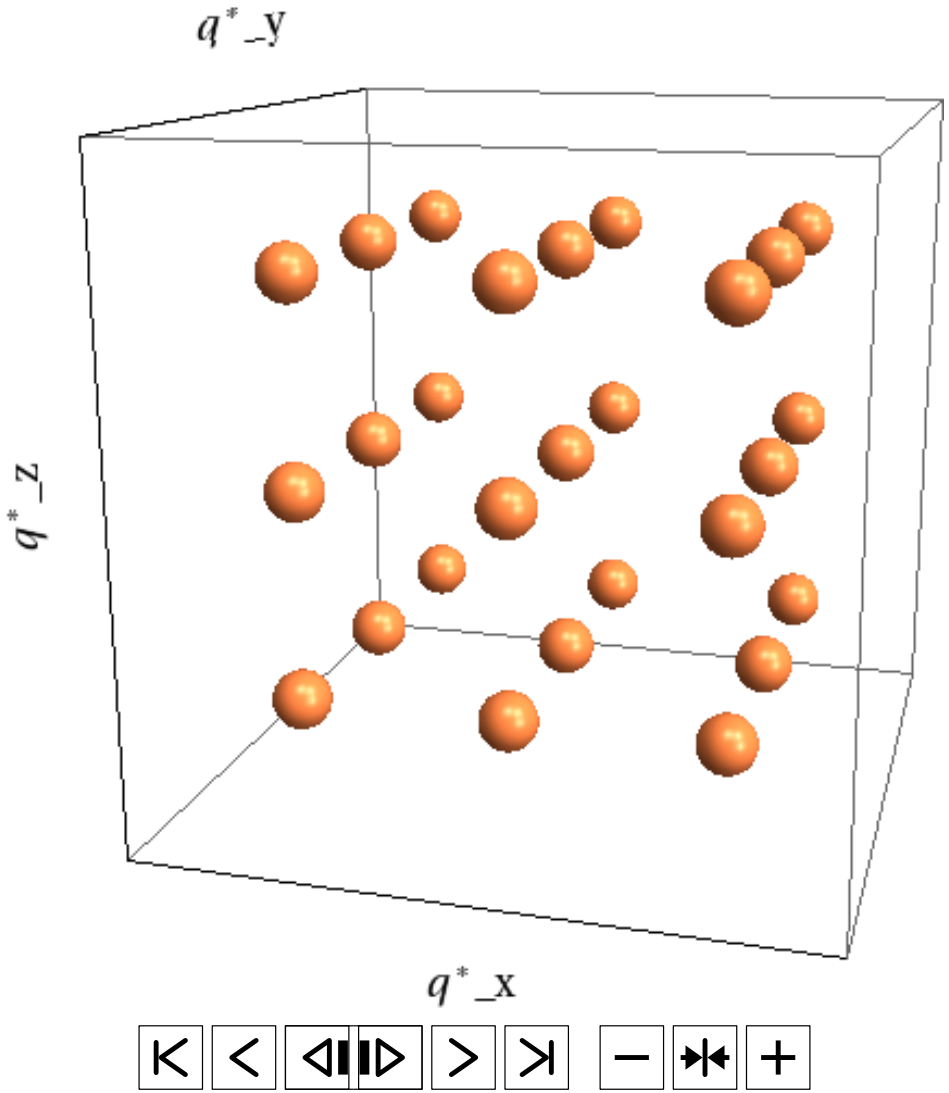

Mixing of partial waves
Example: S- and P-waves

- Finite volume & boost: Cubic symmetry $\rightarrow$ subgroups of cubic symmetry

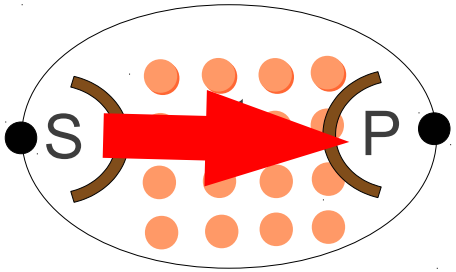

$$\frac{1}{L^3}\sum_{\vec{n}} g(|\vec{q}|)\; Y_{\ell m}(\theta,\phi)\, Y^*_{\ell' m'}(\theta,\phi) \sim A_{\ell\ell' mm'}.$$

- For boost $P = \frac{2\pi}{L}$ (0,1,1):

S→S	0	S→P_0	0
0	$P_{-1} \rightarrow P_{-1}$	0	$P_{-1} \rightarrow P_1$
P_0→S	0	$P_0 \rightarrow P_0$	0
0	$P_1 \rightarrow P_{-1}$	0	$P_1 \rightarrow P_1$

Mixing of partial waves
Example: S- and P-waves

- Finite volume & boost: Cubic symmetry $\rightarrow$ subgroups of cubic symmetry

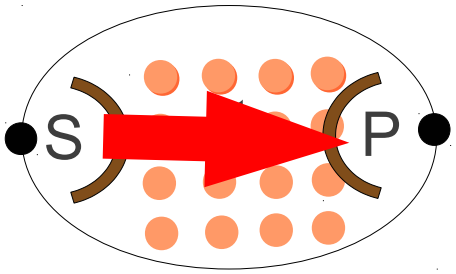

$$\frac{1}{L^3}\sum_{\vec{n}} g(|\vec{q}|)\; Y_{\ell m}(\theta,\phi)\, Y^*_{\ell' m'}(\theta,\phi) \sim A_{\ell\ell' mm'}.$$

- More complicated boosts:

$S \rightarrow S$	$S \rightarrow P_{-1}$	$S \rightarrow P_0$	$S \rightarrow P_1$
$P_{-1} \rightarrow S$	$P_{-1} \rightarrow P_{-1}$	$P_{-1} \rightarrow P_0$	$P_{-1} \rightarrow P_1$
$P_0 \rightarrow S$	$P_0 \rightarrow P_{-1}$	$P_0 \rightarrow P_0$	$P_0 \rightarrow P_1$
$P_1 \rightarrow S$	$P_1 \rightarrow P_{-1}$	$P_1 \rightarrow P_0$	$P_1 \rightarrow P_1$

Disentanglement of partial waves

Example: S- and P-waves for the $\kappa(800)/K^*(892)$ system

Knowledge of P-wave (from separate analysis of lattice data) allows to disentangle the S-wave:

$$p\,\cot\delta_S = -8\pi\,E\,\frac{p\,\cot\delta_P\,\hat{G}_{SS} - 8\pi E(\hat{G}_{SP}^2 - \hat{G}_{SS}\hat{G}_{PP})}{p\,\cot\delta_P + 8\pi\,E\,\hat{G}_{PP}}$$

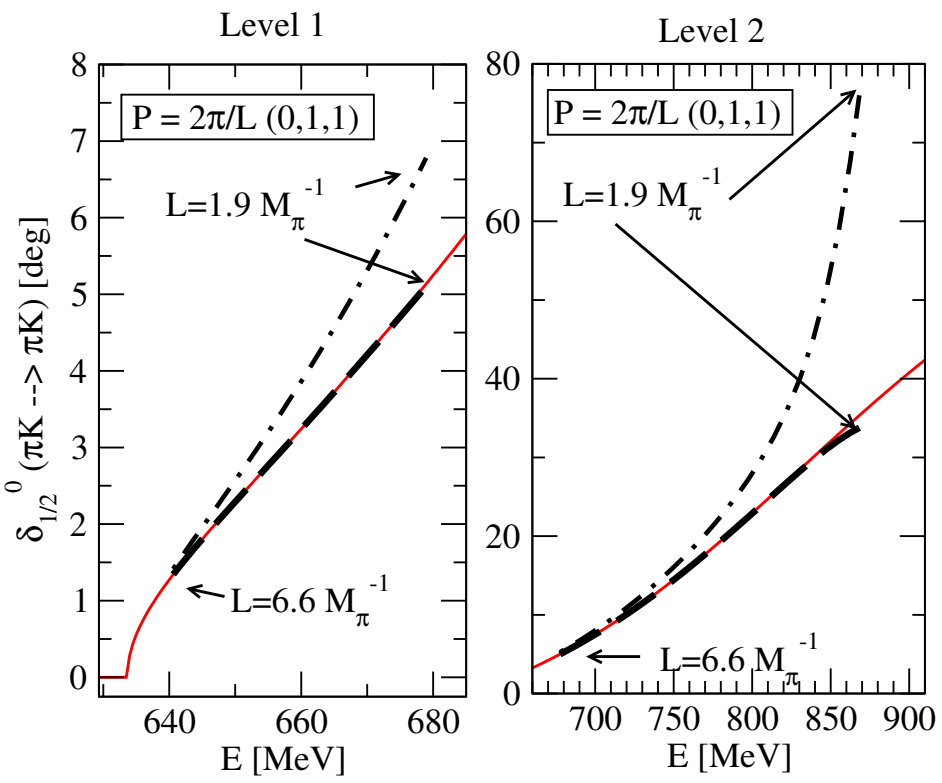

- $\delta_S \equiv \delta^0_{1/2}(\pi K \to \pi K)$
- Red solid: Actual S-wave phase shift.
- Dash-dotted: Reconstructed S-wave phase shift, PW-mixing ignored.
- Dashed: Reconstructed S-wave phase shift, PW-mixing disentangled.
- small p-wave: Level shift $\Delta E \simeq -\dfrac{6\pi E_S \delta_P}{L^3 p \omega_1 \omega_2}$

Mixing of partial waves in boosted multiple channels: $\sigma(600)$

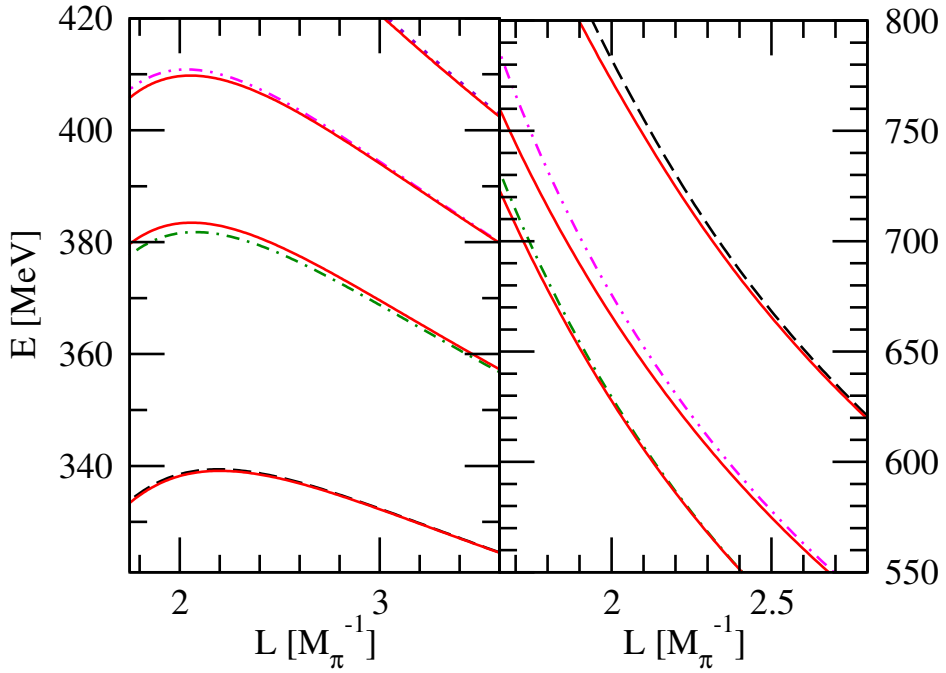

Solid: Levels from A_1^+.
Non-solid: Neglecting the D-wave.

- $\pi\pi$ & $\bar{K}K$ in S-wave, $\pi\pi$ in D-wave.
- Organization in Matrices (A_1^+), e.g. $\vec{P} = (2\pi/L)(0,0,1)$, $(2\pi/L)(1,1,1)$, and $(2\pi/L)(0,0,2)$:

$$V = \begin{pmatrix} V_S^{(11)} & V_S^{(12)} & 0 \\ V_S^{(21)} & V_S^{(22)} & 0 \\ 0 & 0 & V_D^{(22)} \end{pmatrix}$$

$$\tilde{G} = \begin{pmatrix} \tilde{G}^{R\,(1)}_{00,00} & 0 & 0 \\ 0 & \tilde{G}^{R\,(2)}_{00,00} & \tilde{G}^{R\,(2)}_{00,20} \\ 0 & \tilde{G}^{R\,(2)}_{20,00} & \tilde{G}^{R\,(2)}_{20,20} \end{pmatrix}$$

- Phase extraction (κ): Expand and fit V_S, V_P *simultaneously* to different representations instead of
  1. P-wave from B_1, B_2, E
  2. S-wave from P and A_1

  (reduction of error).

Phase shifts from a moving frame: the $\sigma(600)$

Comparison: *Variation of L vs moving frames*

- The first two levels for the first five boosts:

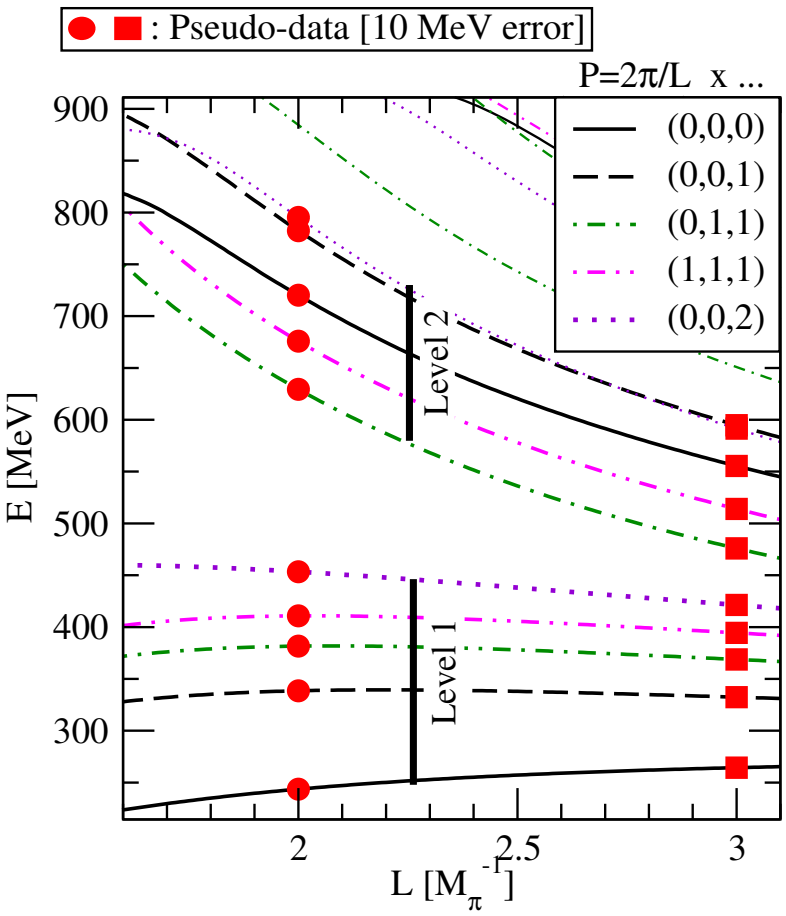

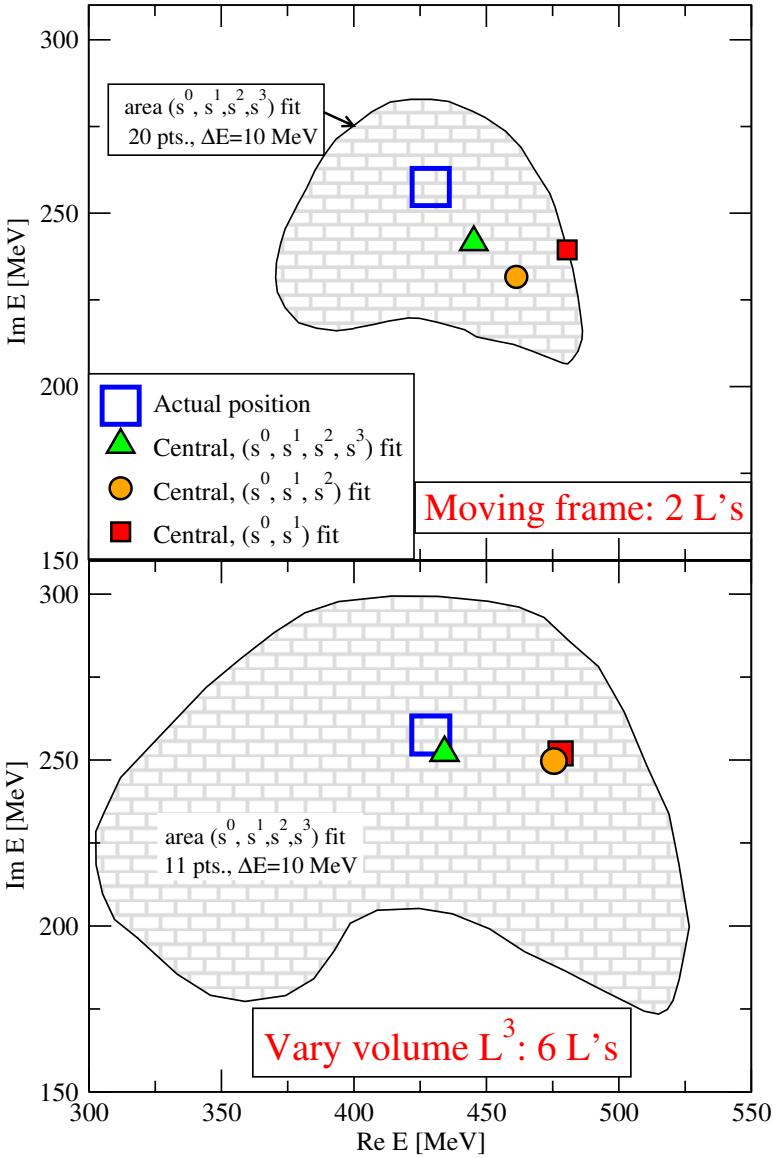

Unitary isobars in the finite volume: the $a_1(1260)$

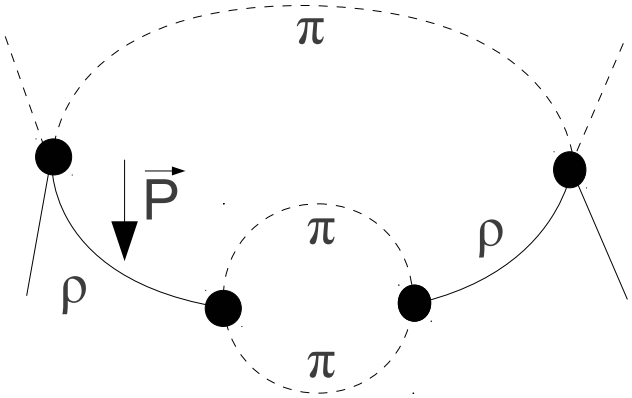

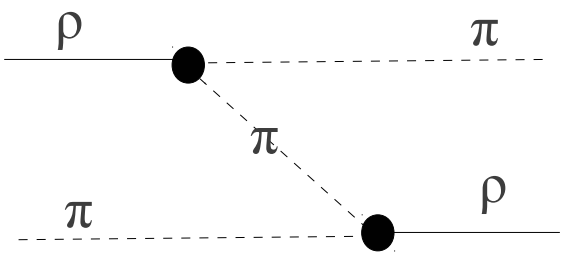

Boosted $\pi\pi$ self energy:

$$\tilde{\Pi}_{\lambda\lambda} = J\,\frac{4\pi}{3}\,\frac{1}{L^3}\sum_{\vec{n}}(q^*)^2\,Y_{1\lambda}(\theta_{q^*},\phi_{q^*}) \times Y^*_{1\lambda'}(\theta_{q^*},\phi_{q^*})\,f(q^*)$$

3×3 self energy:

$$\tilde{\Pi} = \begin{pmatrix} \tilde{\Pi}_{1,1} & \tilde{\Pi}_{1,0} & \tilde{\Pi}_{1,-1} \\ \tilde{\Pi}_{0,1} & \tilde{\Pi}_{0,0} & \tilde{\Pi}_{0,-1} \\ \tilde{\Pi}_{-1,1} & \tilde{\Pi}_{-1,0} & \tilde{\Pi}_{-1,-1} \end{pmatrix},$$

Dressed propagator

$$\tilde{S}^D_{\pi\rho} = \frac{1}{2\omega_1}\left((S^B_{\pi\rho}\,\mathbb{1})^{-1} - \tilde{\Pi}\right)^{-1}$$

Sum over boosts $\vec{P}$:

$$\tilde{G}_{\pi\rho} = \frac{1}{L^3}\sum_{\vec{P}}\tilde{S}^D_{\pi\rho}\ .$$

$\pi\rho$ scattering equation:

$$\tilde{T}_{\pi\rho} = (\mathbb{1} - \hat{V}_{\pi\rho}\,\tilde{G}_{\pi\rho})^{-1}\,\hat{V}_{\pi\rho}, \quad \hat{V}_{\pi\rho} = V_{\pi\rho}\mathbb{1}$$

Lattice levels:

$$\det(\mathbb{1} - \hat{V}_{\pi\rho}\,\tilde{G}_{\pi\rho}) = 0\ .$$

(+ pion exchange, required from 3-body unitarity; certain 3-body singularities cancel [see also K. Polejaeva and A. Rusetsky, EPJA 48 (2012)]).